Activity 10: Ambient air quality monitoring

Activity 10.2: E-BAM deployment and air quality assessment for eZamokuhle for 2023

Document by:

ARM
AIR RESOURCE MANAGEMENT

Final Report

7th March 2024

Document Title

Client	**Eskom**
Title	**E-bam deployment and air quality (AQ) assessment (baseline) for eZamokuhle**
Our Reference	**ESKPMV-2024- ACT-10.2-02**
Issued to Client	**7th March 2024**
Classification	**Company Confidential**

Document Change Record

Revision Number	Date	Description of Revision
00A	13 December 2023	Creation of Document
00B	30th January 2024	Peer Review of Document
00	8th February 2024	Draft Document issued to Eskom
01	28th February 2024	Revised Document issued to Eskom
02	7th March 2024	Final Document issued to Eskom

Document Approval

	Name	Date
Prepared by	Avishkar Ramandh & Anesu Shamu	5th March 2024
Reviewed by	Fred Goede	6th March 2024
Approved by	Fred Goede	7th March 2024

TABLE OF CONTENTS

TABLE OF FIGURES

EXECUTIVE SUMMARY

1. STUDY OBJECTIVE

The objective of this study component was to conduct ambient air quality monitoring utilising the Environmental Beta Attenuation Monitors (E-BAM) to measure baseline particulate matter (PM_{10} and $Pm_{2.5}$) ambient concentrations in eZamokuhle. It's noted that these measurements at eZamokuhle were conducted prior to the large-scale rollout of the Eskom AQO Project interventions in the eZamokuhle community and thus still serves as the status quo air quality baseline herein. Its noted due to constraints and delays encountered by the insulation contractors in eZamokuhle, the roll-out of the Eskom AQO Project interventions herein was not at a significant scale for the sampling period.

2. STUDY METHODOLOGY

Three E-BAM monitors were commissioned outdoors at three residential sampling sites in the eZamokuhle airshed. The E-BAM instrument is a portable, real-time beta gauge comparable to U.S.-EPA methods for $PM_{2.5}$ and PM_{10} particulate measurements. The E-BAM automates particulate measurement by continuously sampling and reporting concentration data. The first sampling assessment (survey 1) was conducted from mid-August to mid-October 2022, whilst the second sampling assessment (survey 2) was conducted from mid-May to mid-September 2023 at the three residential sampling sites. It's noted that the first sampling survey campaign, no households were completed whilst the in the second survey 450 households were completed in Ezamokuhle (pers comm, Mandava, 2024) The Openair model was utilised to statistically analyse the semi-empirical mathematical relationships between air pollutant concentrations and meteorological parameters for these three stations.

3. STUDY RESULTS

3.1 PARTICULATE MATTER (PM_{10} & $PM_{2.5}$)

It was evident that the highest elevated particulate matter concentrations were recorded during hours 06:00 to 08:00 and 17:00 to 19:00 for both the 2022 (survey 1) and 2023 (survey 2) campaign. This bi-modal particulate matter peak is a typical profile for residential fuel burning. A morning peak occurs at 07:00 whilst the evening peak occurs at 18:00. The morning peaks reduces towards midday as the inversion layer rises & improves the mixing height of the planetary boundary layer.

The daily NAAQS for particulate matter (both PM_{10} & $PM_{2.5}$) was exceeded at all three residential sampling sites in eZamokuhle. These elevated concentrations were predominant during the colder winter months. The colder ambient temperatures lead to an increase in residential fuel burning activities. The Openair model analysis further supported that the highest concentrations occurred during low temperatures, which is attributable to residential fuel burning. Its noted, fewer particulate matter exceedances were recorded for the warmer month of October as the need for space heating herein declines.

3.2 SULPHUR DIOXIDE (SO_2)

An analysis of the Eskom eZamokuhle ambient air quality stations (AQMS) showed that there were no recorded exceedances of the hourly NAAQS SO_2 standard. The highest mean concentrations were recorded around midday and 18:00 for the Eskom eZamokuhle AQMS. The midday peak indicates a typically industrial signature as tall stack plumes are brought down to ground-level due to the break-up of the surface inversion layer in convective conditions. The Openair model results demonstrated that the SO_2 concentrations observed at the Eskom eZamokuhle station showed two distinct wind directions, namely from the south-west and the north-west.

The higher SO_2 concentrations associated with the south-westerly winds are most likely due to emissions from the Eskom Majuba power station. Whereas the SO_2 concentrations from the north- west indicate a distinct tall stack emission source. Its plausible the impact of source is due to other Power Stations (Tutuka, Kriel, Matla) and possibly a petrochemical facility which are all located in the north west from eZamokuhle. Furthermore, the Openair results supported that the 18:00 peak recorded for the Eskom eZamokuhle station is indicative of the impact of residential fuel burning emissions.

3.3 Nitrogen Dioxide (NO_2)

An analysis of the Eskom eZamokuhle ambient air quality stations (AQMS) showed that there were no recorded exceedances of the hourly NAAQS NO_2 standard. The highest mean concentrations were recorded during hours 06:00 to 08:00 and 16:00 to 18:00 for the Eskom eZamokuhle AQMS. The Openair analysis explicitly revealed that the variability of this pollutant concentration is conditioned by vehicle emissions. The diurnal cycle corresponds to the cyclical nature of traffic volume with marked peaks in concentration on weekdays around the early-morning and late-afternoon rush-hours.

4. Conclusion

Both the 2022 and 2023 survey campaigns have consistently demonstrated that elevated short term particulate matter (both PM_{10} & $PM_{2.5}$) in the winter months are clearly attributable to residential fuel burning in Ezamokuhle. The daily NAAQS for particulate matter (both PM_{10} & $PM_{2.5}$) was again exceeded at the three eZamokuhle residential sampling sites in the 2023 survey. The Openair analysis further supported that the elevated particulate matter concentrations occurring during winter were associated with localized non-bouyant sources (residential fuel burning) as opposed to tall stack emissions. It’s clear from both survey campaigns that residential fuel burning poses a significant health risk to the community of eZamokuhle. Thus, there is an opportunity

herein to reduce human exposure to harmful levels of air pollution by reducing emissions from residential burning. Hence supporting the roll-out of Eskom's PMV air quality offset intervention project in Ezamokuhle.

1. BACKGROUND

1.1 Air Quality Offsets Guideline

An environmental offset is an action(s), designed to compensate for a negative environmental impact of resource use, a discharge, emission, or other activity. The Department of Environment, Forestry & Fisheries (DEFF) defines air emissions offsets as an intervention, or interventions, specifically implemented to counterbalance the adverse and residual environmental impact of atmospheric emissions in order to deliver a net ambient air quality benefit within, but not limited to, the affected airshed where ambient air quality standards are being or have the potential to be exceeded and whereby opportunities and need for offsetting exist (Notice 333 of 2016).

1.2 ESKOM'S Approach to Air Quality Offsets

DEFF's Air Quality Offset Guideline has shaped and informed Eskom's Air Quality Offsets Implementation Plan. This Plan has been based on a scientific process of feasibility studies, testing and demonstration, and on consultation with key stakeholders. Figure 1 illustrates the concept schedule for the phased implementation of Eskom's air quality offsets.

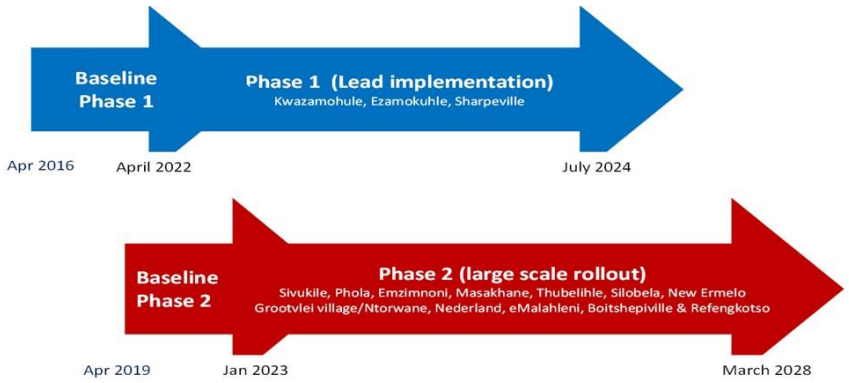

Figure 1: Concept Schedule for the implementation of Eskom's air quality offsets (Matimolane, 2023).

Eskom has adopted the phased approach (Figure 2) herein to increase the probability of success and to ensure that learnings from early phases are incorporated into the large-scale roll-out. (Matimolane, 2020).

Phase 1	Phase 2	Phase 3
• Lead Phase • The intervention is tested on an entire community in order to determine the best way forward for sclaing up the inititiative.	• Full implementation on the remaining households in the larger settlements • Learnings from the Lead Phase incorporated herein. • Intervention will be rolled out simultaneously at several large communities across the three district municipalities and selected areas in the Vaal.	• Full implementation on the remaining households in the smaller settlements • Learnings from the Lead Phase incorporated herein. • The intervention will be rolled out simultaneously at several small semi-rural communities the three district municipalities and selected areas in the Vaal.

Figure 2: Eskom's Phased approach to the rollout of air quality offset interventions (Matimolane, 2020).

Eskom's air quality offsets programme is designed to reduce human exposure to harmful levels of air pollution by reducing emissions from local sources, like domestic coal burning and waste burning. Thus, air quality offsets can improve ambient air quality in low-income communities in the vicinity of Eskom's power stations. Eskom has developed air quality offset (AQO) implementation plans for Majuba Power Station (eZamokuhle township); Hendrina Power Station (KwaZamokuhle township) and Lethabo Power station (Sharpeville).

1.3 ESKOM'S PLANNING, MONITORING AND VERIFICATION (PMV) PROJECT

For Eskom's PMV Project, interventions to reduce household emissions from domestic coal/wood burning will be rolled out in KwaZamokuhle and eZamokuhle in the Mpumalanga Highveld. For formal dwellings the intervention will be a thermal insulation retrofit and an electricity starter pack and installation. The intervention for informal dwellings still needs to be selected and tested. Interventions also need to be identified and implemented to improve air quality in Sharpeville, Gauteng. Since domestic coal burning is less prevalent in Sharpeville, it is expected that a community-scale intervention, like reducing waste burning, will be more suitable there.

Air Resource Management (ARM) (Pty) Ltd has been appointed by Eskom to support the PMV services in support of the *Phase 1: Lead implementation* at: KwaZamokuhle; eZamokuhle and Sharpeville. Its ARM (Pty) Ltd understanding that the overall objective *Lead Implementation Phase* is to benefit the specific local communities, minimize implementation risk, increase practical and scientific knowledge, and develop and refine monitoring, reporting and verifications processes. To achieve this, Eskom has included sixteen targeted work package Activities (Table 1) for these respective communities. This report focuses on *Activity 10.1 The E-bam deployment and AQ assessment (baseline) for eZamokuhle.*

Table 1: Eskom PMV Activity Schedule (Eskom PMV NEC Contract,27082020)

Activities	Kwazamokuhle	Ezamokuhle	Sharpeville
Activity 1: Preliminary air quality assessment		✓	
Activity 2: Gather Area intelligence		✓	
Activity 3: Rapid in situ assessment		✓	
Activity 4: Obtain ethical clearance		✓	
Activity 5: Census	✓	✓	✓
Activity 6: Community source survey		✓	
Activity 7: Fuel source survey		✓	
Activity 8: Household surveys		✓	
Activity 9: Annual (household/community) surveys and monitoring of project effectiveness	✓	✓	✓
Activity 10: Ambient air quality monitoring	✓	✓	✓
Activity 11: Conduct indoor air quality monitoring	✓	✓	
Activity 12: Atmospheric Dispersion Model	✓	✓	✓
Activity 13: Design of Intervention		✓	✓
Activity 14: Development of Database Reporting	✓	✓	✓
Activity 15: Strategic Assistance and offsets methodology	✓	✓	✓
Activity 16: Research and Development	✓	✓	✓

1.4 Scope of Work

In accordance with the scope of work, for Activity 10: *Conduct Ambient Air Quality Monitoring*, ARM is to conduct ambient air quality monitoring utilising the Environmental beta Attenuation Monitors to monitor baseline PM concentrations in eZamokuhle before the implementation and rollout of the intended Eskom household interventions.

2. METHODOLOGY

2.1 SAMPLING METHODOLOGY

Three E-BAM Environmental Beta Attenuation Mass Monitors were commissioned at three residential sampling sites in the eZamokuhle region. The E-BAM instrument is a portable, real-time beta gauge comparable to U.S.-EPA methods for $PM_{2.5}$ and PM_{10} particulate measurements. The E-BAM automates particulate measurement by continuously sampling and reporting concentration data. Data records are updated every minute. Figure 3 is a graphical representation of the E-BAM instrument.

Figure 3: E-Bam Instrument.

2.2 SAMPLING LOCATIONS

Table 2 is a summary of the E-BAM site locations as well as the sampling duration. Figure 4 is a picture of the E-BAM instrument commissioned at House 5 whereas Figure 5 is a close-up of these sampling locations in the eZamokuhle residential region. Figure 6 is

locality map of the E-BAM samplers in relation to the Eskom eZamokuhle and Eskom Majuma AQMS, whilst Figure 7 is indicative of the eZamokuhle residential region in the Highveld.

Table 2: Summary of E-BAM sampling locations as well as the sampling dates

Site	Pollutant Measured	Latitude (°S)	Longitude (°E)	Survey 1: Sampling Duration	Survey 2: Sampling Duration
House 1	$PM_{2.5}$	27.000325°	29.853501°	6 August 2022 to 21 October 2022	20 May 2023 to 22 September 2023
House 4	PM_{10}	27.001456°	29.856803°	14 August 2022 to 21 October 2022	20 May 2023 to 20 September 2023
House 5	$PM_{2.5}$	27.000133°	29.855321°	8 August 2022 to 19 October 2022	20 May 2023 to 22 September 2023

Figure 4: E-Bam instrument commissioned at House 5

Figure 5: Close-up of the sampling sites in eZamokuhle community

Figure 6: Map indicating the sampling sites in relation to the Majuba Power Station.

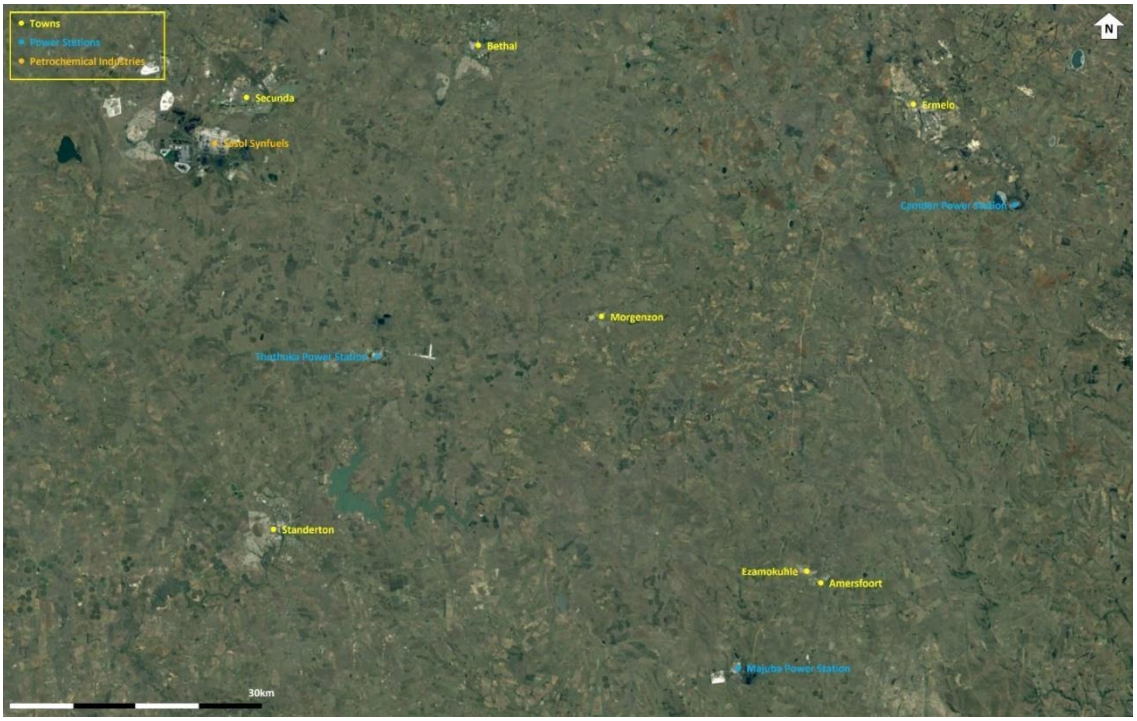

Figure 7: Layout of eZamokuhle in the Highveld.

3. RESULTS AND DISCUSSION

3.1 METEOROLOGICAL RESULTS

Air quality is strongly influenced by meteorology. Meteorological mechanisms govern the dispersion and eventual removal of pollutants from the atmosphere (Seaman, 2000). The analysis of hourly average meteorological data is necessary to facilitate a comprehensive understanding of the dispersion potential of the site. The horizontal dispersion of pollution is largely a function of the wind field. The wind speed determines both the distance of downward transport and the rate of dilution of pollutants. The wind rose is a very useful way for showing how wind speed and wind direction conditions vary by year. Meteorological data for the sampling period were obtained from the Eskom eZamokuhle and Eskom Majuba AQMS.

3.1.1 WIND SPEED AND WIND DIRECTION

Wind drives the atmospheric transport and strongly affects vertical air mixing and thus the ventilation of the urban air (Grundstrom et al., 2015). The understanding of how wind speed affects ground–level air pollution concentrations is relatively well established.

Stagnant atmospheric conditions with calm, clear weather often led to stable atmospheric stratification which can transform into strong nocturnal temperature inversions due to rapid surface cooling. The resulting restriction in vertical air mixing near the surface consequently leads to poor air quality (Delaney and Dowding, 1998; Janhall et. al., 2006; Olofson et al., 2009). Low wind speeds deteriorate air quality with respect to pollutants emitted near the ground due to restricted air ventilation (Jones et al., 2010). In contrast higher wind speeds are associated with increased dispersion and mixing of atmospheric pollutants which may result in low ambient pollution concentrations. Figure 8 illustrates

the predominant wind directions for the two sampling surveys at the Eskom eZamokuhle and Eskom Majuba AQMS during the two sampling surveys.

During 2022 the Eskom eZamokuhle AQMS station the average wind speed for the sampling period (Figure 8) was recorded at 3.04m/s with calm condition 0%. Calm condition means that wind speed is recorded at zero meter/second (Carlaw, 2015). The predominant wind direction was westerly (≈17% frequency of occurrence) followed by north westerly and easterly winds (≈13% frequency of occurrence) with maximum wind speed of 8 – 11m/s. The eZamokuhle AQMS indicated the same predominant wind directions during 2023, with the westerly component still prominent.

For the Eskom Majuba AQMS station the average wind speed for the sampling period (Figure 8) was recorded at 4.31m/s with calm condition 0.3%. Calm condition means that wind speed is recorded at zero meter/second (Carlaw, 2015). The predominant wind direction was south westerly (≈16% frequency of occurrence) followed by westerly and north easterly winds (≈13% frequency of occurrence) with maximum wind speed of 8 – 11m/s. The Majuba AQMS indicated the same predominant wind directions during 2023, however the north easterly components are substantially less than in 2022.

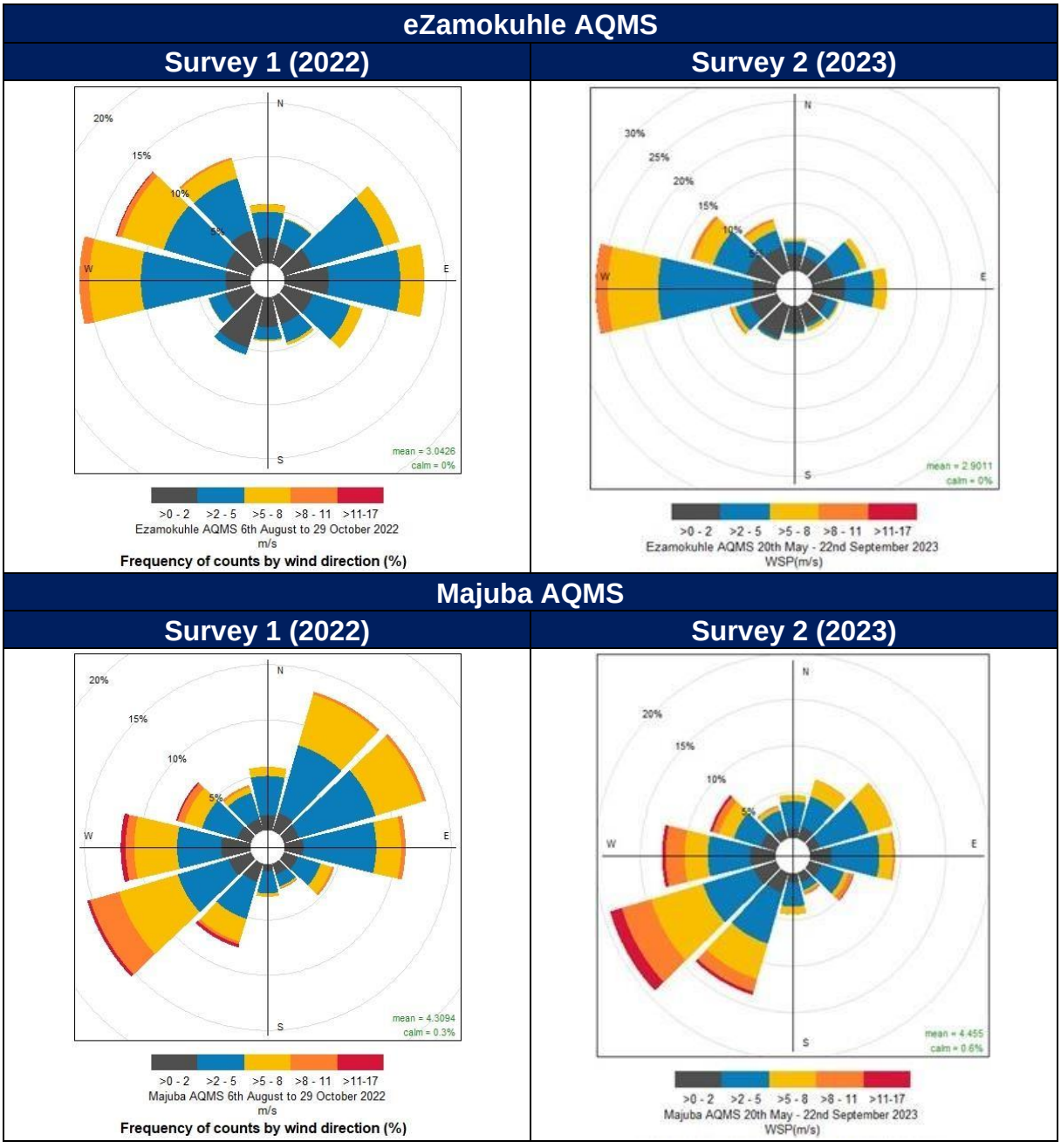

Figure 8: Wind roses for the Eskom eZamokuhle and Eskom Majuba AQMS for the two sampling surveys.

Figure 9A and Figure 9B box plots provide the diurnal wind speeds, whilst Figure 11A and Figure 10B are indicative of the monthly mean ambient wind speeds recorded at the Eskom eZamokuhle and Eskom Majuba AQMS respectively. The box plots highlight the distribution of the wind speed values by showing the minimum values, lower quartile, median, upper quartile and maximum values, and outlier values (circles outside of the box area depicted on the y-axis).

It is evident from Figure 9A and Figure 9B that the wind speed for both stations increase at 08:00 with a decrease at around 17:00. Maximum wind speeds are recorded for both stations at 15:00. Figure 11A illustrates slightly higher monthly mean wind speeds for the Majuba AQMS in comparison to the eZamokuhle AQMS during the same period.

As a norm, wind speeds in excess of 5.4m/s potentially have sufficient energy to pick-up and transport loose and/or disturbed particulate matter, which gives rise to visible nuisance dust and clouds of dust at ground level. The extent, to which this occurs / can occur, depends on several parameters, such as the properties and characteristics of the particulate matter, moisture content, etc.

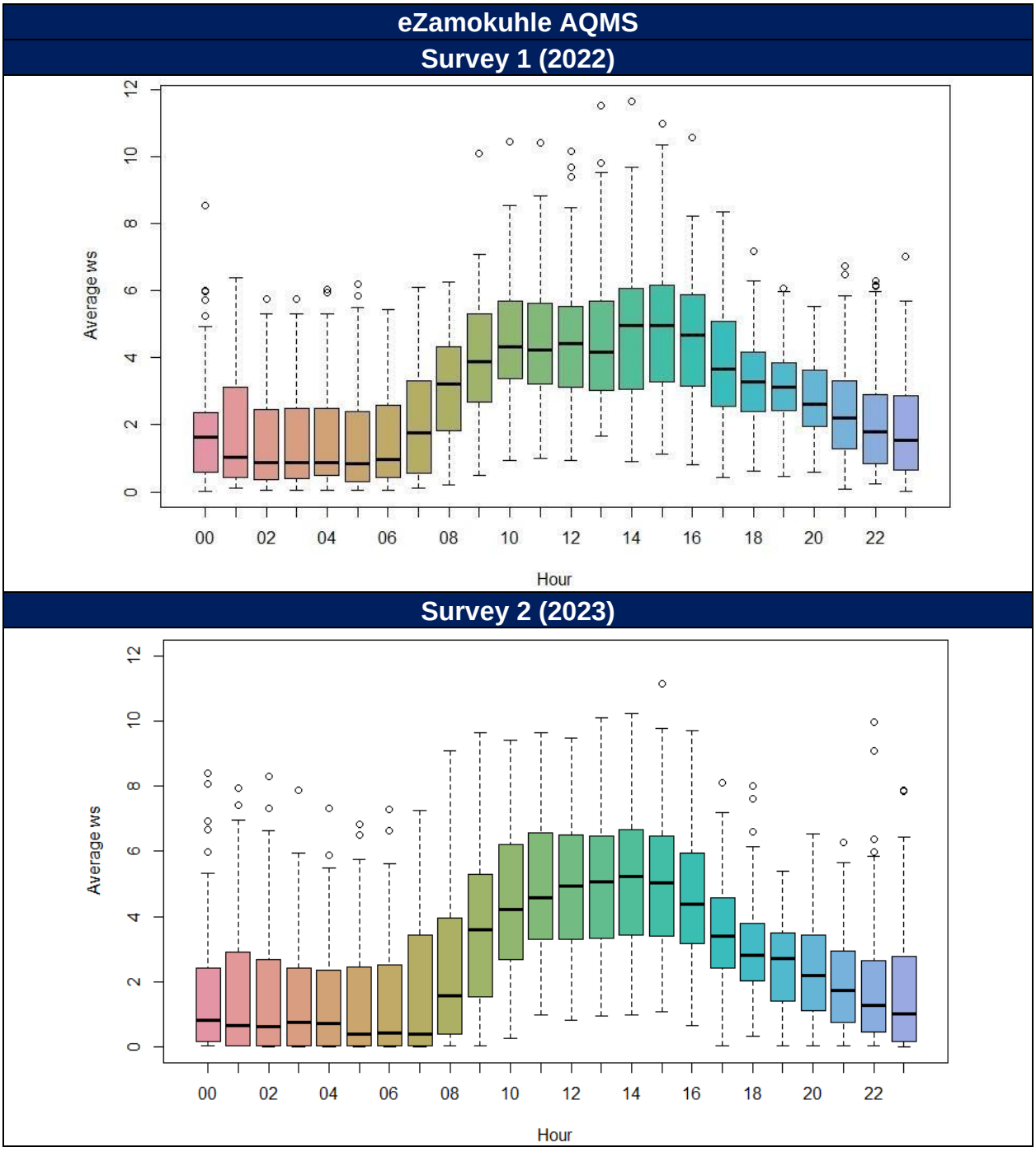

Figure 9A: Diurnal wind speeds recorded at the eZamokuhle AQMS (m/s) for the two sampling surveys.

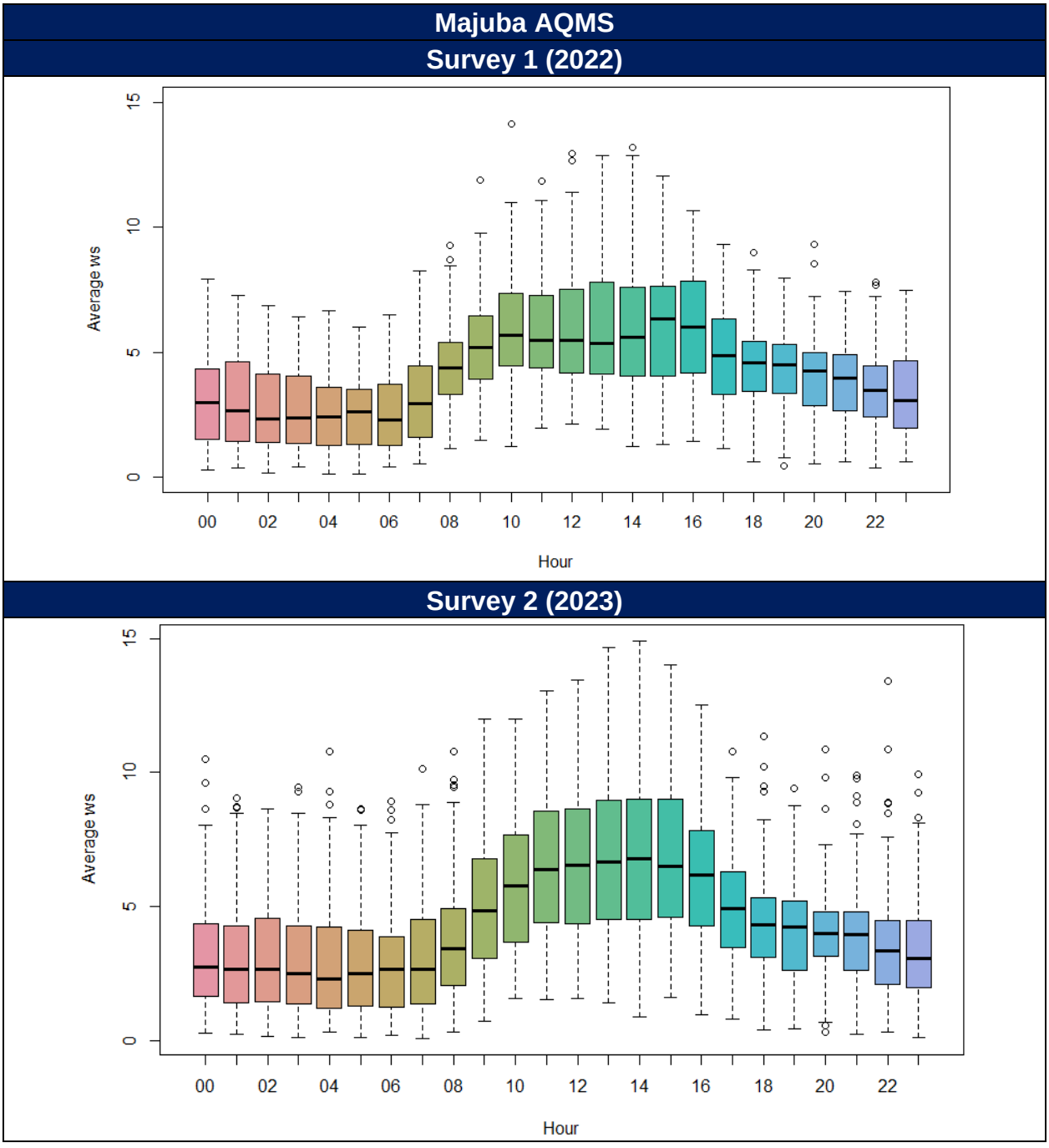

Figure 10B: Diurnal wind speeds recorded at the Majuba AQMS (m/s) for the two sampling surveys.

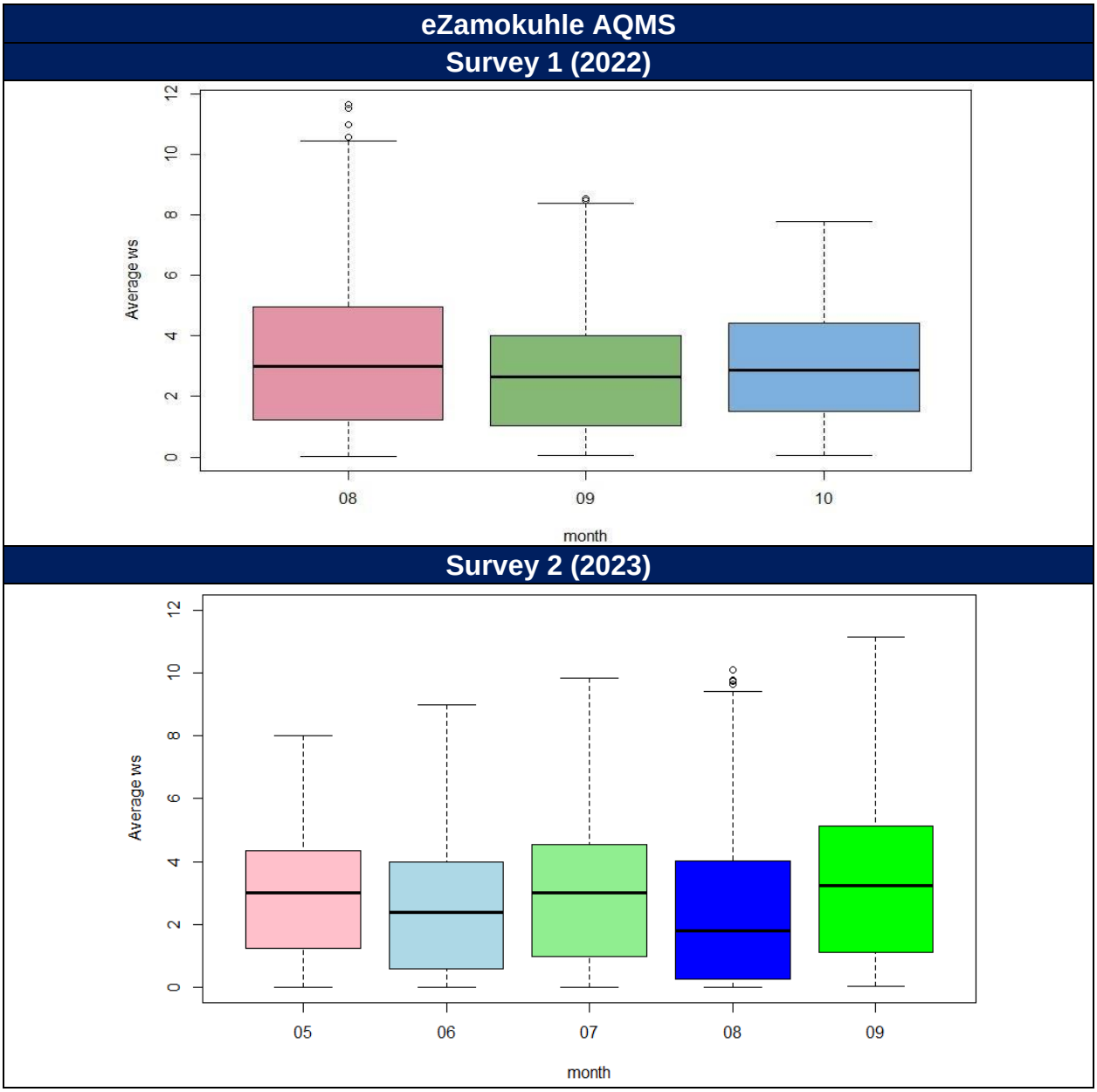

Figure 11A: Monthly mean wind speeds recorded at the eZamokuhle (m/s) for the two sampling surveys.

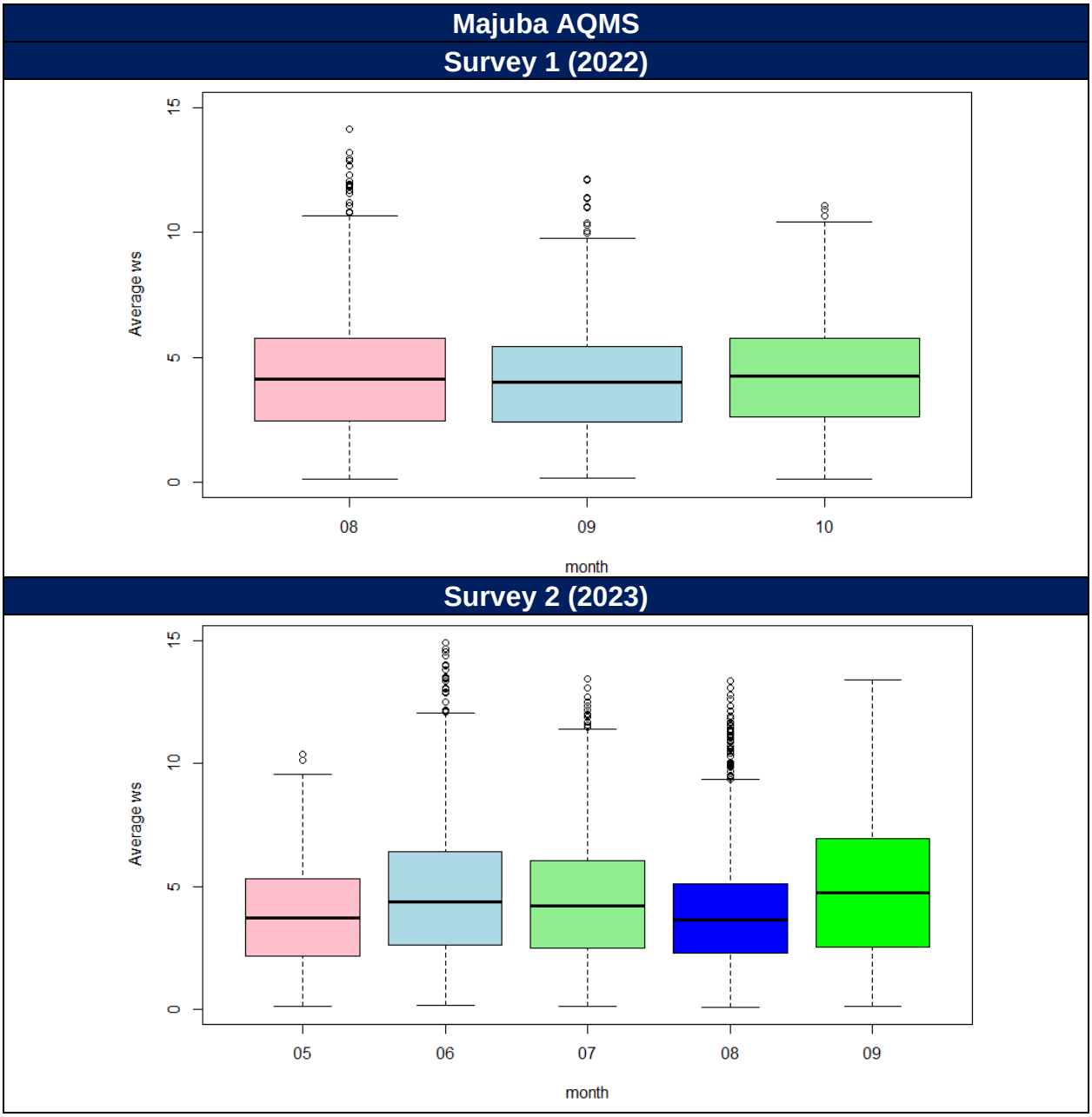

Figure 12B: Monthly mean wind speeds recorded at the Majuba AQMS (m/s) for the two sampling surveys.

3.1.2 TEMPERATURE

Air temperature is important, both for determining the effect of plume buoyancy (the larger the temperature difference between the plume and the ambient air, the higher the plume can rise), and determines the development of the mixing and inversion layers. Figure 13A and Figure 11B provides daily mean ambient temperatures for the Eskom eZamokuhle and Eskom Majuba AQMS respectively. From Figure 13A and Figure 11B, it is evident how the average ambient air temperatures are between 5 and 15°C for August, and slowly increasing to 15 and 22°C for the month of October. An increase in wind speed and ambient temperature improves the dispersion of air pollutants in the air.

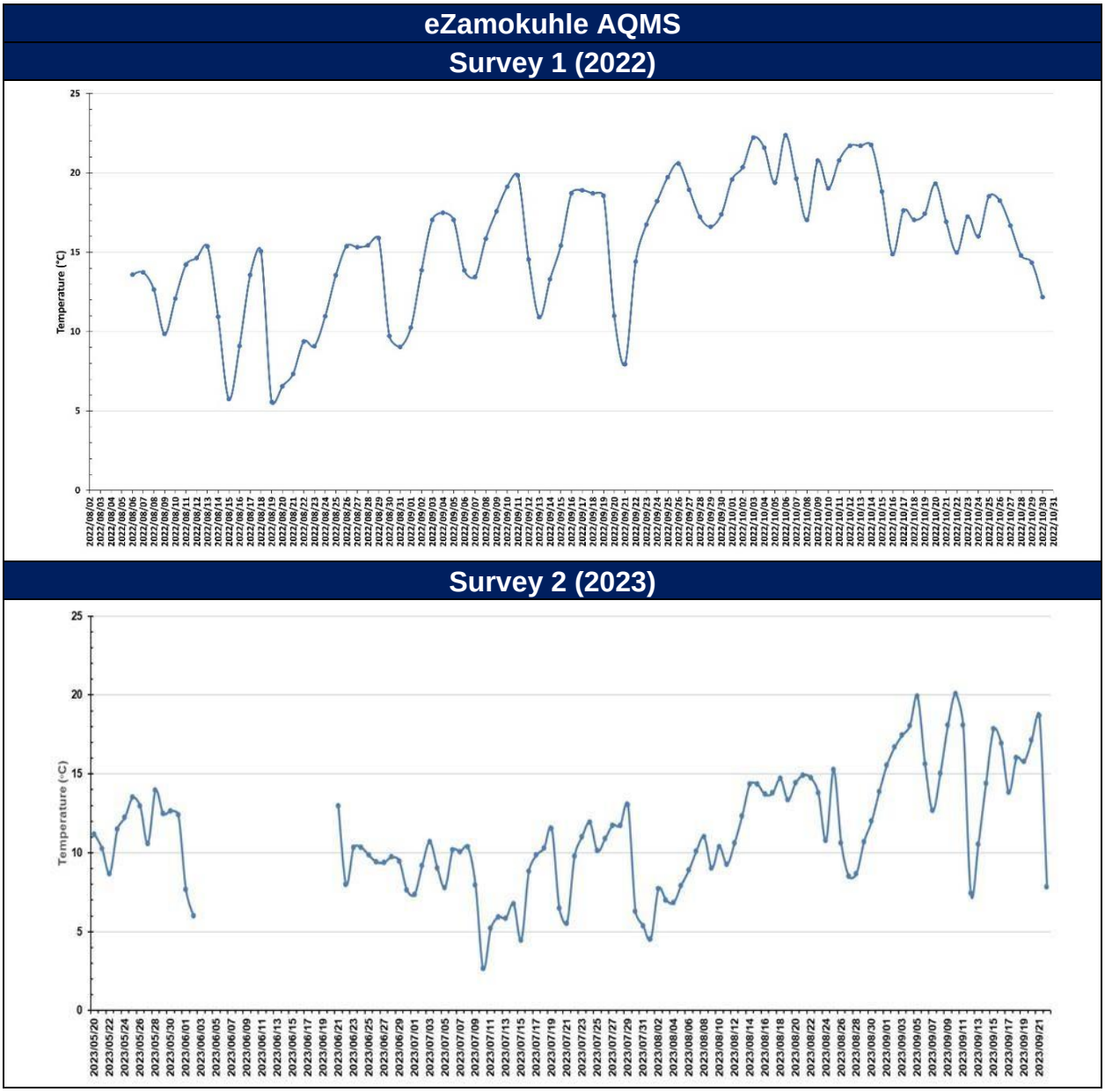

Figure 13A: Daily average temperature at the eZamokuhle AQMS (°C) for the two sampling surveys.

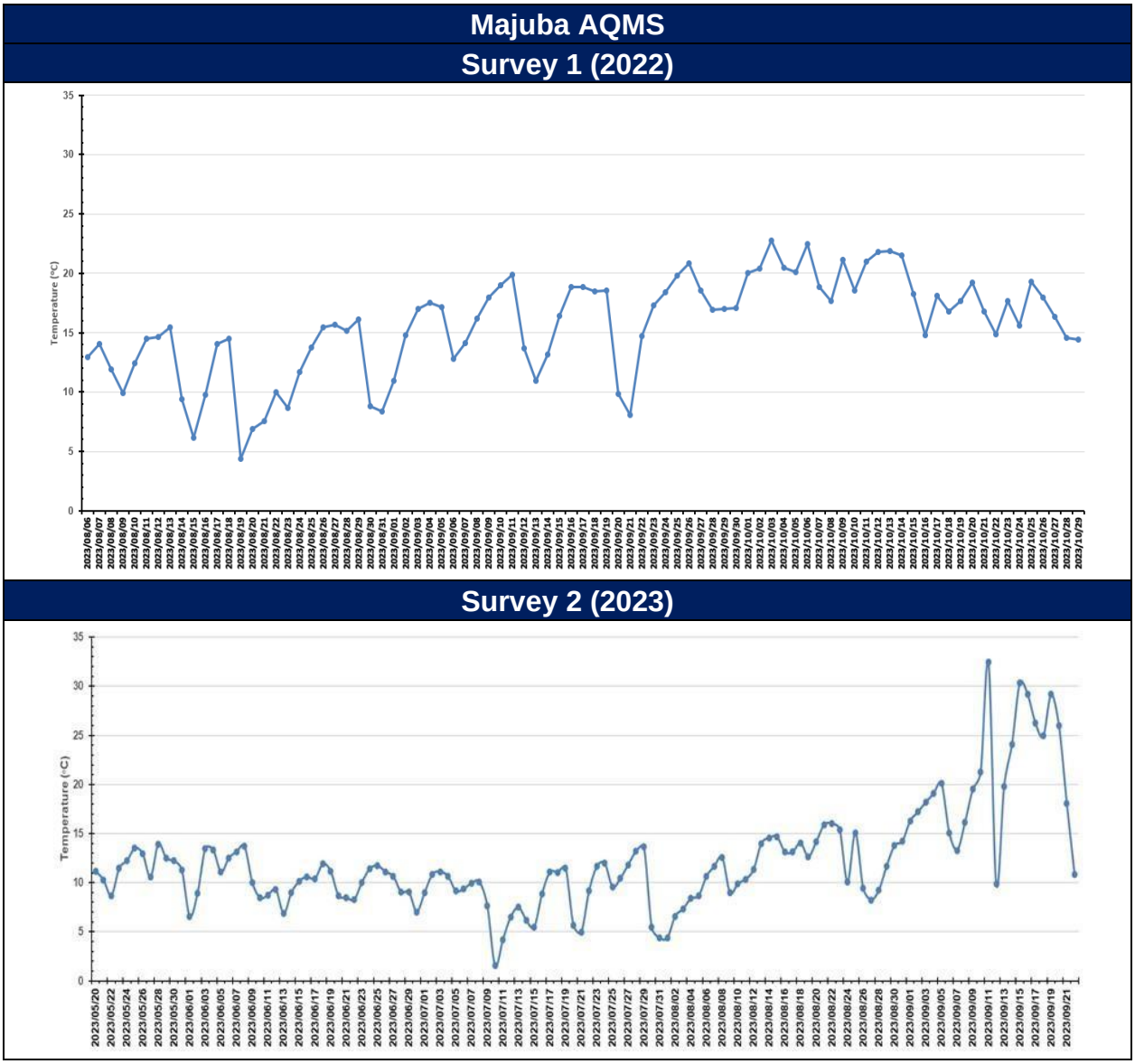

Figure 14B: Daily average temperature at the Majuba AQMS (°C) for the two sampling surveys.

3.1.3 RAINFALL (PRECIPITATION)

Figure 15A and Figure 12B provides daily total rainfall/precipitation recorded for the Eskom eZamokuhle and Eskom Majuba AQMS respectively. From Figure 15A and Figure 12B, it is evident both stations recorded a maximum rainfall of 17mm on 20 August 2022. Frequent rainfall events were recorded for both stations from 18 to 28 October 2022.

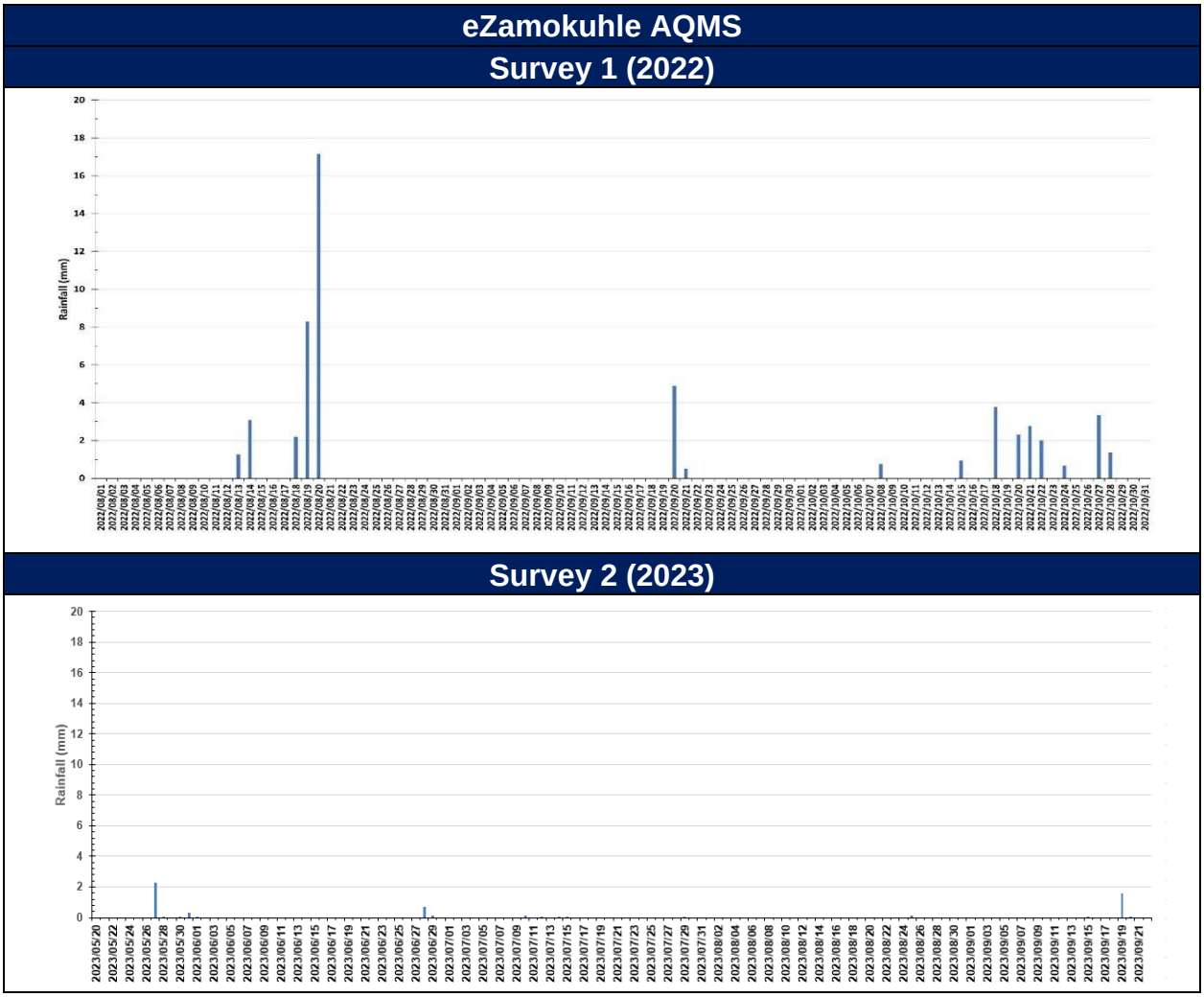

Figure 15A: Daily total precipitation (rainfall) at the eZamokuhle AQMS (mm) for the two sampling surveys.

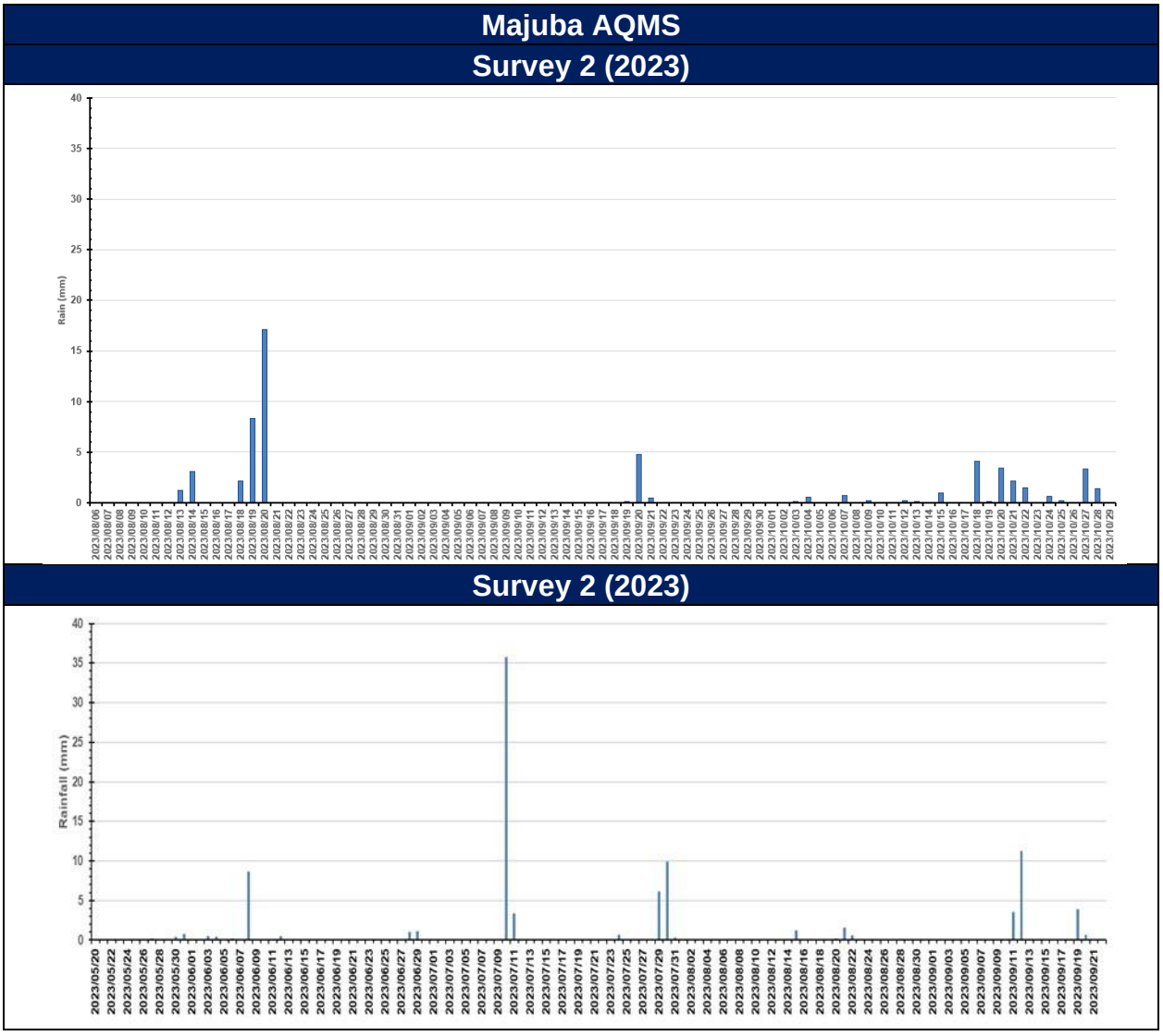

Figure 16B: Daily total precipitation (rainfall) at the Majuba AQMS (mm) for the two sampling surveys.

3.2 POLLUTANT TREND & ANALYSIS

Openair is an air quality model for statistically analysing semi-empirical mathematical relationships between air pollutant concentration and other factors that may affect it (Tiwary, 2010). The Openair model can analyse emissions of pollutant sources, pollutant characteristics, trend estimates and model evaluations. Additionally, Openair model has the advantage of data manipulation or interpolation, statistical data analysis, creation, and visualization of high-quality graphics (Carslaw, 2015).

The Openair model has been successfully applied to determine the potential emission sources based on urban air quality measurements (Munir et al., 2016, Czernecki et al., 2016) as well as for air quality research campaigns (Crilley et al. 2017), studies concerning pollution exposure (Pattinson et al. 2016), and natural events (Salvador et al. 2014; Schweizer, Cisneros 2014). Often multiple functions provided in Openair are combined to provide comprehensive information & insight for the analysed data (Crilley et al., 2015 and Jang et al., 2016).

The relationship and trends of concentrations, including PM_{10}, $PM_{2.5}$, SO_2, NO_2 and meteorological parameters such as wind speed and direction, temperature for the five sampling sites were examined using the Openair model.

3.2.1 PARTICULATE MATTER (PM_{10})

Figure 17 indicate the ambient hourly PM_{10} concentrations recorded at the Eskom eZamokuhle, Eskom Majuba and House 4 sampling sites. Although no NAAQS exists for hourly PM_{10} concentrations, Figure 17 highlight that for both the eZamokuhle and Majuba sites maximum hourly concentrations of 500ug/m^3 were recorded, whilst House 4 indicate maximum concentrations of 400ug/m^3 during the first sampling survey. During the second sampling survey House 4 also recorded hourly concentrations of 500ug/m^3.

Figure 18 is a graphical representation of the average hourly PM_{10} concentrations for the sampling period. It is evident from Figure 18 that the highest average values are recorded during hours 06:00 to 08:00 for both the eZamokuhle and House 4 sites, but all three sites indicate elevated hourly values from 17:00 to 19:00 during the first sampling survey. The same trend continues during the second sampling survey if the winter months are compared. These diurnal profiles are also illustrated in Figure 19. The bi-modal particulate matter peak for both the Eskom eZamokuhle, Majuba and House 4 sites (Figure 4-8) is a typical profile for residential fuel burning. A morning peak occurs at 07:00 whilst the evening peak occurs at 18:00. The morning peaks reduces towards midday as the inversion layer rises & improves the mixing height of the planetary boundary layer. The morning peak is not that prevalent at the Majuba AQMS.

Figure 20 indicate the daily ambient PM_{10} concentrations recorded at the Eskom eZamokuhle, Eskom Majuba and House 4 sampling sites for both sampling surveys. The daily NAAQS for PM_{10} of 75 ug/m^3 is exceeded at all three stations, especially during the colder months of August and September, which indicate higher daily ambient concentrations (Figure 20). This trend is highlighted during the second sampling survey. Daily maximum PM_{10} concentrations of 200 ug/m^3 were recorded for both the Eskom eZamokuhle and Eskom Majuba sampling sites, whilst House 4 recorded maximum concentrations of approximately 120 ug/m^3 during the first sampling survey, however during the second sampling survey both the Eskom eZamokuhle and Eskom Majuba sampling sites recorded lower maximum daily concentrations. Few exceedances were recorded for October. These elevated daily concentrations during the colder months are indicated in the calendar plots (Figure 21). These elevated concentrations could be attributed to colder ambient temperatures leading to an increase in residential fuel burning. Figure 22 highlights the average weekday PM_{10} concentrations. The Eskom eZamokuhle and House 4 sampling sites indicate elevated concentrations on Thursdays, whilst the Eskom Majuba AQMS recorded elevated concentrations for Sundays and

Mondays during the first sampling survey. The first sampling survey also highlights lower concentrations for Tuesdays compared to the other days in the week for all three stations. The second sampling survey highlighted higher daily averages for Tuesday for Eskom eZamokuhle and House 4, whilst higher daily concentrations were recorded for the Eskom Majuba station on Thursdays.

Figure 23 illustrates the monthly mean ambient PM_{10} concentrations recorded at the Eskom eZamokuhle, Eskom Majuba and House 4 sampling sites during the two sampling surveys. Both the Eskom eZamokuhle and Eskom Majuba illustrates a decrease in monthly concentrations from August to October, whilst House 4 indicate an increase from August to September, and a significant decrease to October. It is also evident that the all three stations indicate a major increase from May to August during the second sampling survey.

As mentioned previously, the bi-modal particulate matter peak for both the Eskom eZamokuhle, Majuba and House 4 sites (Figure 19) is a typical profile for residential fuel burning. These peaks are evident in Figure 24A to 20C illustrating the weekly diurnal ambient PM_{10} concentrations. A morning peak occurs at 07:00 whilst the evening peak occurs at 18:00. The morning peaks are less prominent at the Eskom Majuba sampling site.

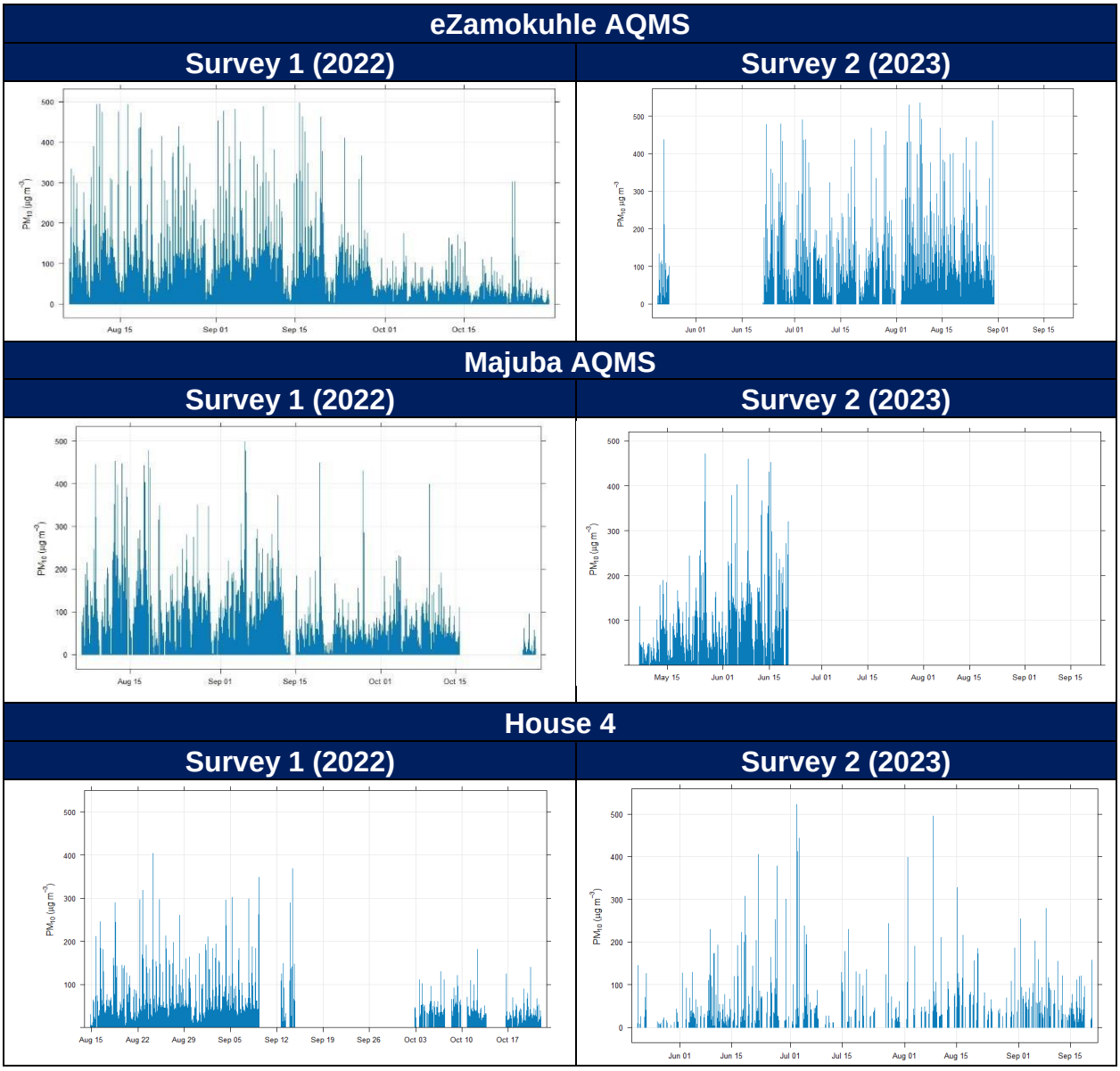

Figure 17: Hourly ambient PM_{10} concentrations ($\mu g/m^3$) measured at the sampling locations during the two sampling surveys.

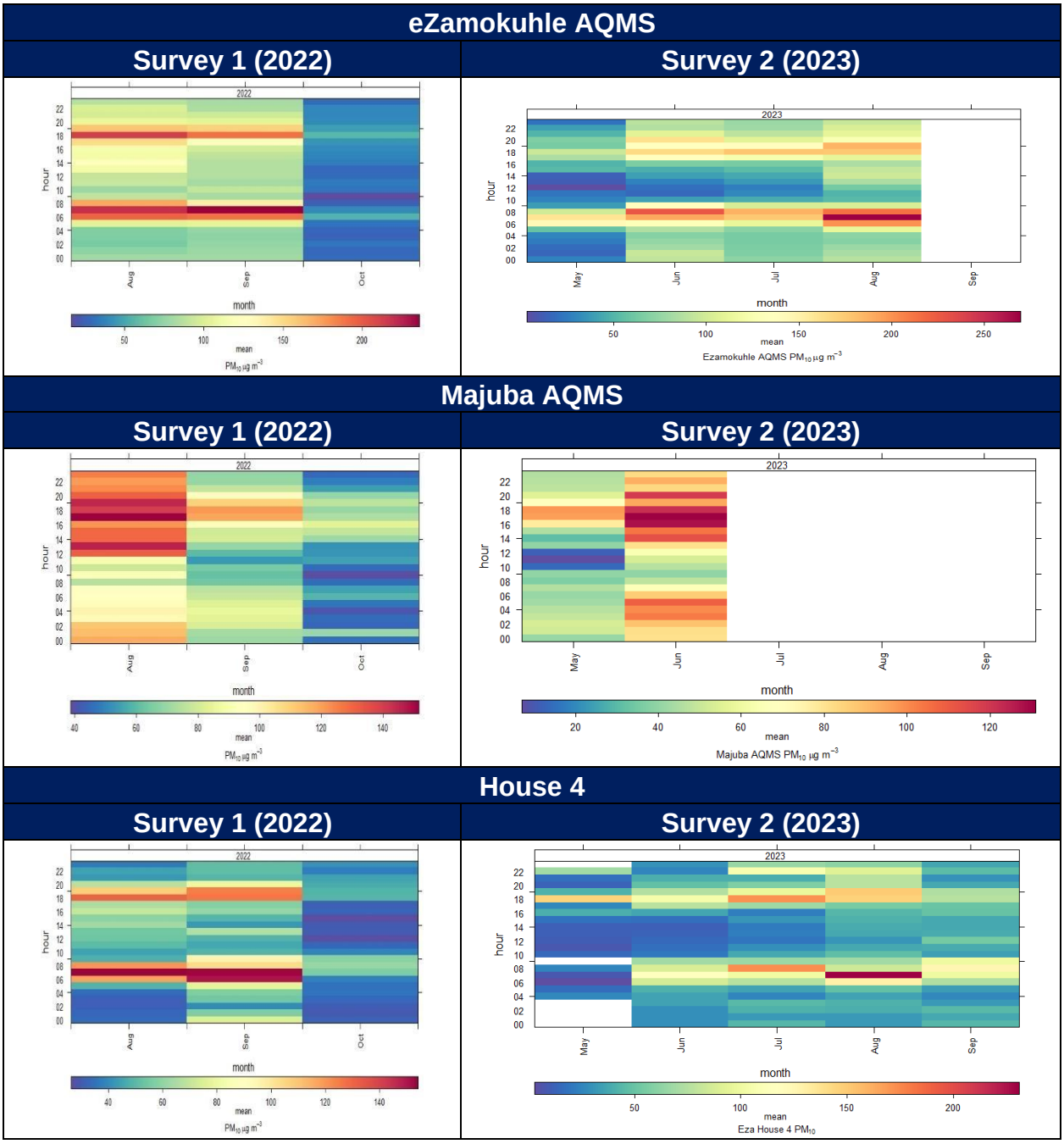

Figure 18: Mean hourly ambient PM_{10} concentrations ($\mu g/m^3$) measured at the sampling locations during the two sampling surveys.

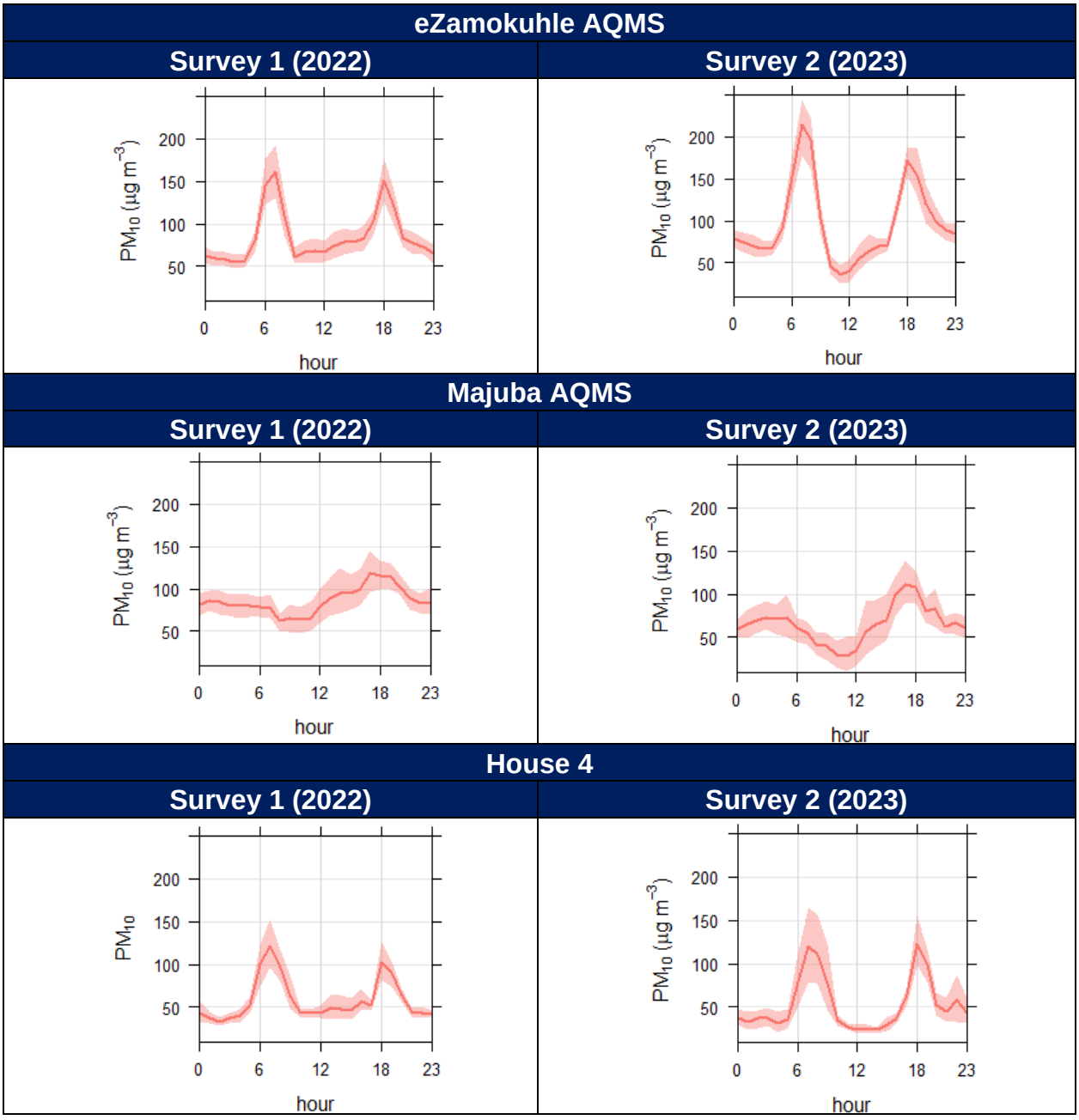

Figure 19: Mean hourly diurnal PM_{10} concentrations ($\mu g/m^3$) measured at the sampling sites during the two sampling surveys.

Figure 20: Daily ambient PM_{10} concentrations ($\mu g/m^3$) measured at the sampling sites during the two sampling surveys.

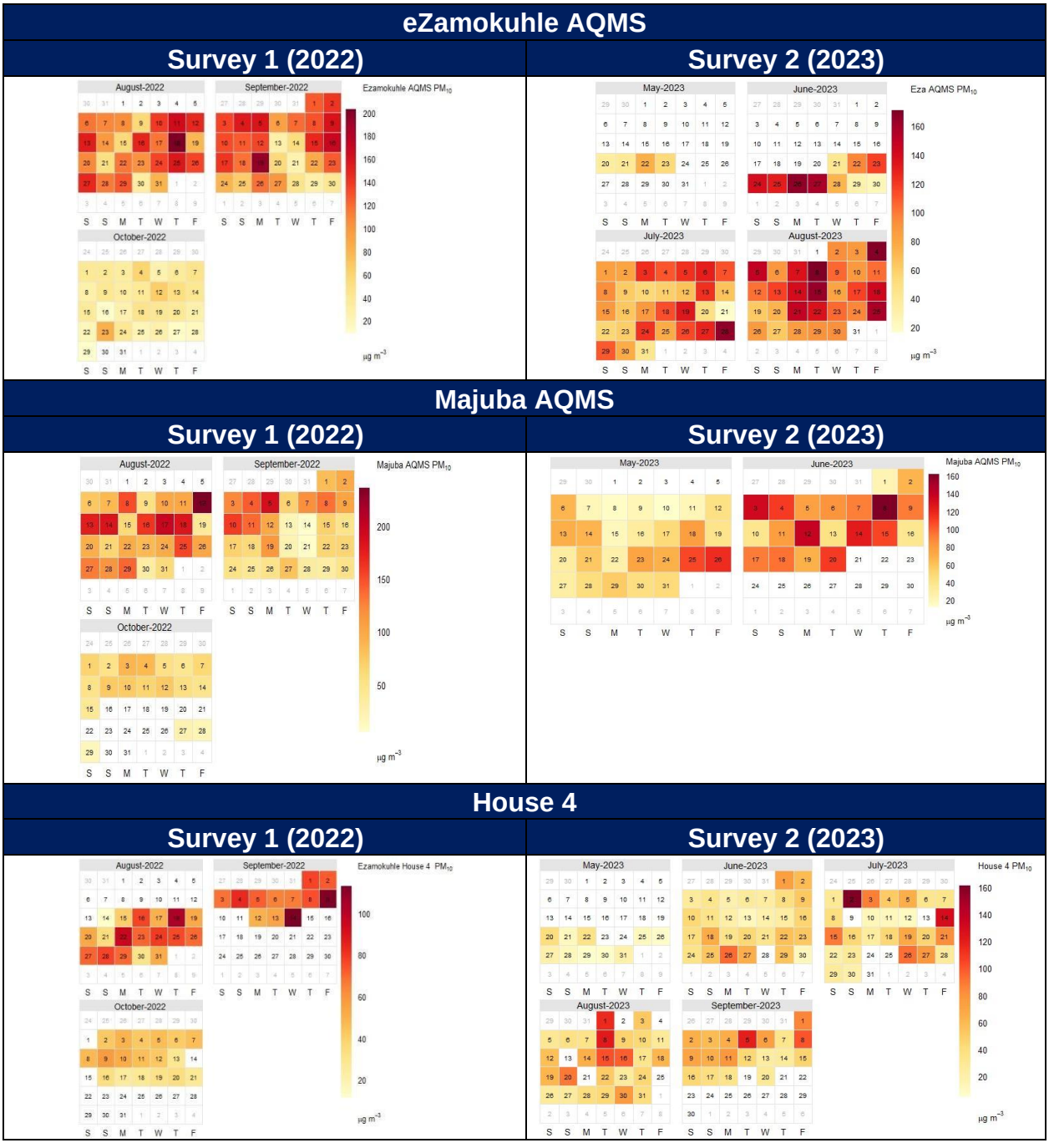

Figure 21: Daily ambient PM_{10} concentrations (µg/m³) measured at the sampling sites during the two sampling surveys.

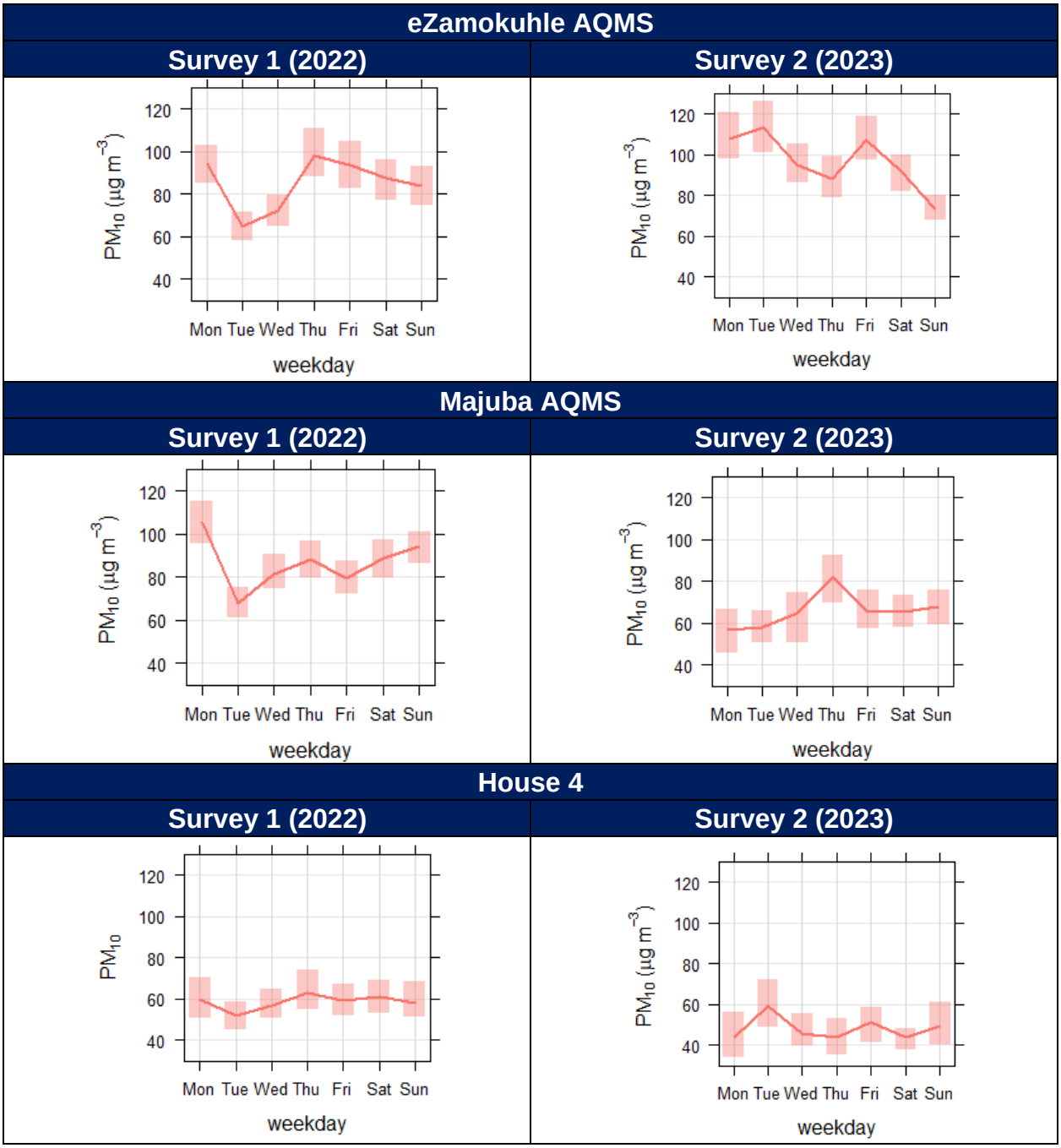

Figure 22: Average weekday ambient PM_{10} concentrations (µg/m³) measured at sampling sites during the two sampling surveys.

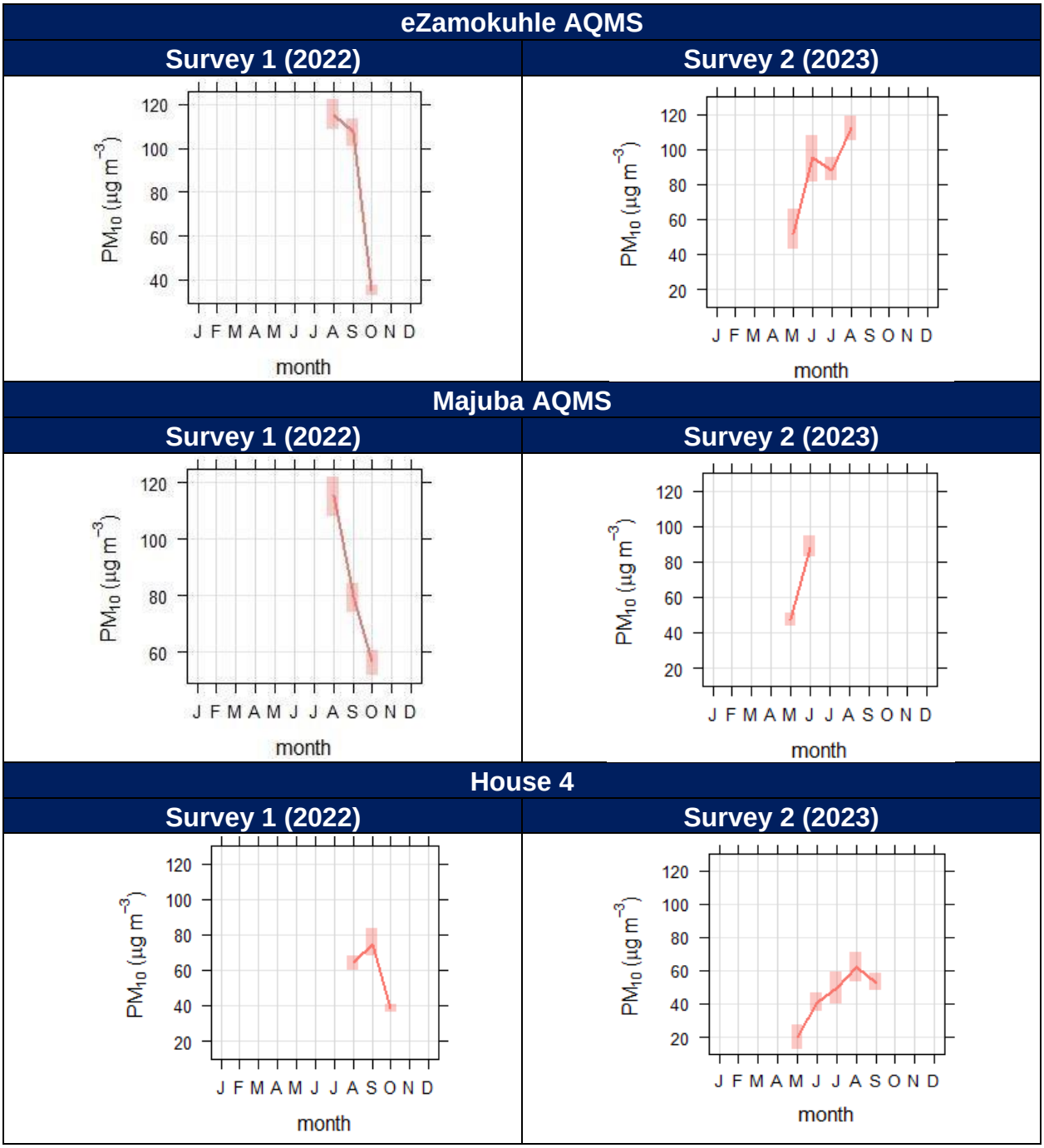

Figure 23: Monthly mean ambient PM_{10} concentrations (µg/m³) measured at sampling sites during the two sampling surveys.

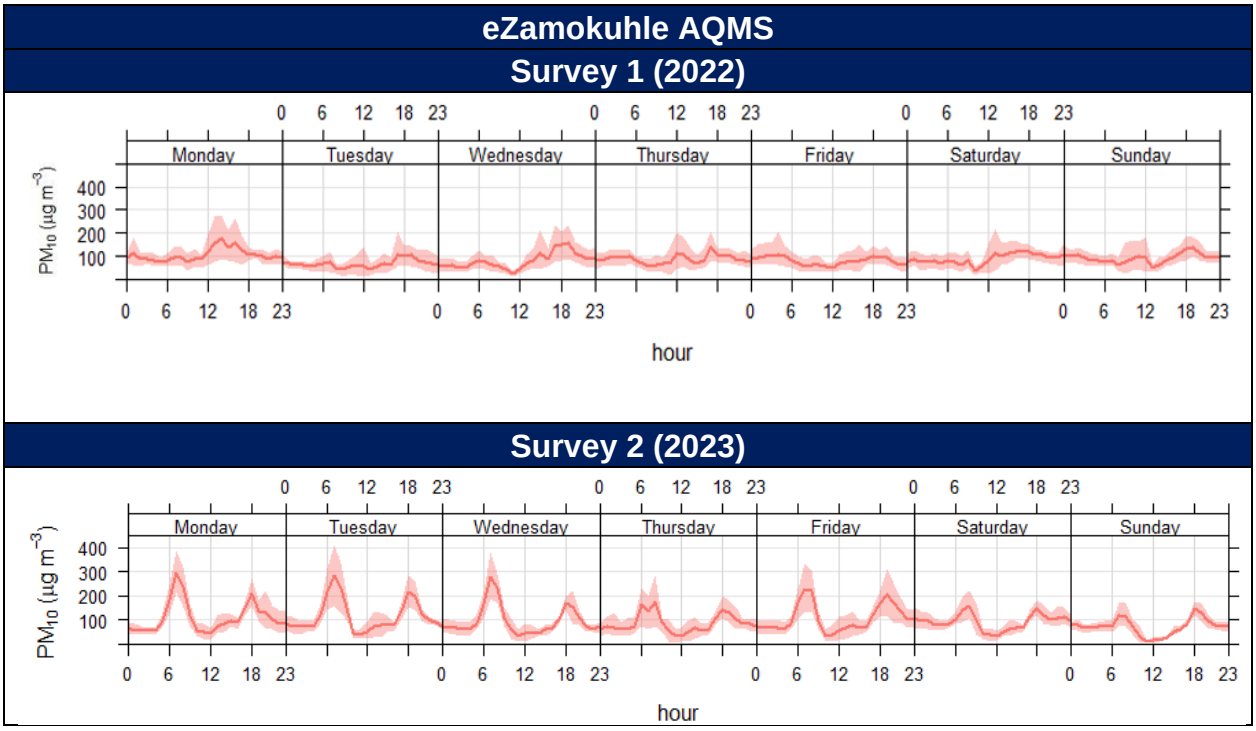

Figure 24A: Weekly diurnal PM_{10} concentrations ($\mu g/m^3$) measured at the eZamokuhle AQMS during the two sampling surveys.

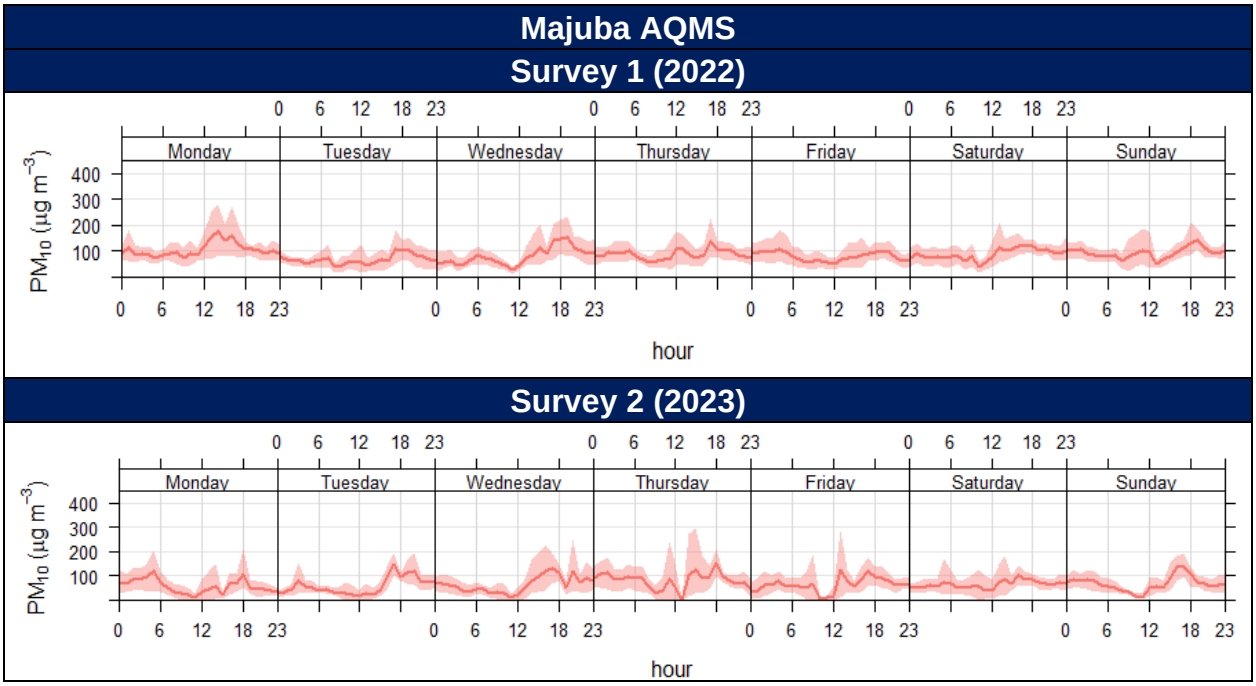

Figure 25B: Weekly diurnal PM_{10} concentrations (µg/m³) measured at the Majuba AQMS during the two sampling surveys.

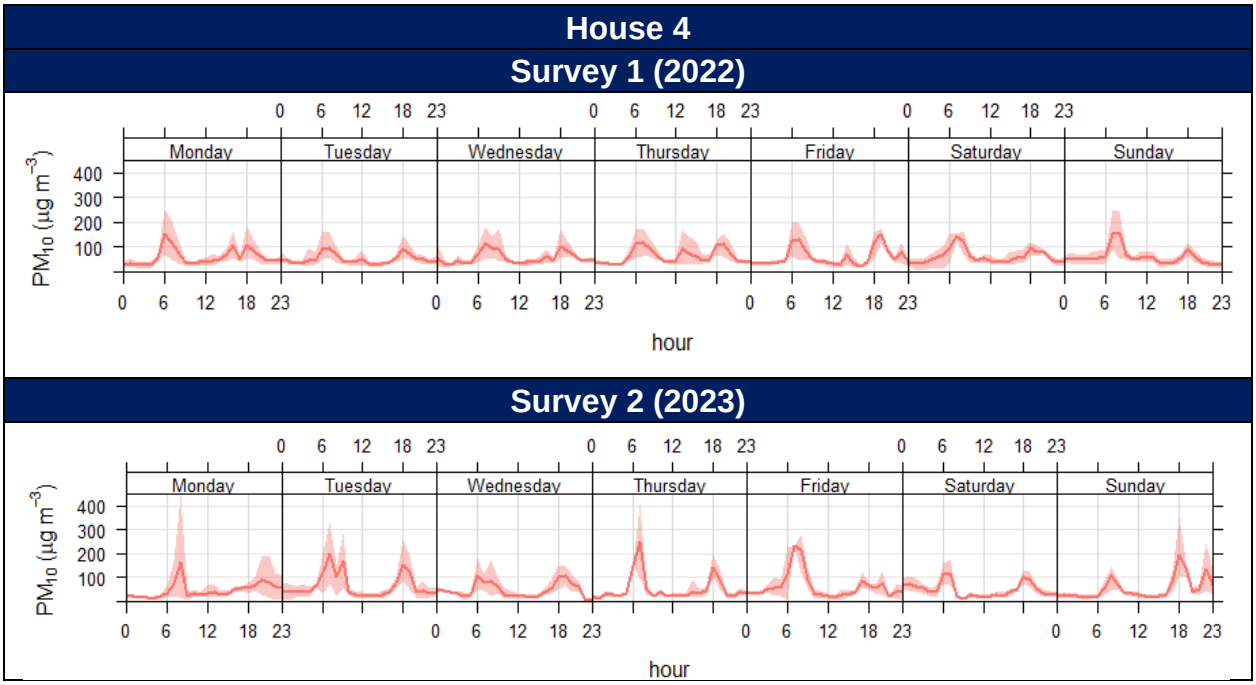

Figure 26C: Weekly diurnal PM_{10} concentrations ($\mu g/m^3$) measured at House 4 during the two sampling surveys.

3.2.2 PARTICULATE MATTER ($PM_{2.5}$)

Figure 27A and Figure 21B indicate the ambient hourly $PM_{2.5}$ concentrations recorded at the Eskom eZamokuhle, Eskom Majuba, House 1, and House 5 sampling sites for both sampling surveys. Although no NAAQS exist for hourly $PM_{2.5}$ concentrations, Figure 27A highlight that for both the eZamokuhle and Majuba sites maximum hourly concentrations of 250 ug/m^3 were recorded, whilst House 1 and House 5 indicate maximum concentrations of 500ug/m^3 (Figure 21B), during the first and second sampling surveys. Figure 29A and 22B are graphical representations of the mean hourly $PM_{2.5}$ concentrations for the first and second sampling surveys. It is evident from Figure 29A and 22B that the highest average values are recorded during hours 06:00 to 08:00 for both the eZamokuhle, House 1 and House 5 sites, but all four sites indicate elevated hourly values from 17:00 to 19:00. These diurnal profiles are also illustrated in Figure 31A and 23B. The bi-modal particulate matter peak for both the Eskom eZamokuhle, Majuba, House 1 and House 5 sites (Figure 31) is a typical profile for residential fuel burning. A morning peak occurs at 07:00 whilst the evening peak occurs at 18:00. The morning peaks reduces towards midday as the inversion layer rises & improves the mixing height of the planetary boundary layer. As with the PM_{10} concentrations, the morning peak is less prevalent at the Eskom Majuba station.

Figure 33A and 24B indicate the daily ambient $PM_{2.5}$ concentrations recorded at the Eskom eZamokuhle, Eskom Majuba, House 1, and House 5 sampling sites respectively. The daily NAAQS for $PM_{2.5}$ of 40 ug/m^3 is exceeded at all four stations, although only once at the Eskom eZamokuhle site during the first sampling survey. The Eskom Majuba, House 1, and House 5 sampling sites recorded multiple exceedances of the daily NAAQS for $PM_{2.5}$ for the first sampling survey. Figure 24B also highlights an increase in daily concentrations for both House 1 and House 5 during the second sampling survey. These elevated daily concentrations are indicated in the calendar plots (Figure 35). These

elevated concentrations could be attributed to colder ambient temperatures leading to an increase in residential fuel burning.

Figure 37A highlights the mean weekday ambient $PM_{2.5}$ concentrations at the Eskom eZamokuhle and Majuba AQMS, whilst Figure 26B is indicative of the House 1 and House 4 sampling sites. Both sampling surveys indicate elevated concentrations on Thursdays, whilst the Eskom Majuba AQMS recorded elevated concentrations for Sundays and Mondays. Survey 2.

Figure 39A and 27B illustrates the mean monthly ambient $PM_{2.5}$ concentrations recorded at the Eskom eZamokuhle, Eskom Majuba, House 1, and House 5 sampling sites. The Eskom Majuba, House 1, and House 5 illustrate a decrease in monthly concentrations from August to October, whilst the Eskom eZamokuhle station indicate an increase from August to September, and a significant decrease to October.

As mentioned previously, the bi-modal particulate matter peak for both the Eskom eZamokuhle, Majuba and House 4 sites (Figure 31) is a typical profile for residential fuel burning. These peaks are evident in Figure 41A to Figure 28D illustrating the weekly diurnal ambient $PM_{2.5}$ concentrations. A morning peak occurs at 07:00 whilst the evening peak occurs at 18:00. These peaks are less prominent at the Eskom Majuba sampling site.

eZamokuhle AQMS	
Survey 1 (2022)	**Survey 2 (2023)**
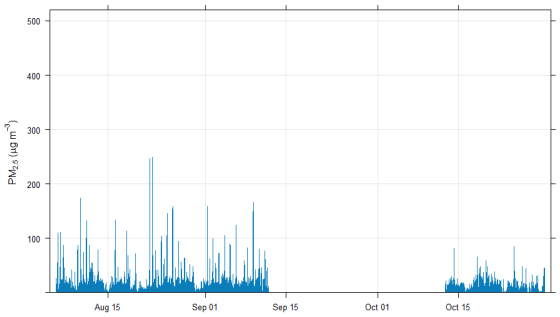	No data available.
Majuba AQMS	
Survey 1 (2022)	**Survey 2 (2023)**
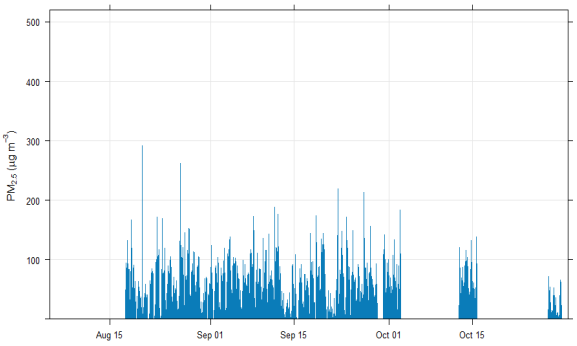	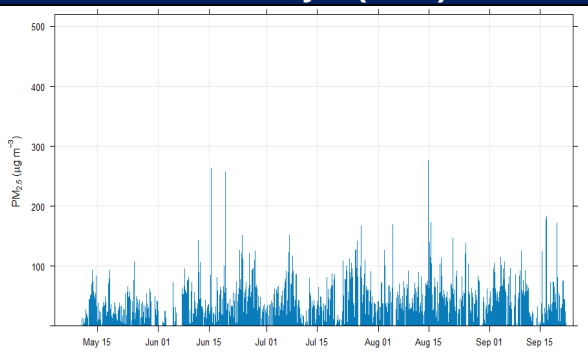

Figure 27A: Hourly ambient $PM_{2.5}$ concentrations ($\mu g/m^3$) measured at the eZamokuhle and Majuba AQMS during the two sampling surveys.

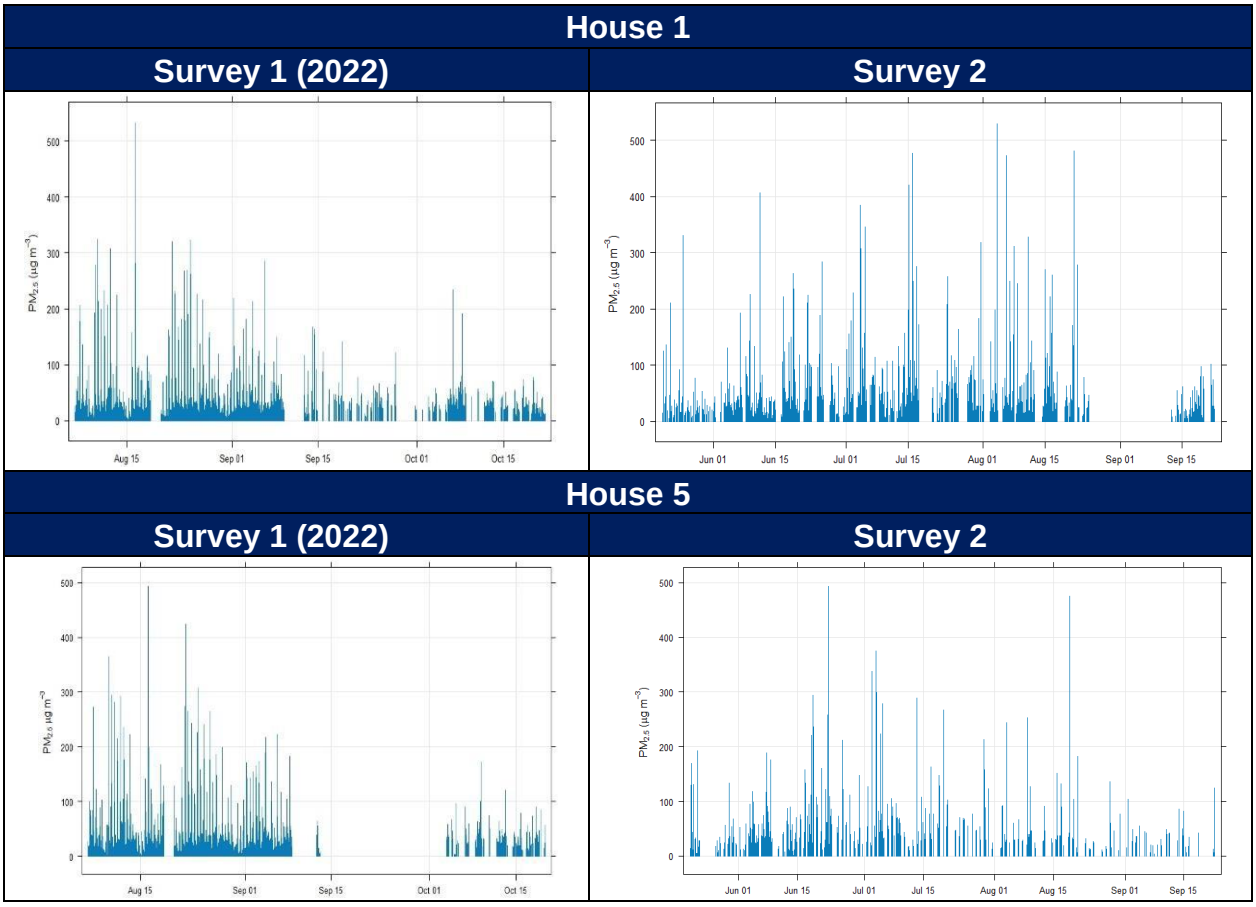

Figure 28B: Hourly ambient $PM_{2.5}$ concentrations (µg/m³) measured at House 1 and House 5 during the two sampling surveys.

eZamokuhle AQMS	
Survey 1 (2022)	**Survey 2 (2023)**
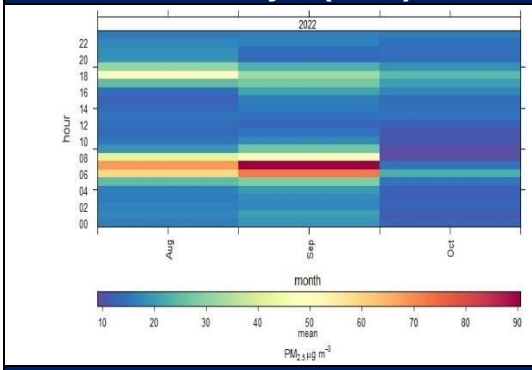	No data available.
Majuba AQMS	
Survey 1 (2022)	**Survey 2 (2023)**
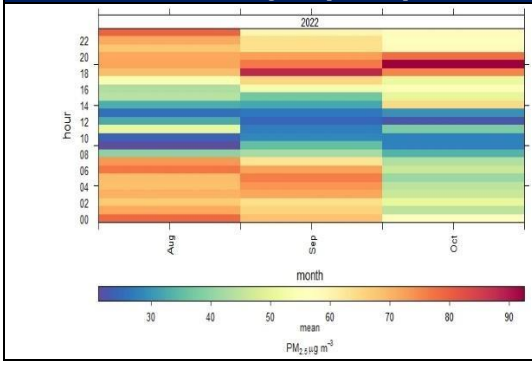	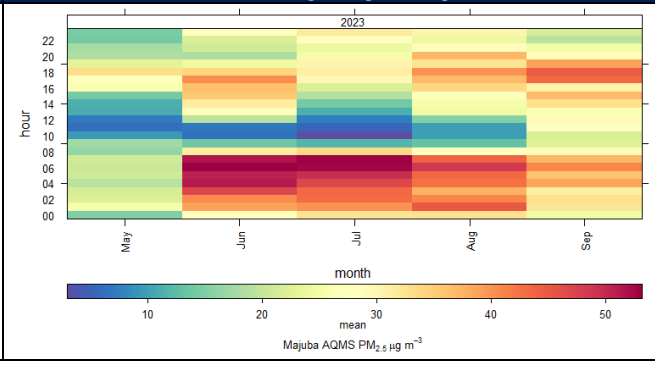

Figure 29A: Mean hourly ambient $PM_{2.5}$ concentrations ($\mu g/m^3$) measured at the eZamokuhle and Majuba AQMS during the two sampling surveys.

Figure 30B: Mean hourly ambient $PM_{2.5}$ concentrations ($\mu g/m^3$) measured at House 1 and House 5 during the sampling survey.

eZamokuhle AQMS	
Survey 1 (2022)	**Survey 2 (2023)**
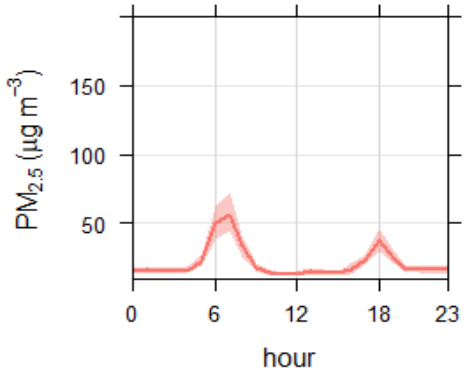	No data available.
Majuba AQMS	
Survey 1 (2022)	**Survey 2 (2023)**
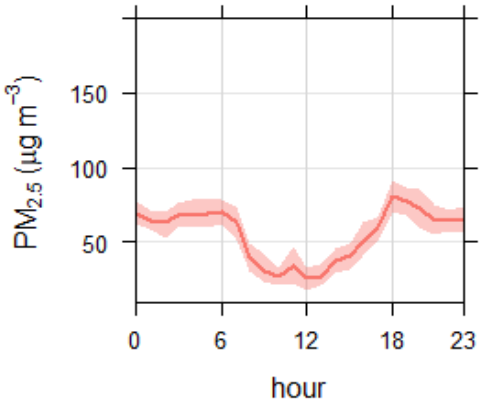	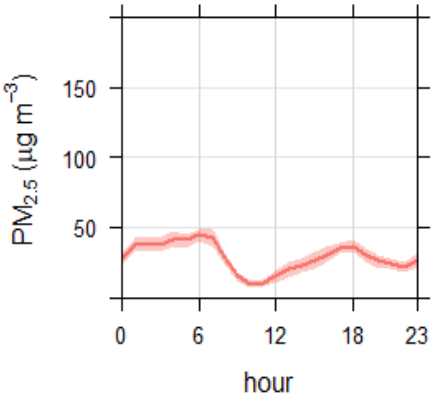

Figure 31A: Hourly diurnal $PM_{2.5}$ concentrations (µg/m³) measured at the eZamokuhle and Majuba AQMS during the two sampling surveys.

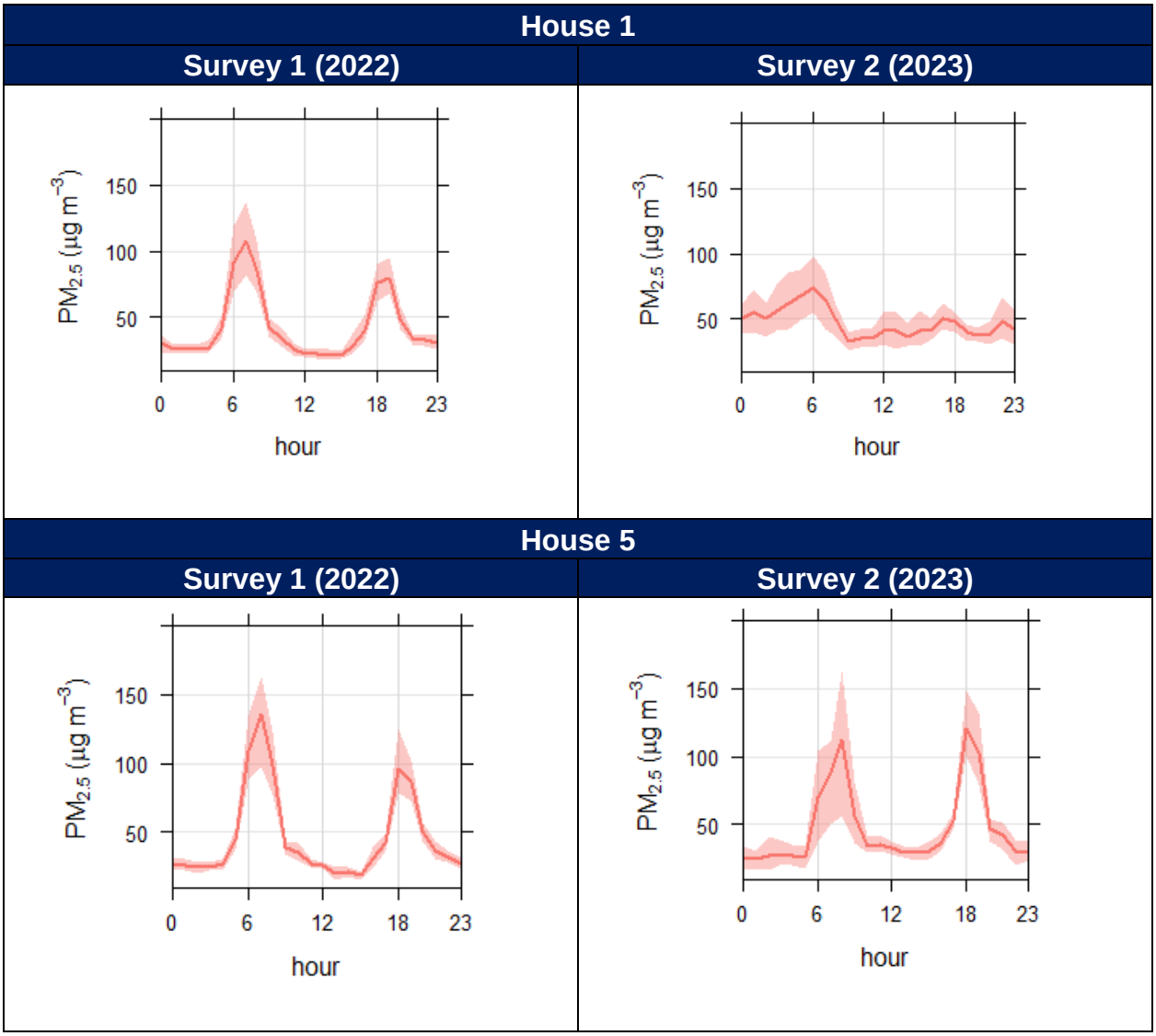

Figure 32B: Hourly diurnal $PM_{2.5}$ concentrations ($\mu g/m^3$) measured at House 1 and House 5 during the two sampling surveys.

eZamokuhle AQMS	
Survey 1 (2022)	**Survey 2 (2023)**
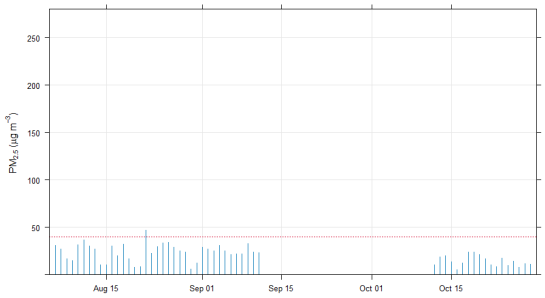	No data available.
Majuba AQMS	
Survey 1 (2022)	**Survey 2 (2023)**
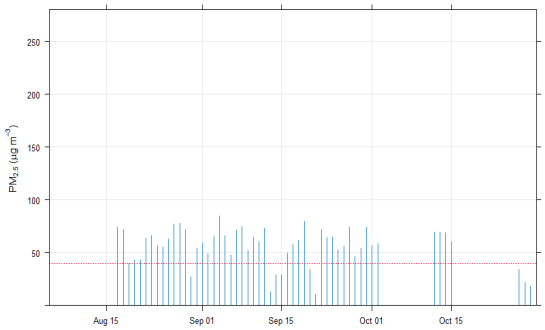	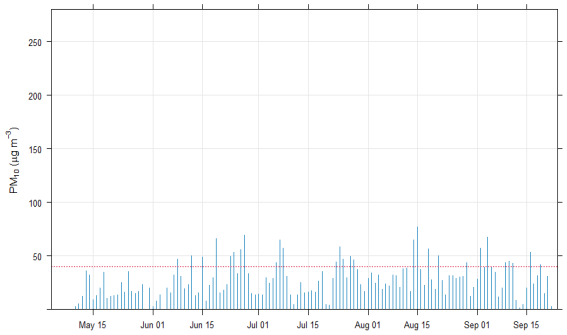

Figure 33A: Daily ambient $PM_{2.5}$ concentrations ($\mu g/m^3$) measured at the eZamokuhle and Majuba AQMS during the two sampling surveys.

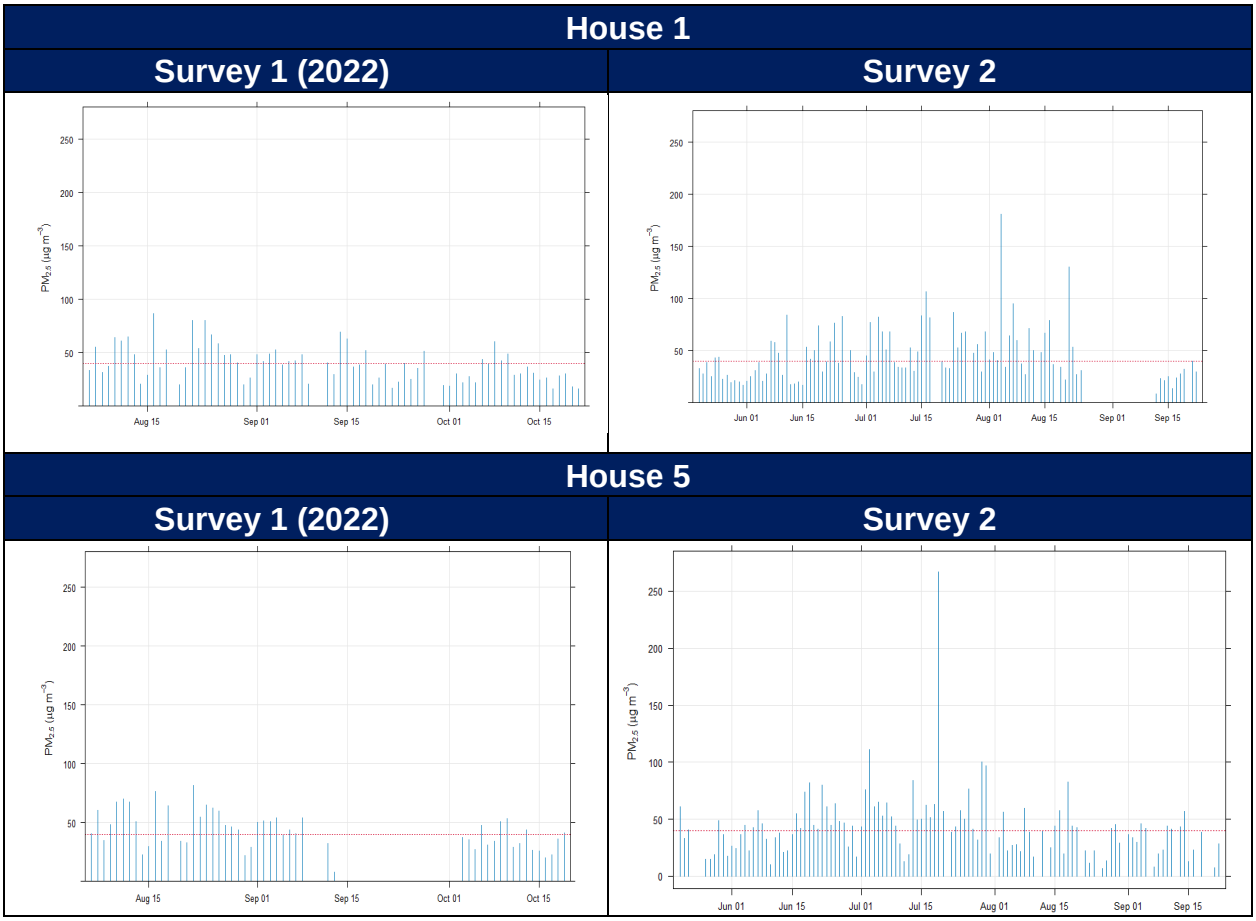

Figure 34B: Daily ambient $PM_{2.5}$ concentrations (µg/m³) measured at House 1 and House 5 during the two sampling surveys.

<table>
<tr><th colspan="2">eZamokuhle AQMS</th></tr>
<tr><th>Survey 1 (2022)</th><th>Survey 2 (2023)</th></tr>
<tr><td> 
</td><td>No data available.</td></tr>
<tr><th colspan="2">Majuba AQMS</th></tr>
<tr><th>Survey 1 (2022)</th><th>Survey 2 (2023)</th></tr>
<tr><td> 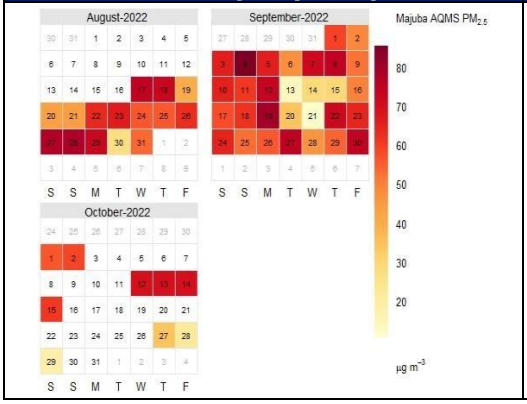
</td><td> 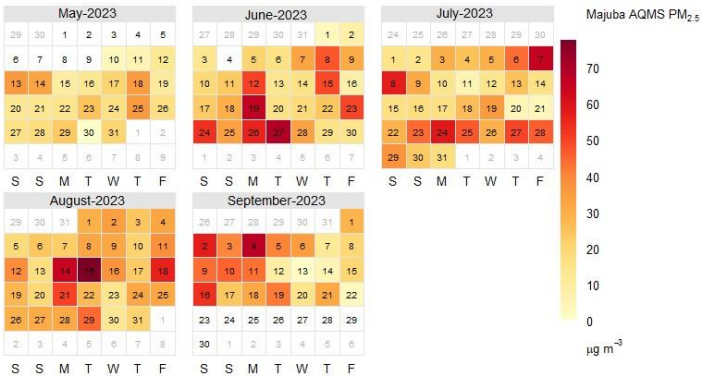
</td></tr>
</table>

Figure 35A: Daily ambient $PM_{2.5}$ concentrations ($\mu g/m^3$) measured at the eZamokuhle and Majuba AQMS during the two sampling surveys.

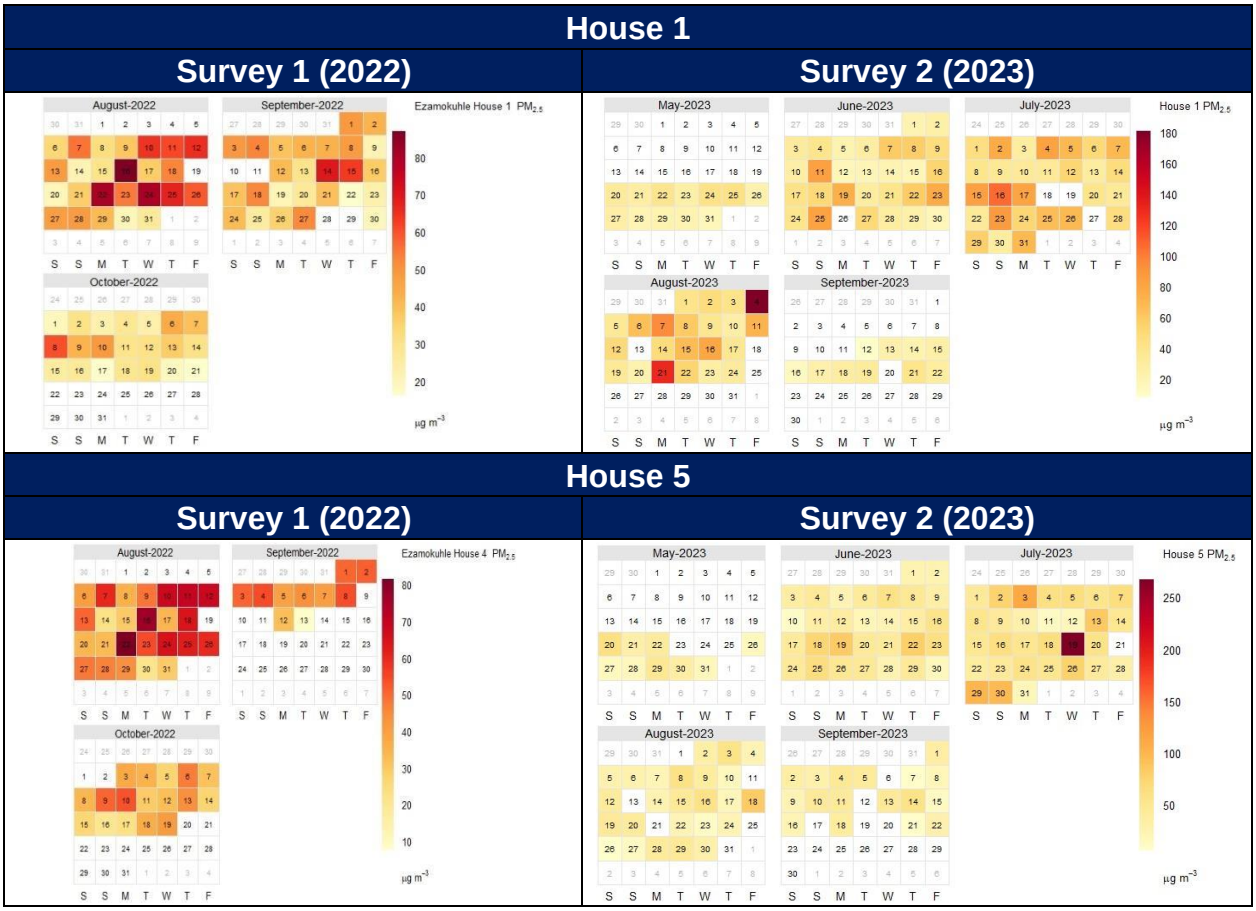

Figure 36B: Daily ambient $PM_{2.5}$ concentrations ($\mu g/m^3$) measured at House 1 and House 5 during the two sampling surveys.

eZamokuhle AQMS	
Survey 1 (2022)	**Survey 2 (2023)**
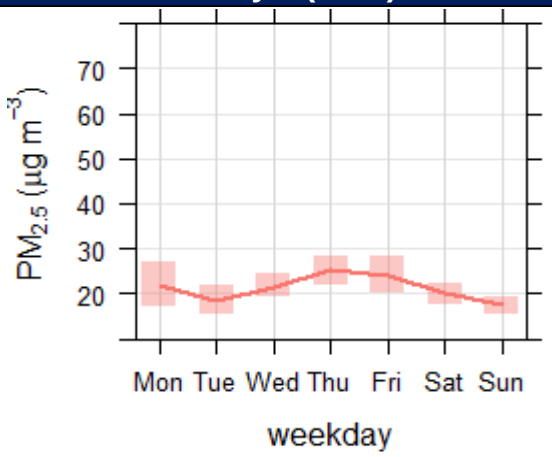	No data available.
Majuba AQMS	
Survey 1 (2022)	**Survey 2 (2023)**
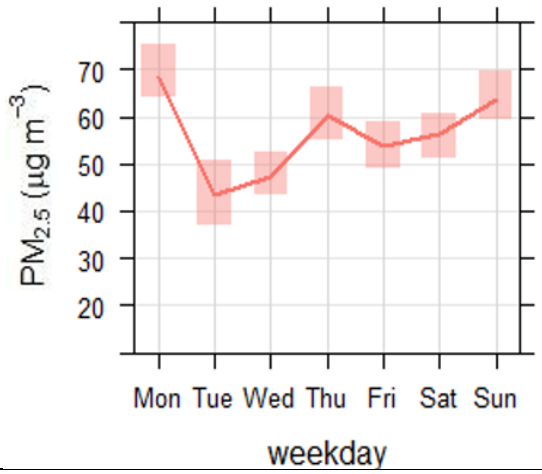	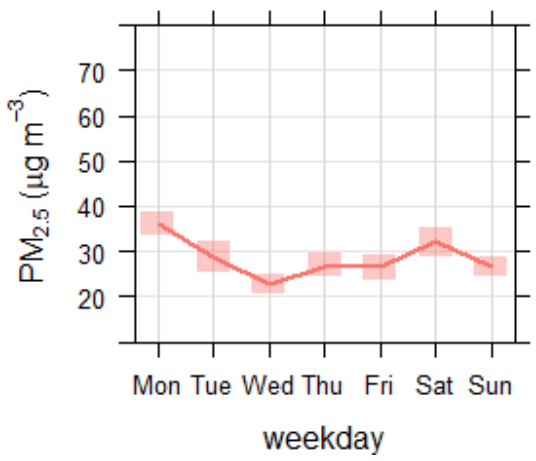

Figure 37A: Weekday ambient $PM_{2.5}$ concentrations (µg/m³) measured at the eZamokuhle and Majuba AQMS during the two sampling surveys.

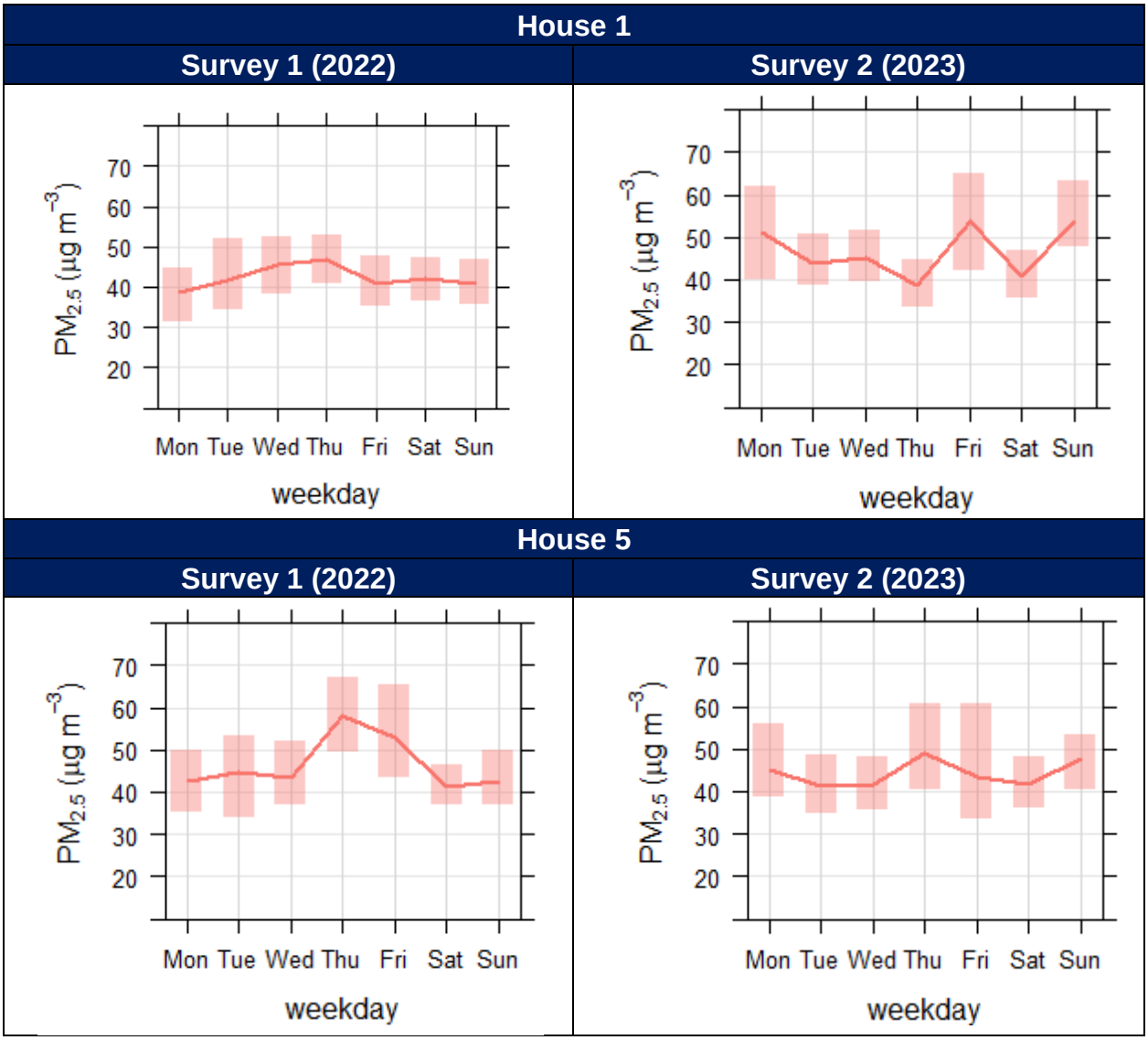

Figure 38B: Weekday ambient $PM_{2.5}$ concentrations (µg/m³) measured at House 1 and House 5 during the two sampling surveys.

eZamokuhle AQMS	
Survey 1 (2022)	**Survey 2 (2023)**
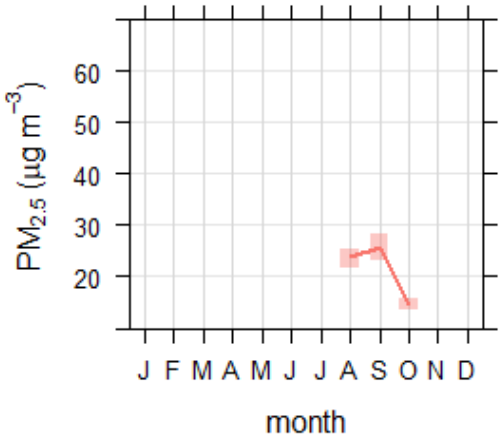	No data available.
Majuba AQMS	
Survey 1 (2022)	**Survey 2 (2023)**
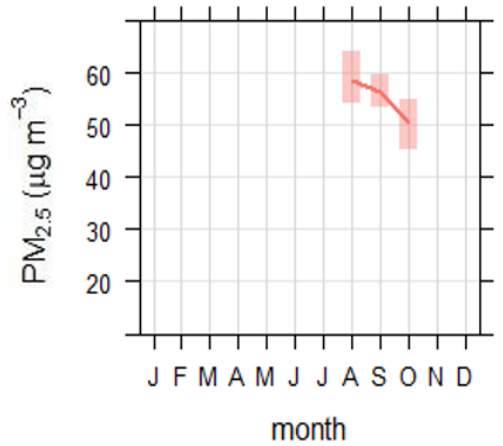	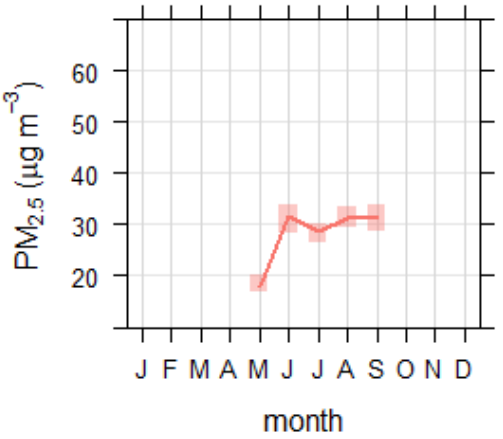

Figure 39A: Mean monthly ambient $PM_{2.5}$ concentrations (µg/m^3) measured at the eZamokuhle and Majuba AQMS during the two sampling surveys.

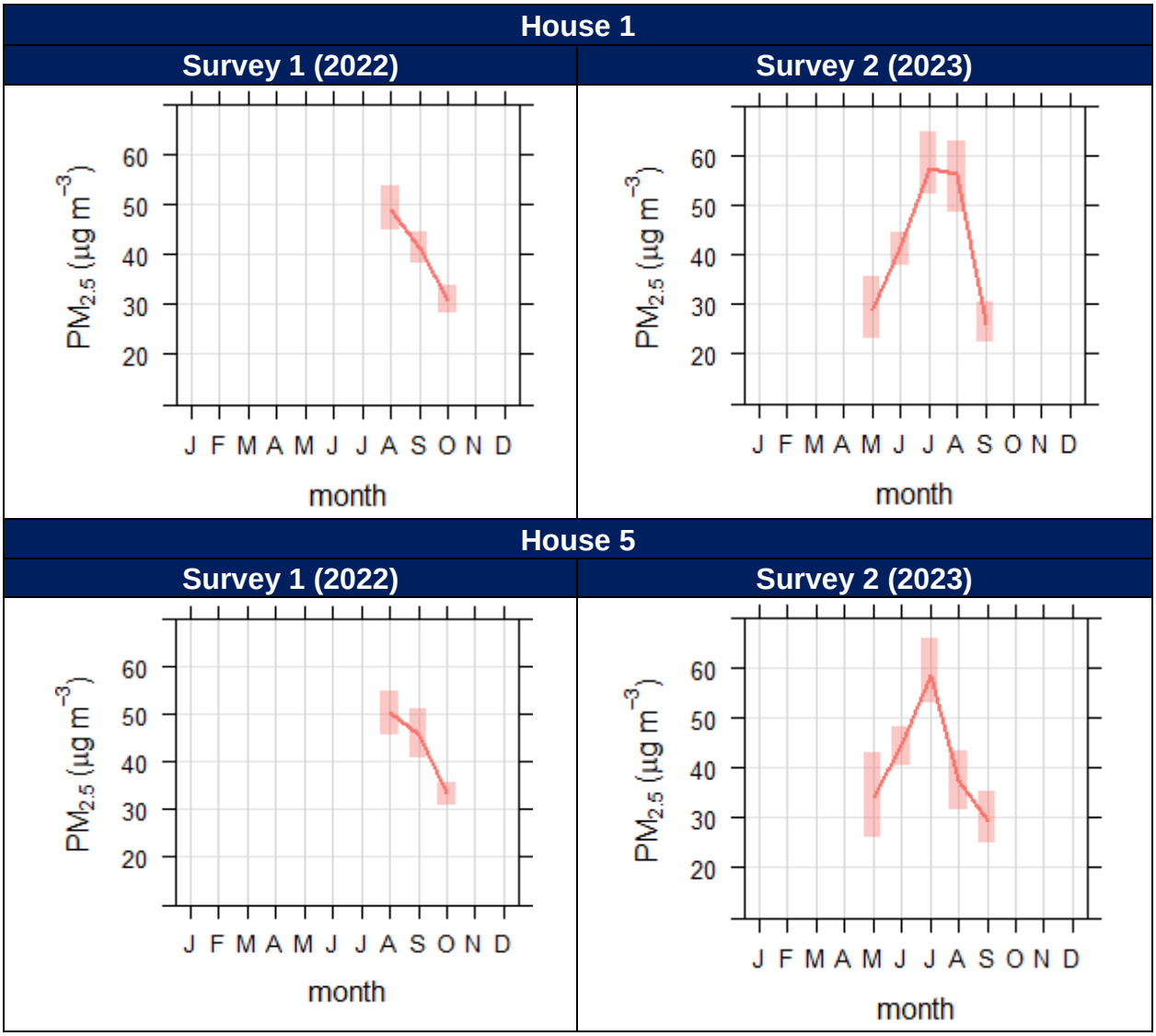

Figure 40B: Mean monthly ambient $PM_{2.5}$ concentrations ($\mu g/m^3$) measured at House 1 and House 5 during the two sampling surveys.

eZamokuhle AQMS

Survey 1 (2022)

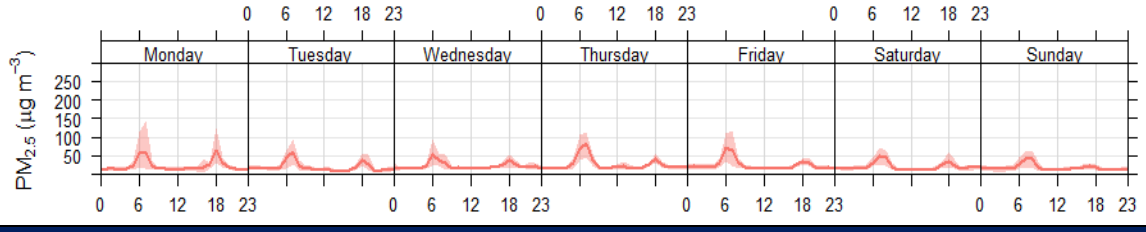

Survey 2 (2023)

No data available.

Figure 41A: Weekly diurnal $PM_{2.5}$ concentrations (µg/m³) measured at the eZamokuhle AQMS during the two sampling surveys.

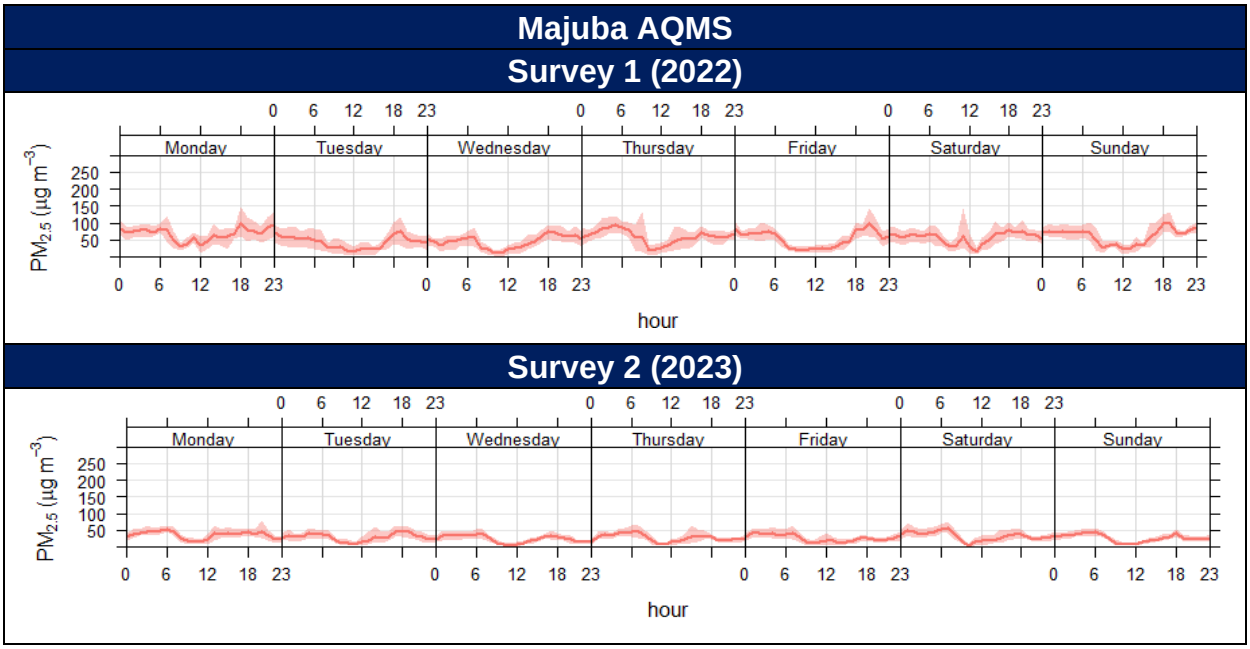

Figure 42B: Weekly diurnal $PM_{2.5}$ concentrations ($\mu g/m^3$) measured at the Majuba AQMS during the two sampling surveys.

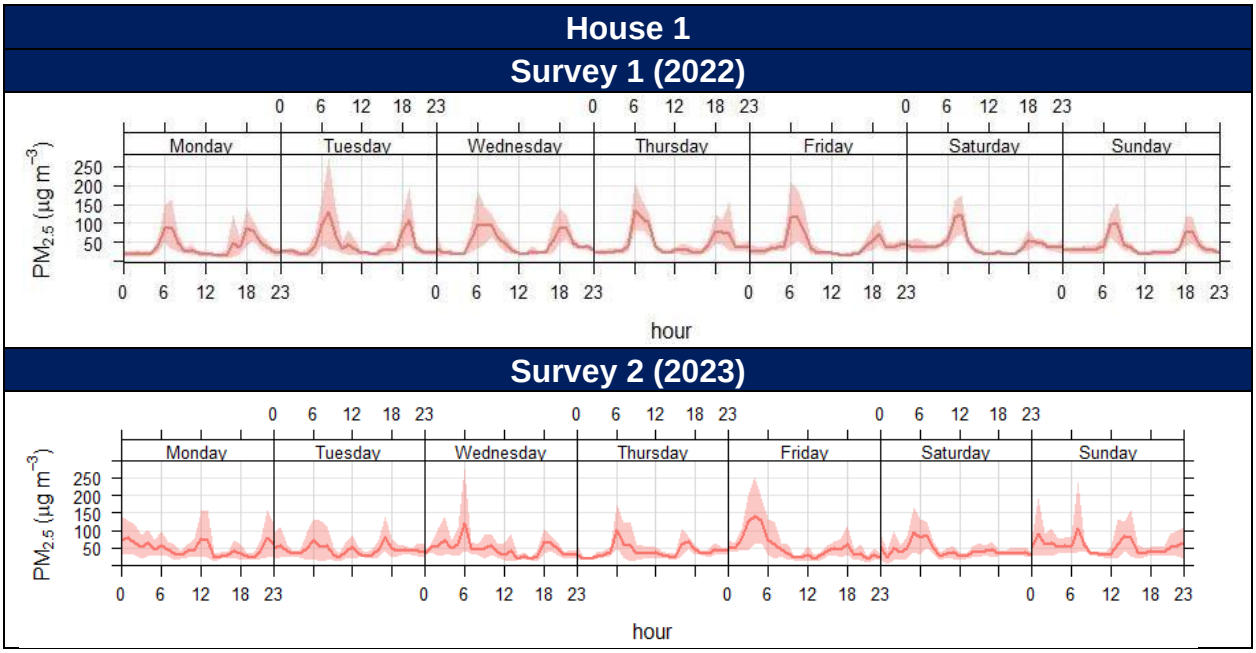

Figure 43C: Weekly diurnal $PM_{2.5}$ concentrations (µg/m³) measured at House 1 during the two sampling surveys.

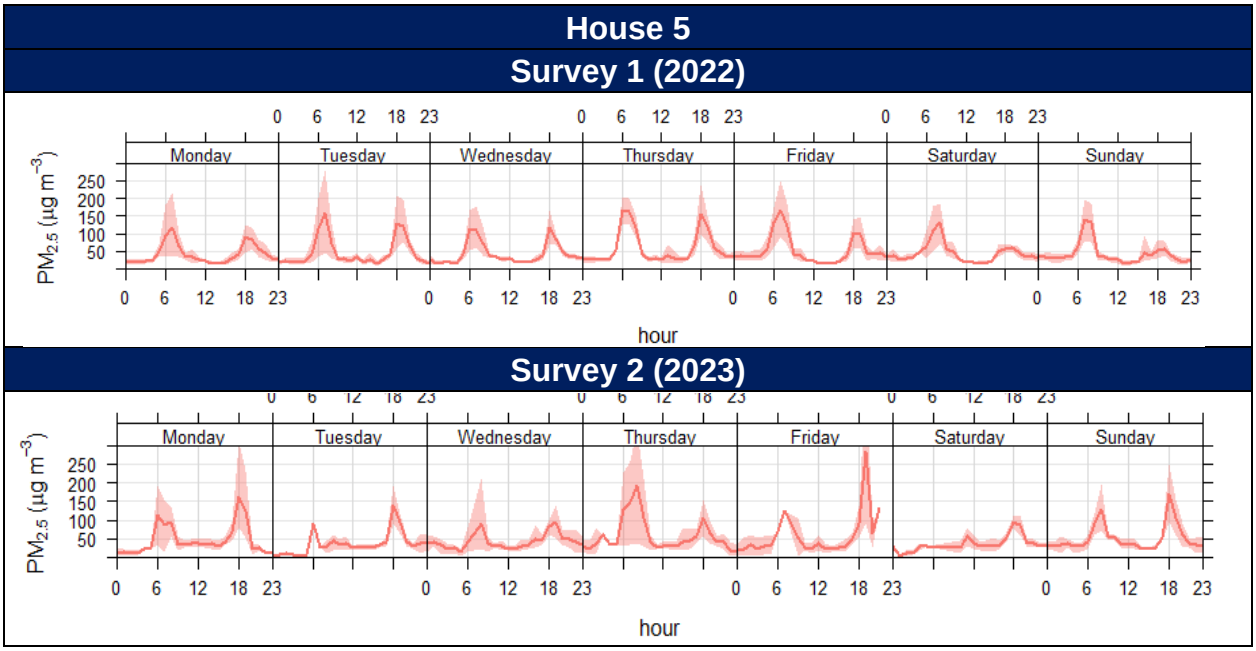

Figure 44D: Weekly diurnal $PM_{2.5}$ concentrations (µg/m³) measured at House 5 during the two sampling surveys.

3.2.3 SULPHUR DIOXIDE (SO_2)

Figure 45A and 29B indicate the hourly ambient SO_2 concentrations recorded at the Eskom eZamokuhle and Eskom Majuba AQMS. The NAAQS for hourly SO_2 concentrations is 134ppb. No exceedances of the hourly NAAQS were recorded for an hourly time average for both stations. Figure 45A highlight maximum hourly SO_2 concentrations of 80ppb at the Eskom eZamokuhle station, whilst maximum concentrations of above 200ppb were recorded for the Eskom Majuba AQMS (Figure 29B).

Figure 47A and 30B are graphical representations of the mean hourly SO_2 concentrations for the sampling period. It is evident from Figure 30A that the highest mean concentrations were recorded during hours 10:00 to 14:00 and 18:00 for the Eskom eZamokuhle station. The 18:00 peak is less prevalent at the Eskom Majuba station (Figure 30B), indicating the highest concentrations recorded during hours 13:00 to 14:00. These diurnal profiles are also illustrated in Figure 49A and 31B. Figure 49B (Eskom Majuba AQMS) indicates a typically industrial signature with increased SO_2 concentrations as just before midday due to the break-up of an elevated inversion layer, in addition to the development of daytime convective conditions causing the plume to be brought down to ground level relatively close to the point of release from tall stacks. The 18:00 peak recorded for the Eskom eZamokuhle station is indicative of the impact of residential fuel burning emissions.

Figure 51A and 32B indicate the daily ambient SO_2 concentrations recorded at the Eskom eZamokuhle and Eskom Majuba AQMS. No exceedances of the daily NAAQS for SO_2 were recorded for both stations during the sampling period. Daily maximum SO_2 concentrations of above 20ppb were recorded for both stations. Figure 51 also indicate lower daily SO_2 concentrations during October for the Eskom eZamokuhle station compared to the Eskom Majuba station. These lower daily concentration in October could

be related to lower domestic fuel burning practices that have a direct impact on the Eskom eZamokuhle station. These daily concentrations are indicated in calendar plots (Figure 53A and 33B). Both stations indicate lower concentrations for October, compared to August and September, and could be attributed to colder ambient temperatures leading to an increase in residential fuel burning.

Figure 55A and 34B highlights the mean weekday and mean monthly ambient SO_2. The Eskom eZamokuhle station as well as the Eskom Majuba station indicate higher recorded ambient concentrations on a Thursday for survey 1, whilst survey 2 highlighted high concentrations on a Tuesday and Friday. Both stations also illustrate a decrease in monthly concentrations from August to September, but a slight elevation in October were recorded for the Eskom Majuba station.

Figure 57A to Figure 35D is indicative of the mean weekly SO_2 concentrations. It is evident for the Eskom eZamokuhle station (Figure 28A) a second less pronounced peak compared to midday, that occurs consistently throughout the entire week at 18:00. A comparison of the trend level plot for eZamokuhle (Figure 47A) clearly indicates that the 18:00 peak occurs in winter (August) thus indicating the impact of residential fuel burning emissions. The evening (18:00) peak is less prominent at the Eskom Majuba sampling site.

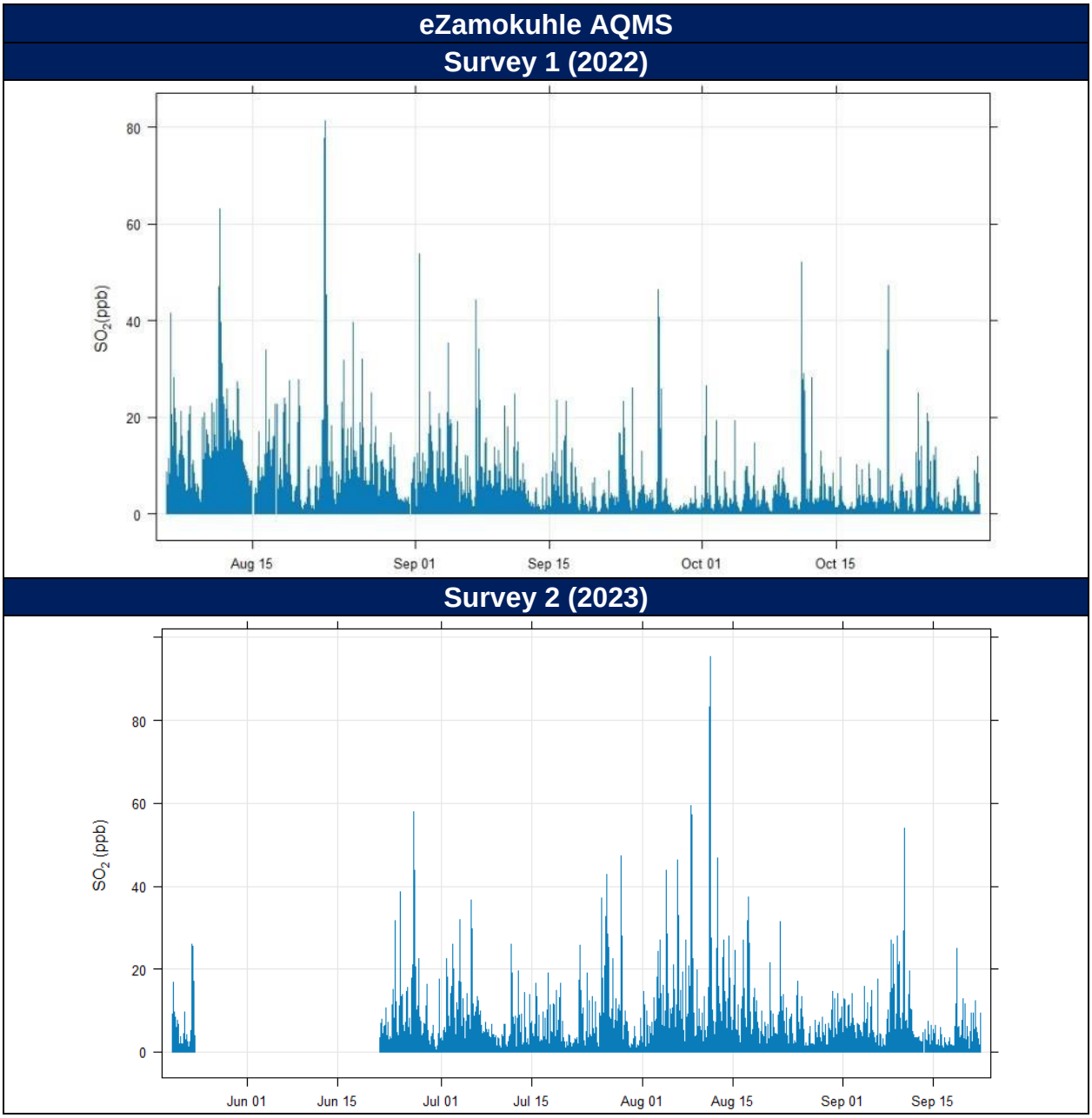

Figure 45A: Hourly ambient SO_2 concentrations (ppb) measured at the Eskom eZamokuhle AQMS during the two sampling surveys (Hourly SO_2 NAAQS = 134ppb).

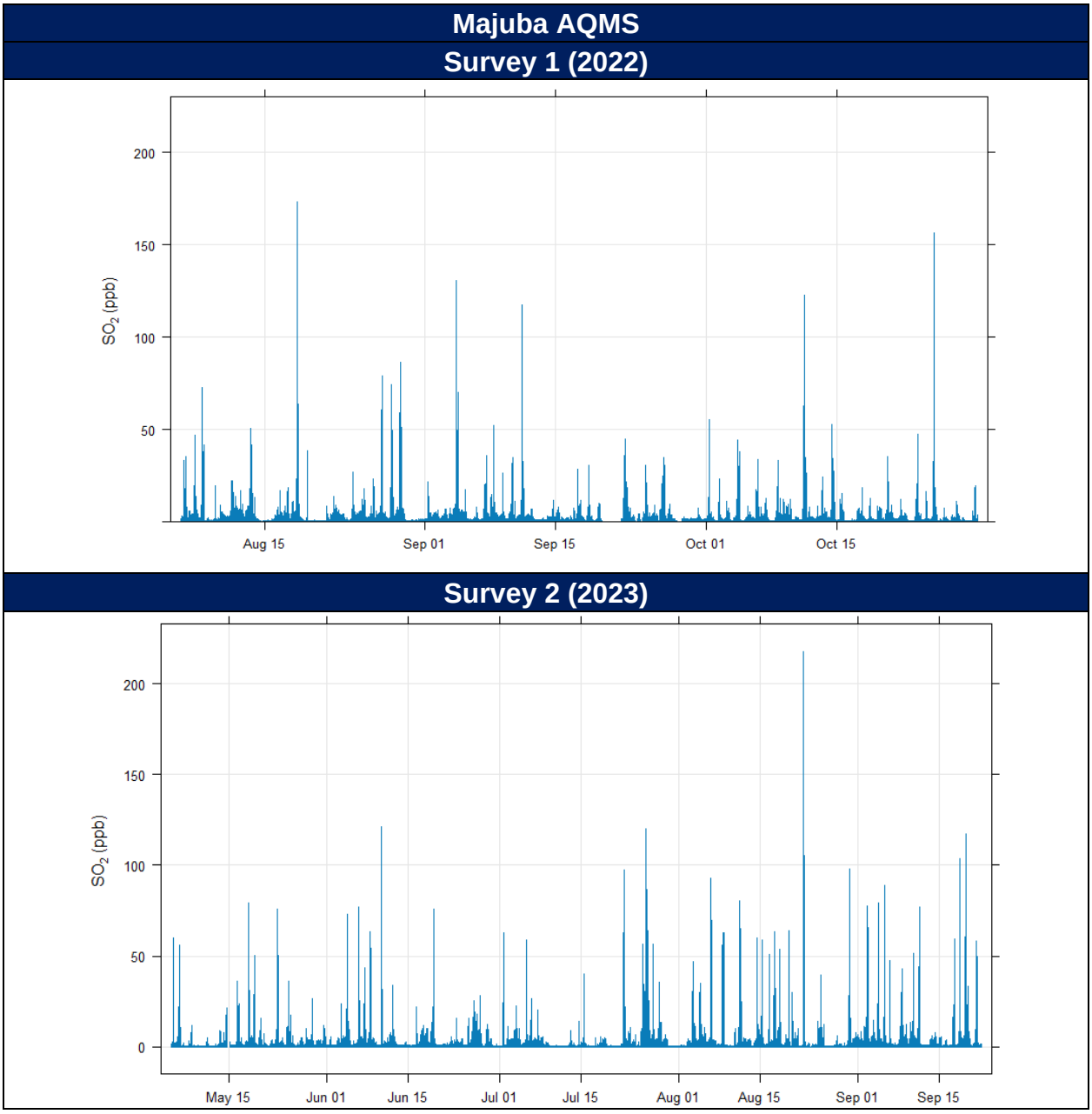

Figure 46B: Hourly ambient SO_2 concentrations (ppb) measured at the Eskom Majuba AQMS during the two sampling surveys (Hourly SO_2 NAAQS = 134ppb).

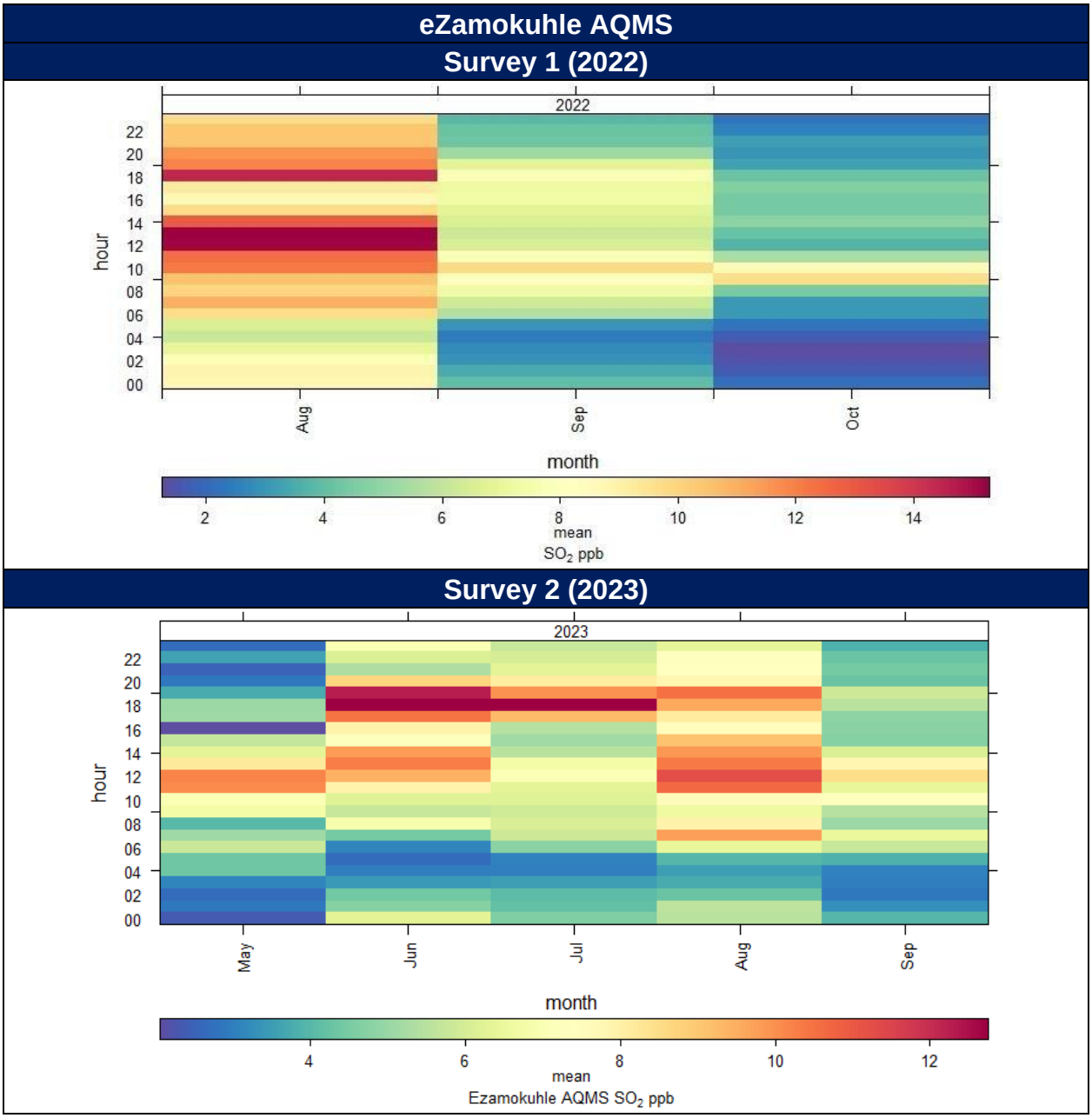

Figure 47A: Hourly mean ambient SO_2 concentrations (ppb) measured at the Eskom eZamokuhle AQMS during the two sampling surveys (Hourly SO_2 NAAQS = 134ppb).

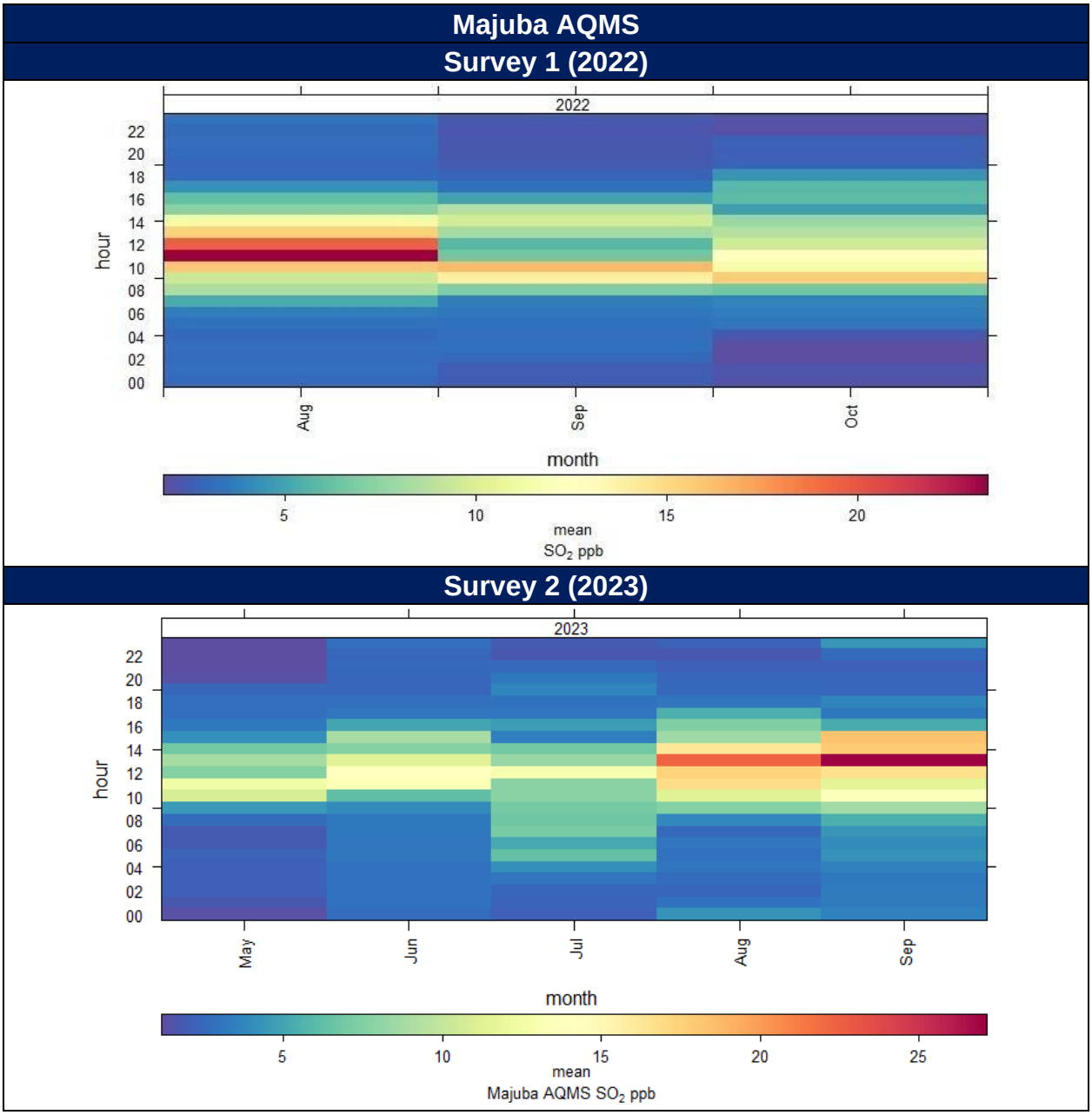

Figure 48B: Hourly mean ambient SO_2 concentrations (ppb) measured at the Eskom Majuba AQMS during the two sampling surveys (Hourly SO_2 NAAQS = 134ppb).

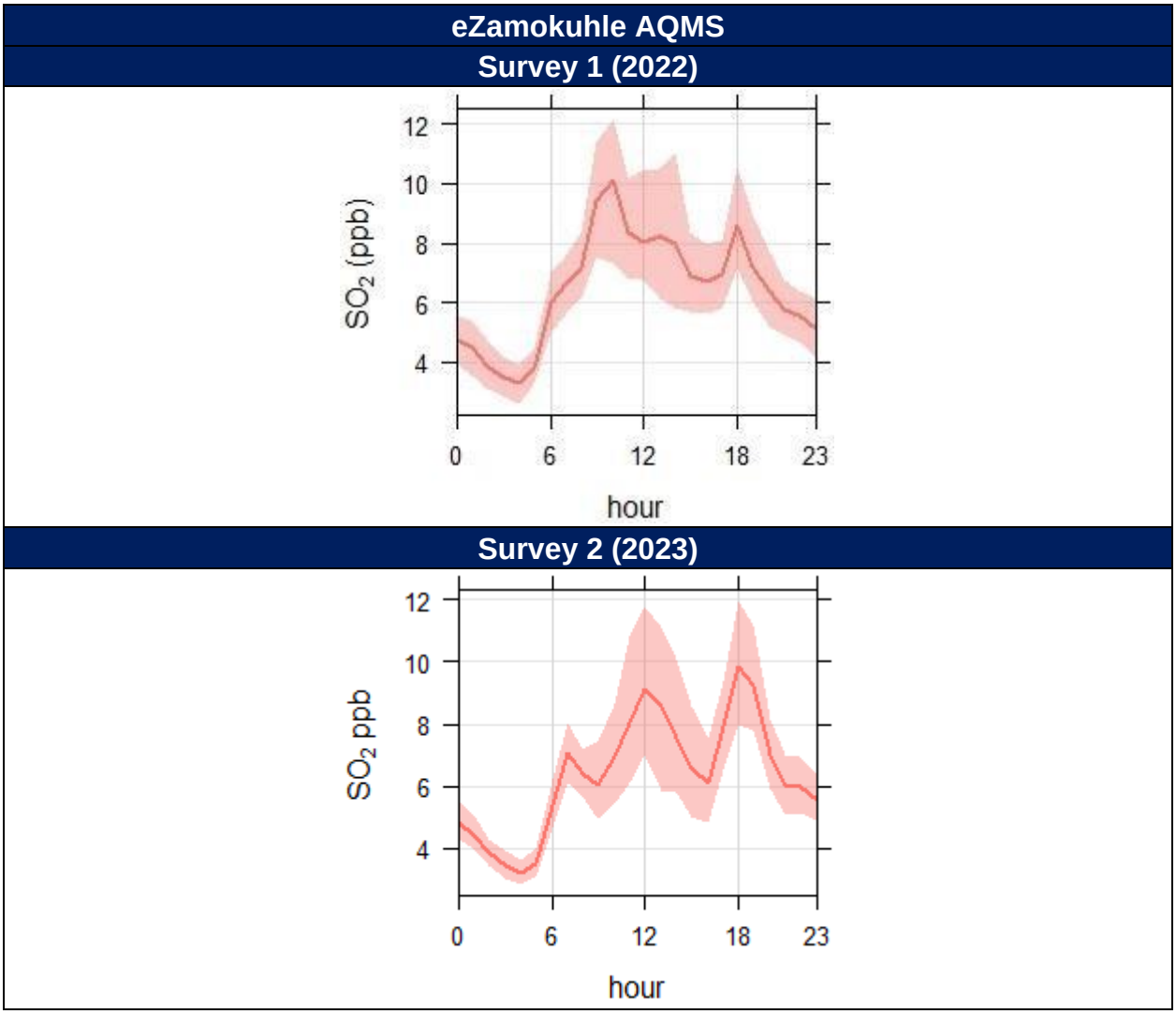

Figure 49A: Mean hourly diurnal ambient SO_2 concentrations (ppb) measured at the eZamokuhle AQMS during the two sampling surveys.

Majuba AQMS

Survey 1 (2022)

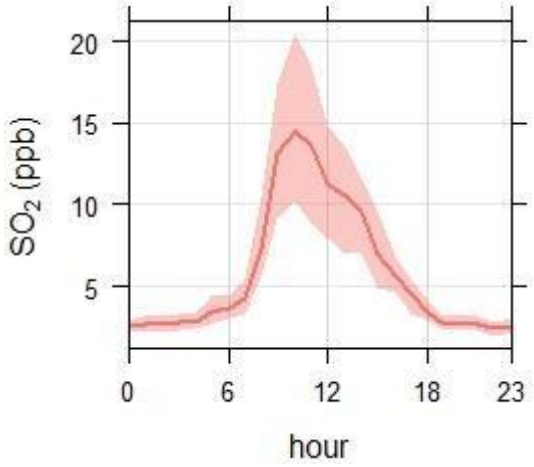

Survey 2 (2023)

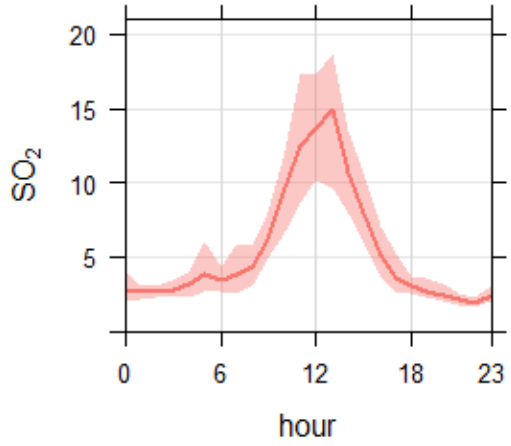

Figure 50B: Mean hourly diurnal ambient SO_2 concentrations (ppb) measured at the Majuba AQMS during the two sampling surveys.

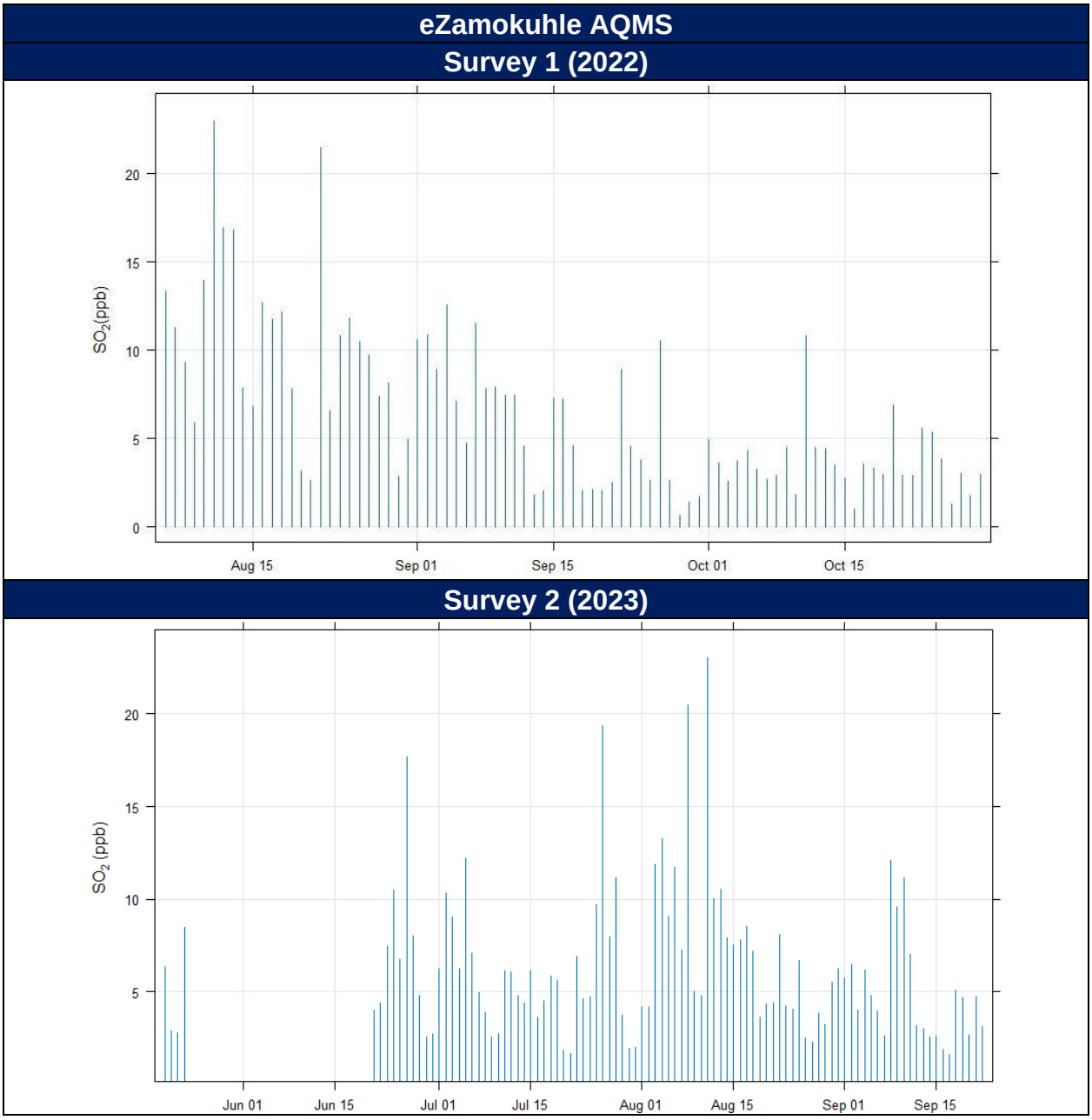

Figure 51A: Daily ambient SO_2 concentrations (ppb) measured at the Eskom eZamokuhle AQMS during the two sampling surveys (Hourly SO_2 NAAQS = 48ppb).

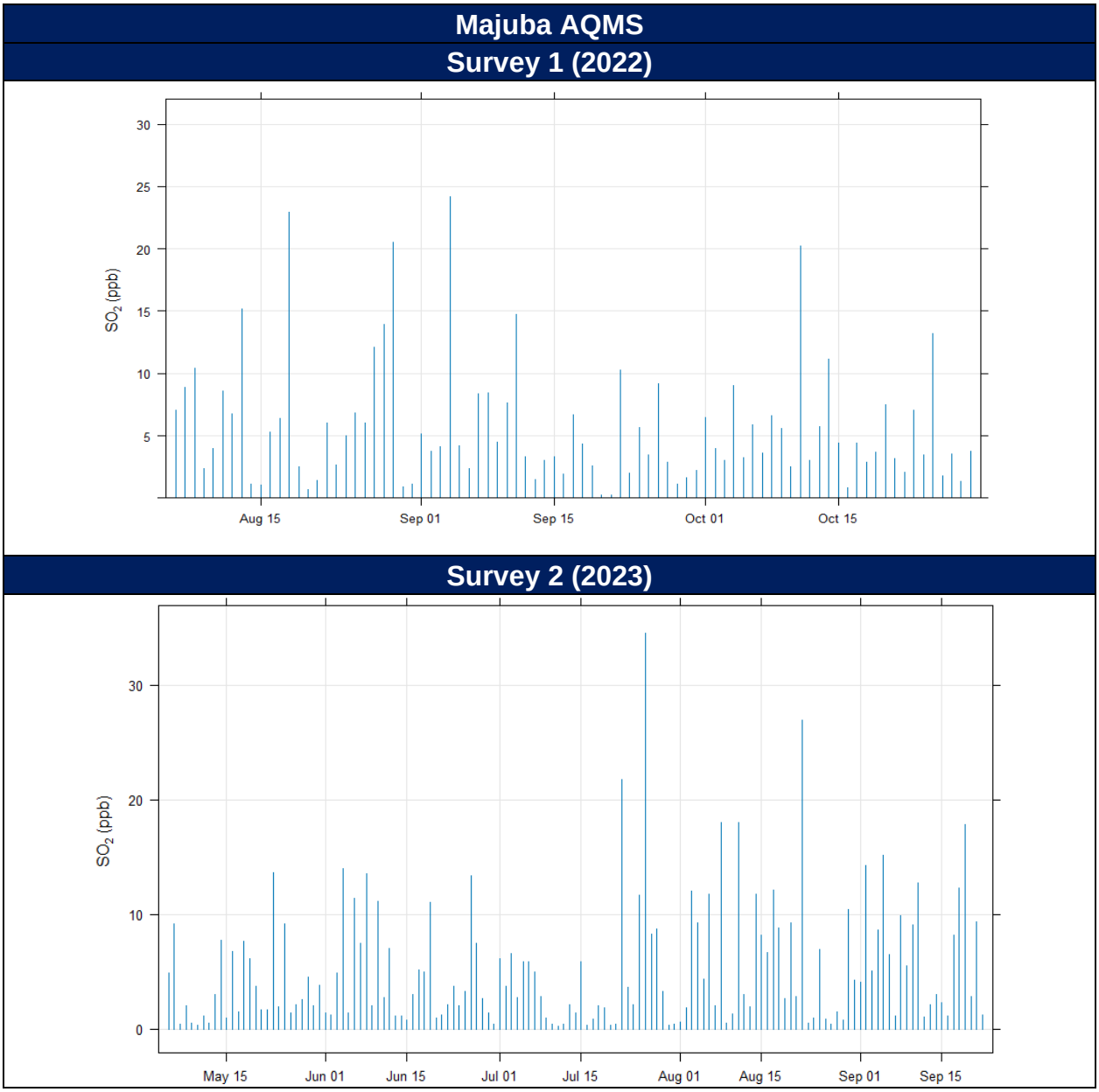

Figure 52B: Daily ambient SO_2 concentrations (ppb) measured at the Eskom Majuba AQMS during the two sampling surveys (Hourly SO_2 NAAQS = 48ppb).

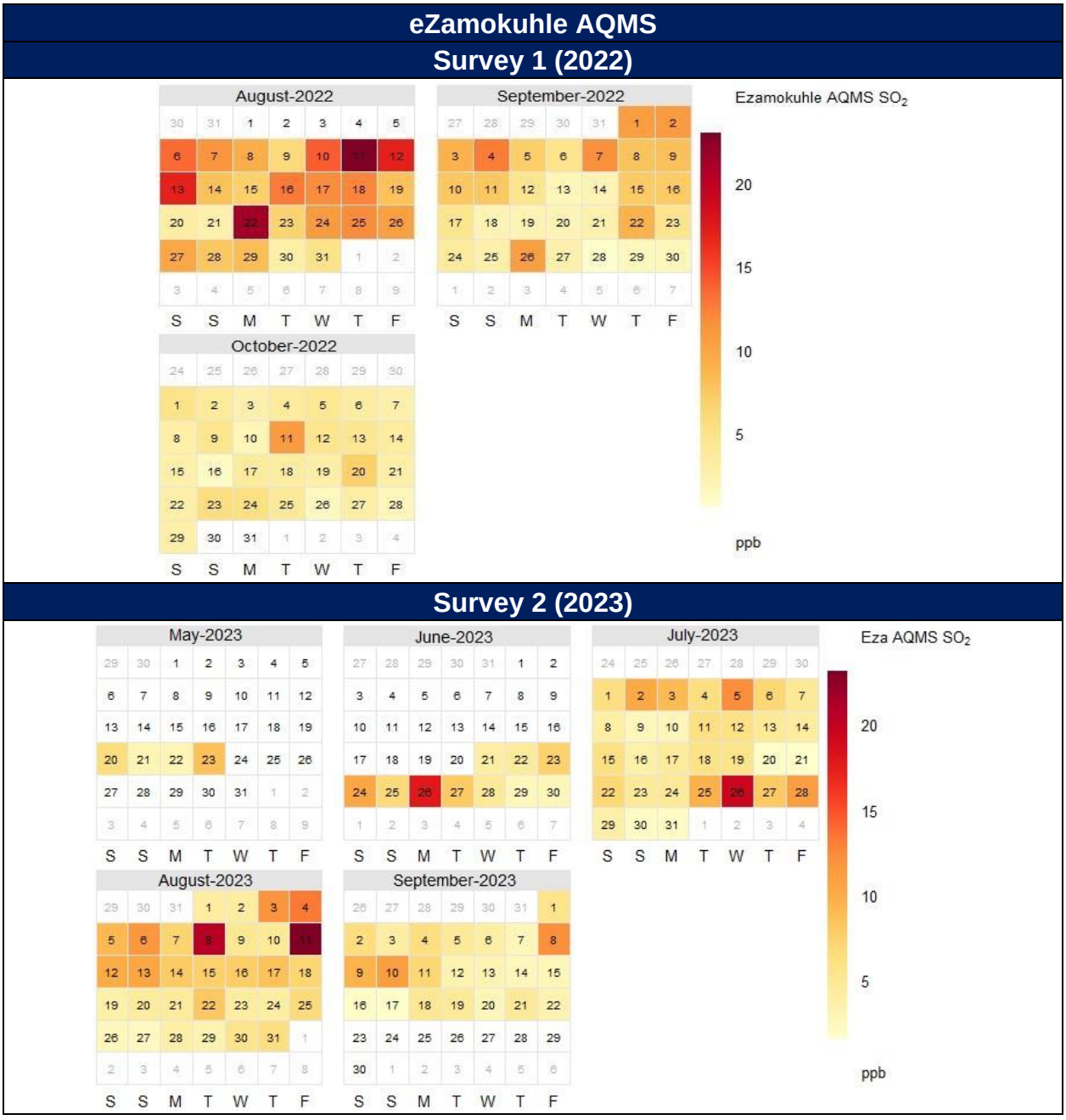

Figure 53A: Daily ambient SO_2 concentrations (ppb) measured at the Eskom eZamokuhle AQMS during the two sampling surveys (Hourly SO_2 NAAQS = 48ppb).

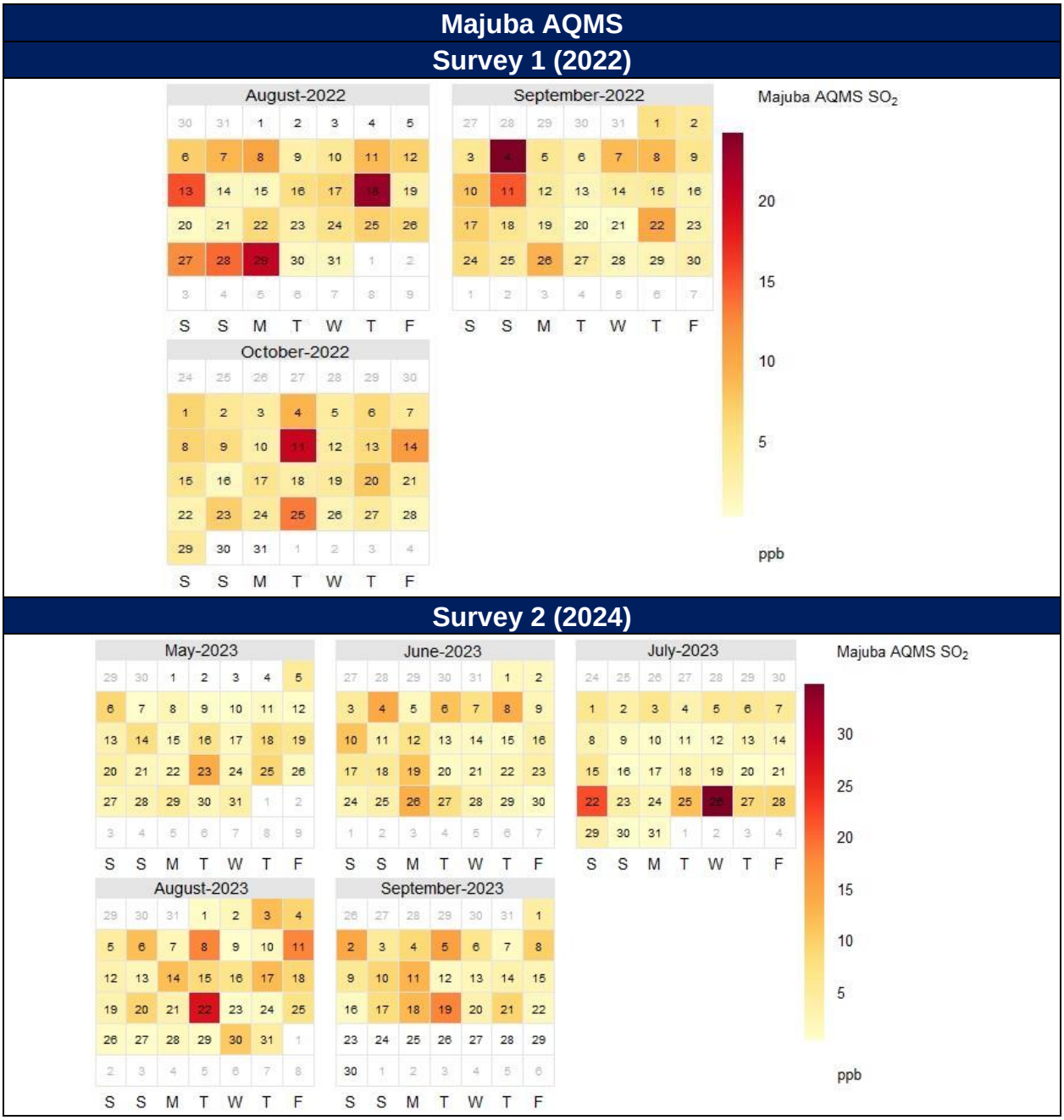

Figure 54B: Daily ambient SO_2 concentrations (ppb) measured at the Eskom Majuba AQMS during the two sampling surveys (Hourly SO_2 NAAQS = 48ppb).

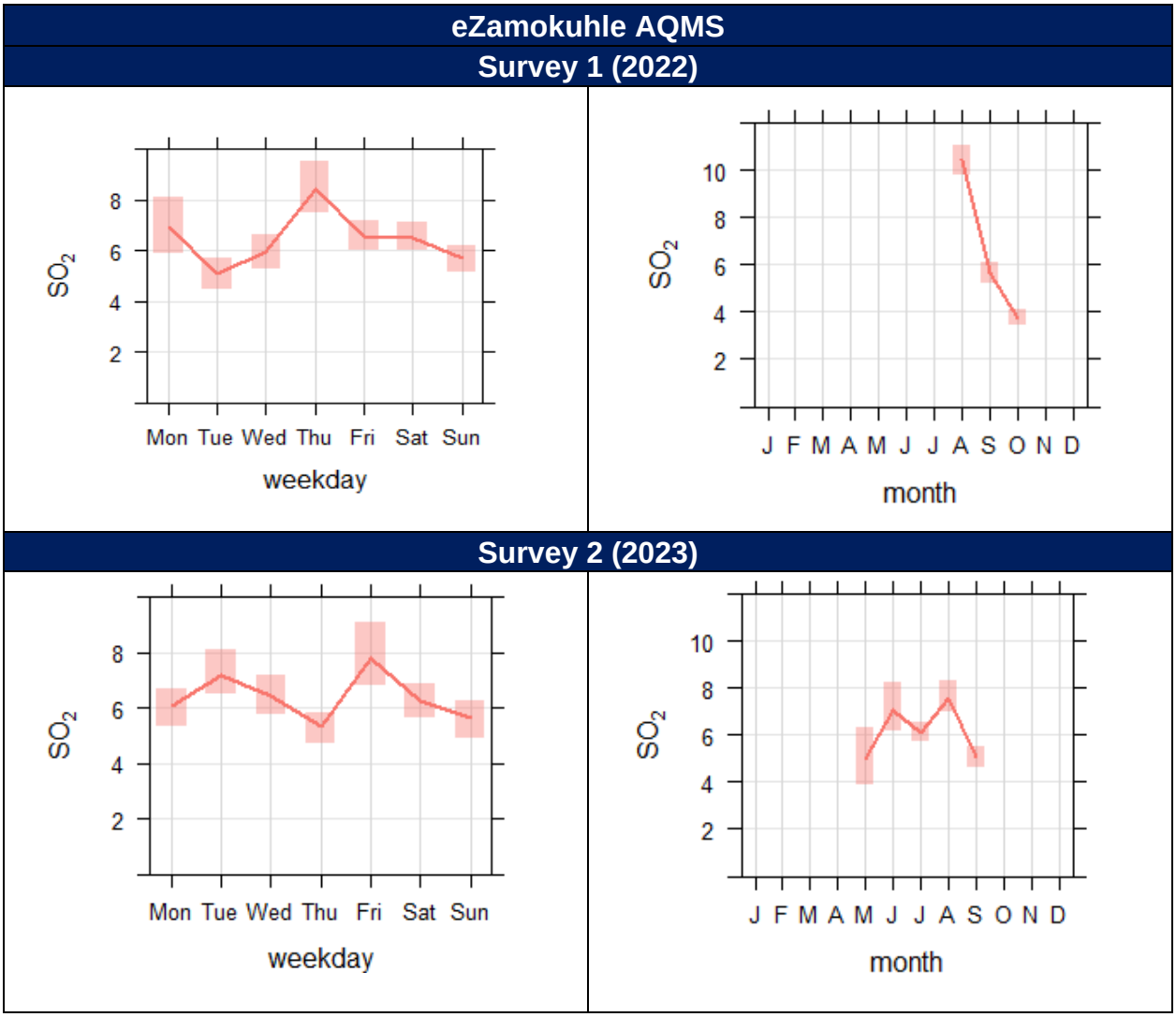

Figure 55A: Mean weekday and mean monthly ambient SO_2 concentrations (ppb) measured at the eZamokuhle AQMS during the two sampling surveys.

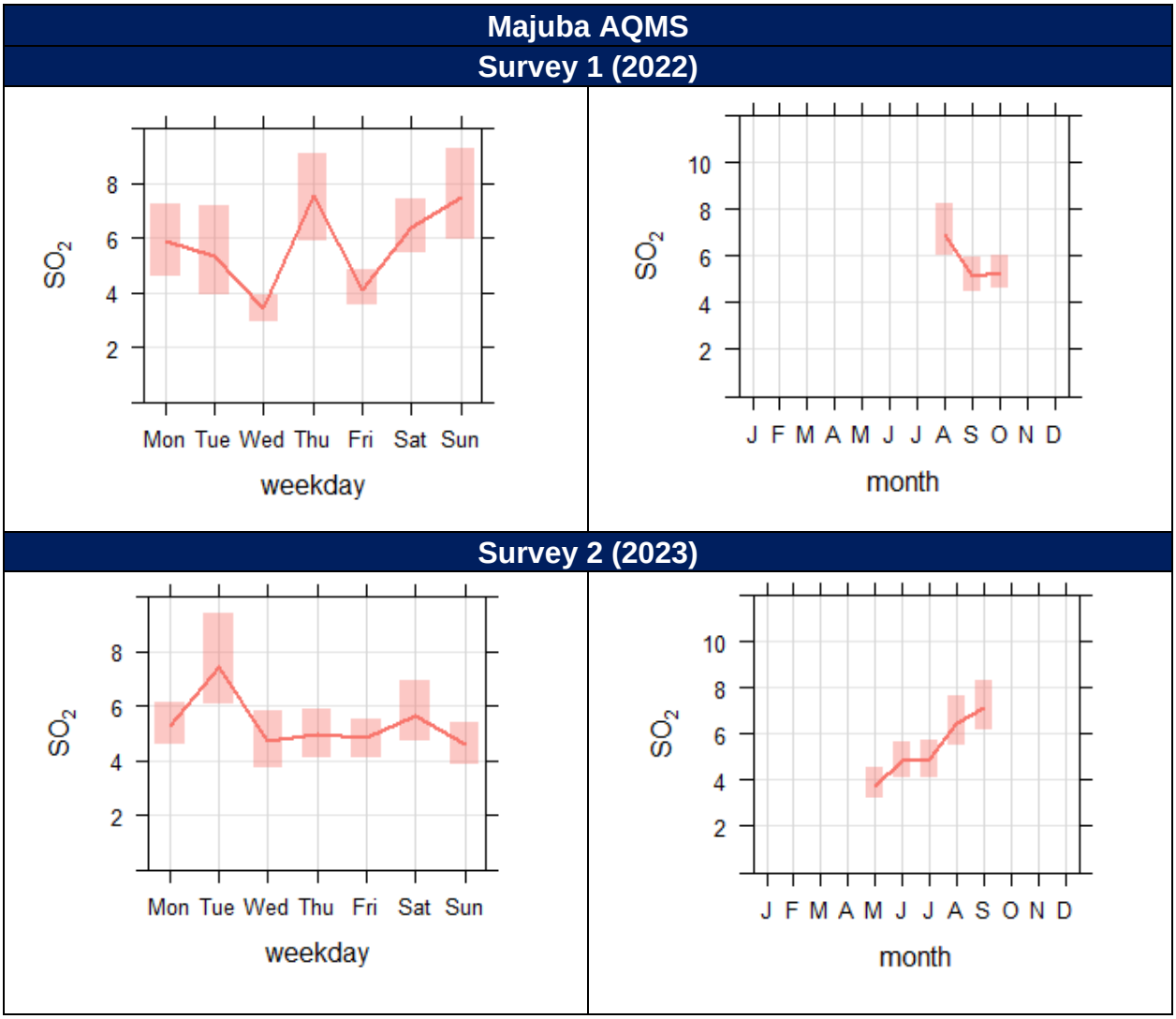

Figure 56B: Mean weekday and mean monthly ambient SO_2 concentrations (ppb) measured at the Majuba AQMS during the two sampling surveys.

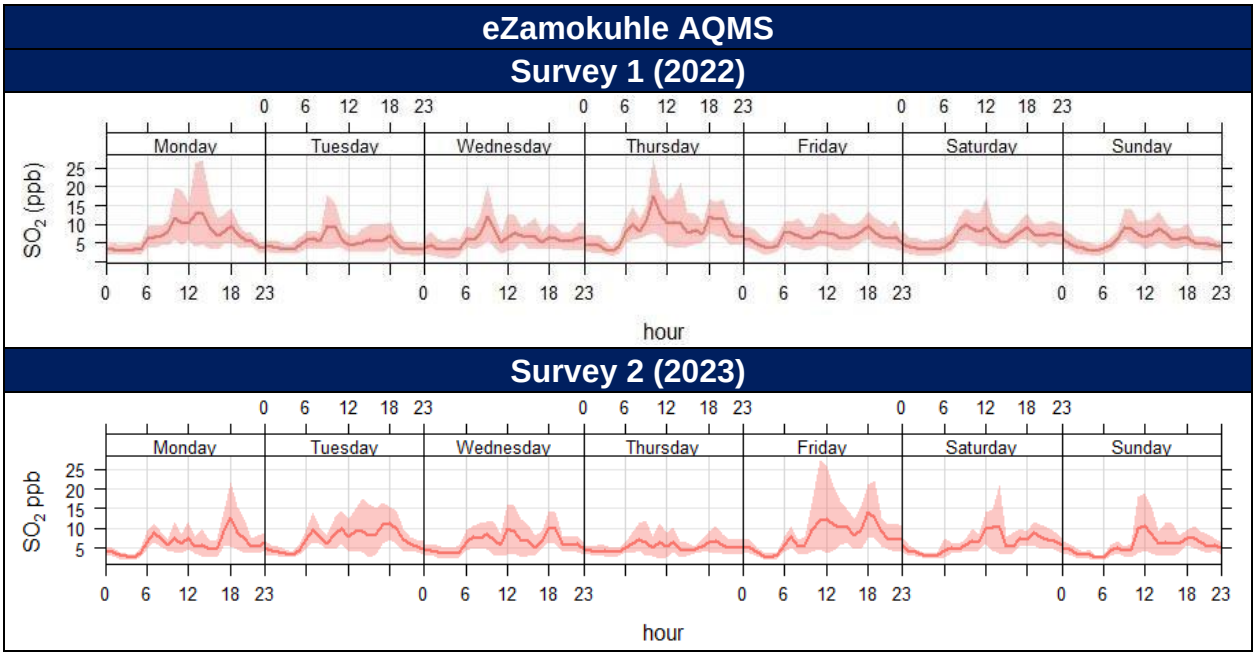

Figure 57A: Weekly diurnal SO_2 concentrations (ppb) measured at the eZamokuhle AQMS during the two sampling surveys.

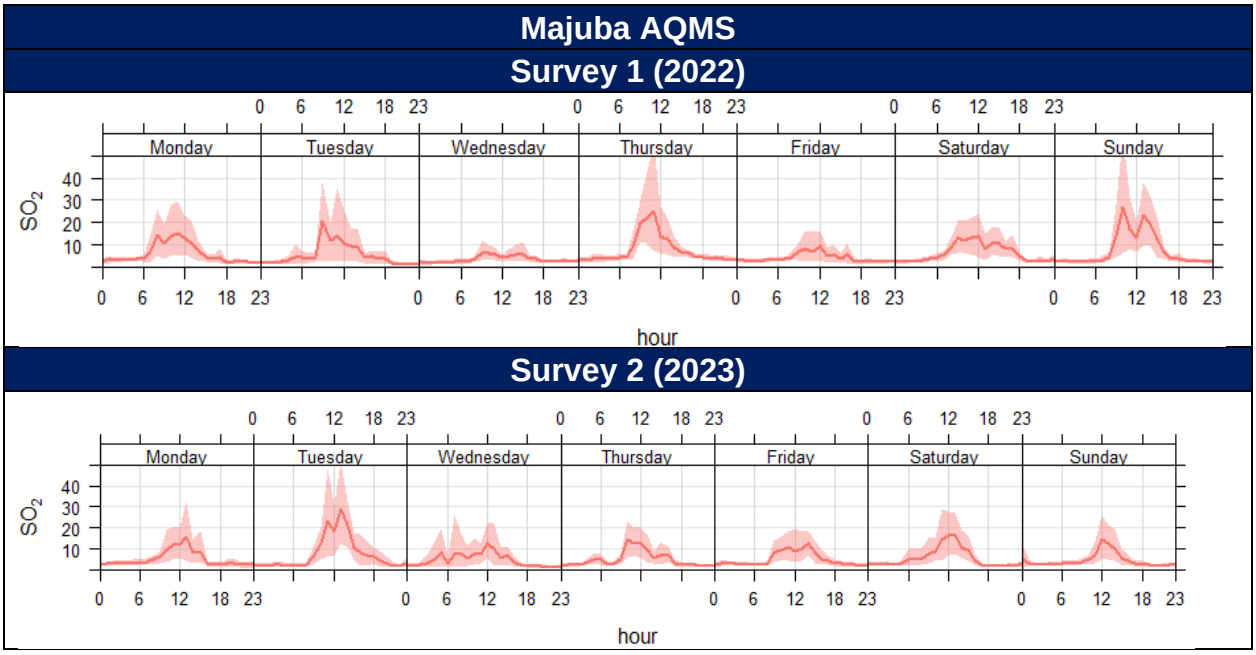

Figure 58B: Weekly diurnal SO_2 concentrations (ppb) measured at the Majuba AQMS during the two sampling surveys.

3.2.4 NITROGEN DIOXIDE (NO_2)

Figure 59A and 36B indicate the hourly ambient NO_2 concentrations recorded at the Eskom eZamokuhle and Eskom Majuba AQMS. The NAAQS for hourly NO_2 concentrations is 106ppb. No exceedances of the hourly NAAQS were recorded for an hourly time average for both stations. Figure 59A highlight maximum hourly NO_2 concentrations of approximately 25ppb at the Eskom eZamokuhle station, whilst maximum concentrations of 40ppb were recorded for the Eskom Majuba AQMS. Unfortunately, no NO_2 data was recorded at the Eskom eZamokuhle AQMS during the survey 2, sampling period.

Figure 61A and 37B are graphical representations of the mean hourly NO_2 concentrations for the sampling periods. It is evident from Figure 37A that the highest mean concentrations were recorded during hours 06:00 to 08:00 and 16:00 to 18:00 for the Eskom eZamokuhle station, whilst elevated concentrations were recorded at 10:00 to 12:00 for the Eskom Majuba station (Figure 37B). These diurnal profiles are also illustrated in Figure 63A and Figure 38B. The Eskom eZamokuhle signature in Figure 63A explicitly reveal that the variability of this pollutant concentration is conditioned by vehicle emissions. The diurnal cycle corresponds to the cyclical nature of traffic volume with marked peaks in concentration on weekdays around the early-morning and late-afternoon rush-hours. For the Eskom Majuba station (Figure 63B), there is an increased NO_2 concentrations at just before midday due to the break-up of an elevated inversion layer, in addition to the development of daytime convective conditions causing the plume to be brought down to ground level relatively close to the point of release from tall stacks.

Figure 65A and 39B indicate the daily ambient NO_2 concentrations recorded at the Eskom eZamokuhle and Eskom Majuba AQMS. No daily NAAQS for NO_2 exists. Daily maximum NO_2 concentrations of approximately 10ppb were recorded for both stations. These daily mean NO_2 concentrations are graphically presented in Figure 67A and Figure 40B.

Figure 67A and Figure 41B highlights the mean weekday and mean monthly ambient NO_2 concentrations. Both stations indicate higher recorded ambient concentrations on a Thursday (both sampling surveys). The Eskom Majuba AQMS highlights a decrease in monthly concentrations from August 2022 to October 2022 (survey 1), whilst an increase in is observed from August 2023 to October 2023 (survey 2) as depicted in Figure 41B.

Figure 69 to Figure 42B is indicative of the mean weekly NO_2 concentrations. It is evident for the Eskom eZamokuhle station that the weekly diurnal cycle corresponds to the cyclical nature of traffic volume with marked peaks in concentration on weekdays around the early-morning and late-afternoon rush-hours. For the Eskom Majuba station (Figure 69), there is an increased NO_2 concentrations at just before midday due to the break-up of an elevated inversion layer, in addition to the development of daytime convective conditions causing the plume to be brought down to ground level relatively close to the point of release from tall stacks.

eZamokuhle AQMS

Survey 1 (2022)

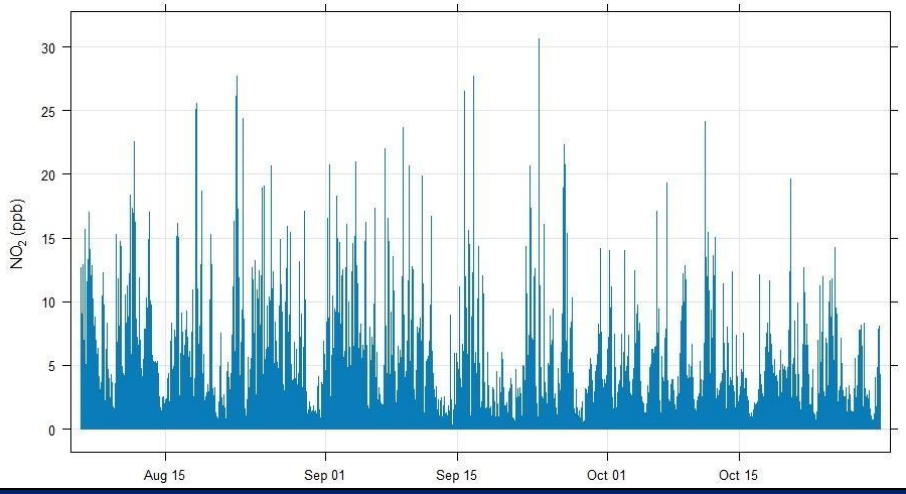

Survey 2 (2023)

No data available.

Figure 59A: Hourly ambient NO_2 concentrations (ppb) measured at Eskom eZamokuhle AQMS during the two sampling surveys (Hourly NO_2 NAAQS = 106ppb).

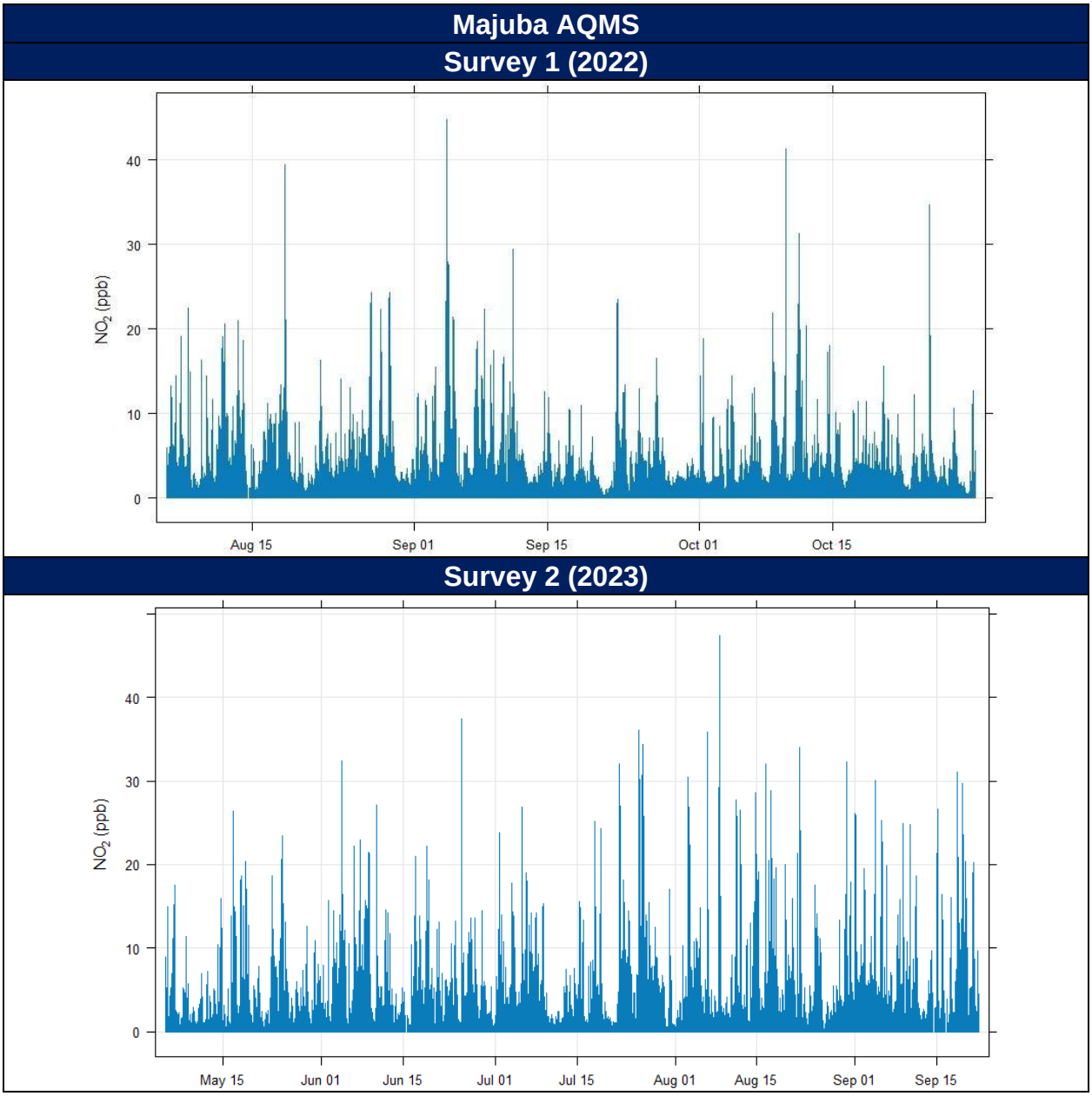

Figure 60B: Hourly ambient NO_2 concentrations (ppb) measured at Eskom Majuba AQMS during the two sampling surveys (Hourly NO_2 NAAQS = 106ppb).

eZamokuhle AQMS

Survey 1 (2022)

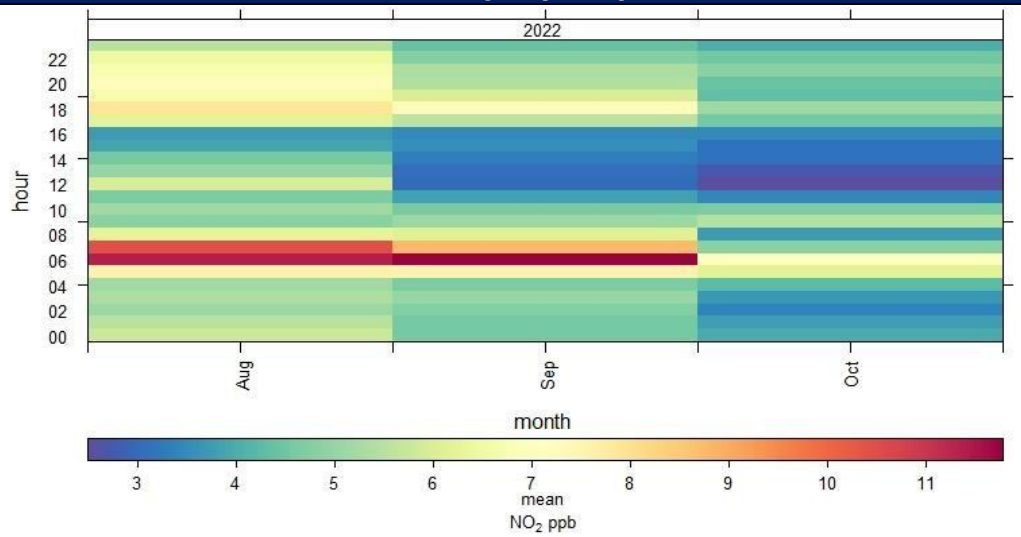

Survey 2 (2023)

No data available.

Figure 61A: Hourly mean ambient NO_2 concentrations (ppb) measured at Eskom eZamokuhle AQMS during the two sampling surveys (Hourly NO_2 NAAQS = 106ppb).

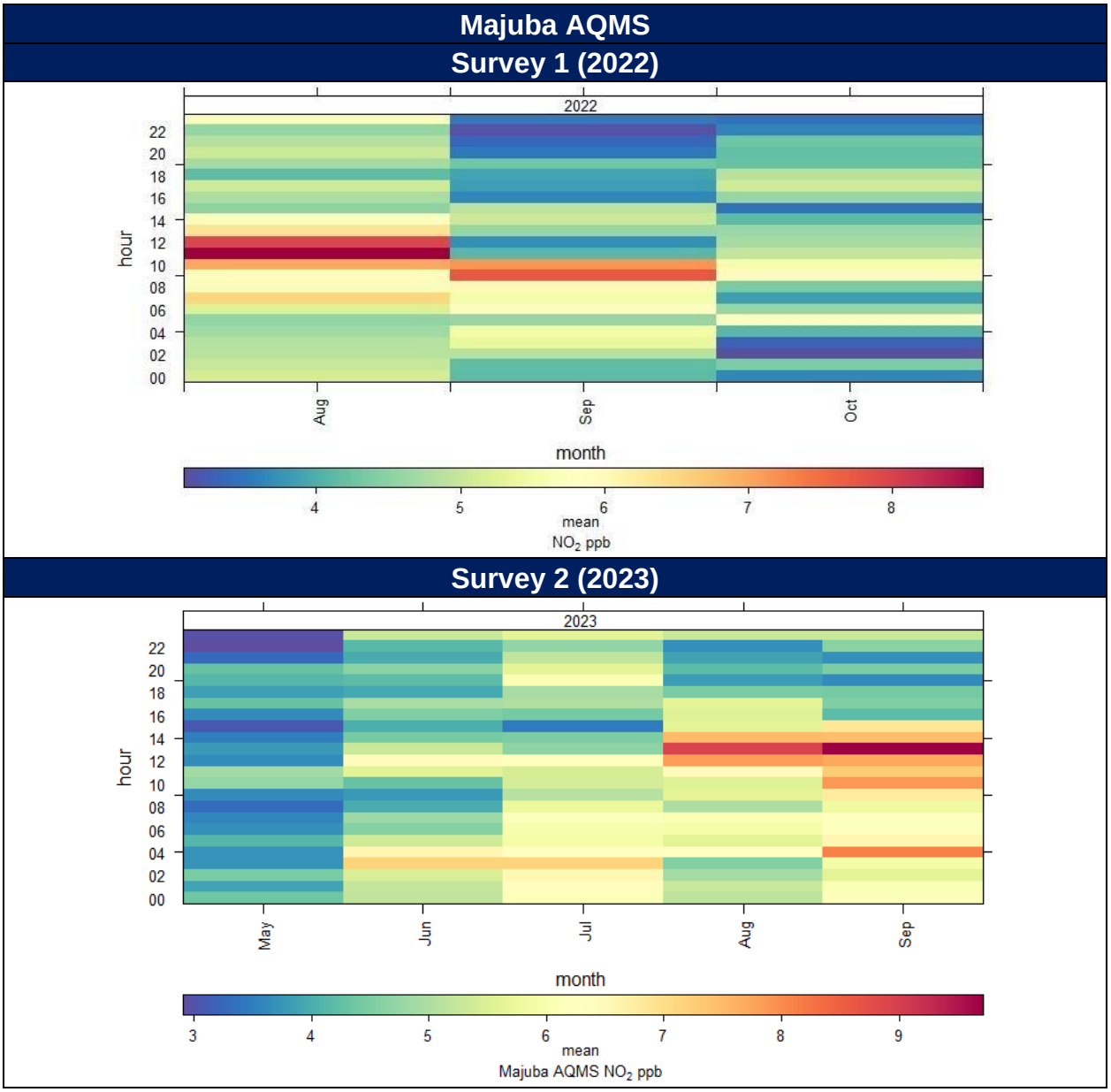

Figure 62B: Hourly mean ambient NO_2 concentrations (ppb) measured at Eskom Majuba AQMS during the two sampling surveys (Hourly NO_2 NAAQS = 106ppb).

eZamokuhle AQMS

Survey 1 (2022)

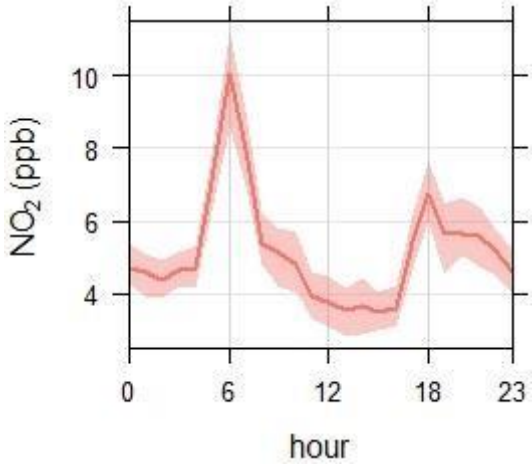

Survey 2 (2023)

No data available.

Figure 63A: Mean hourly diurnal NO_2 concentrations (ppb) measured at the eZamokuhle AQMS during the two sampling surveys.

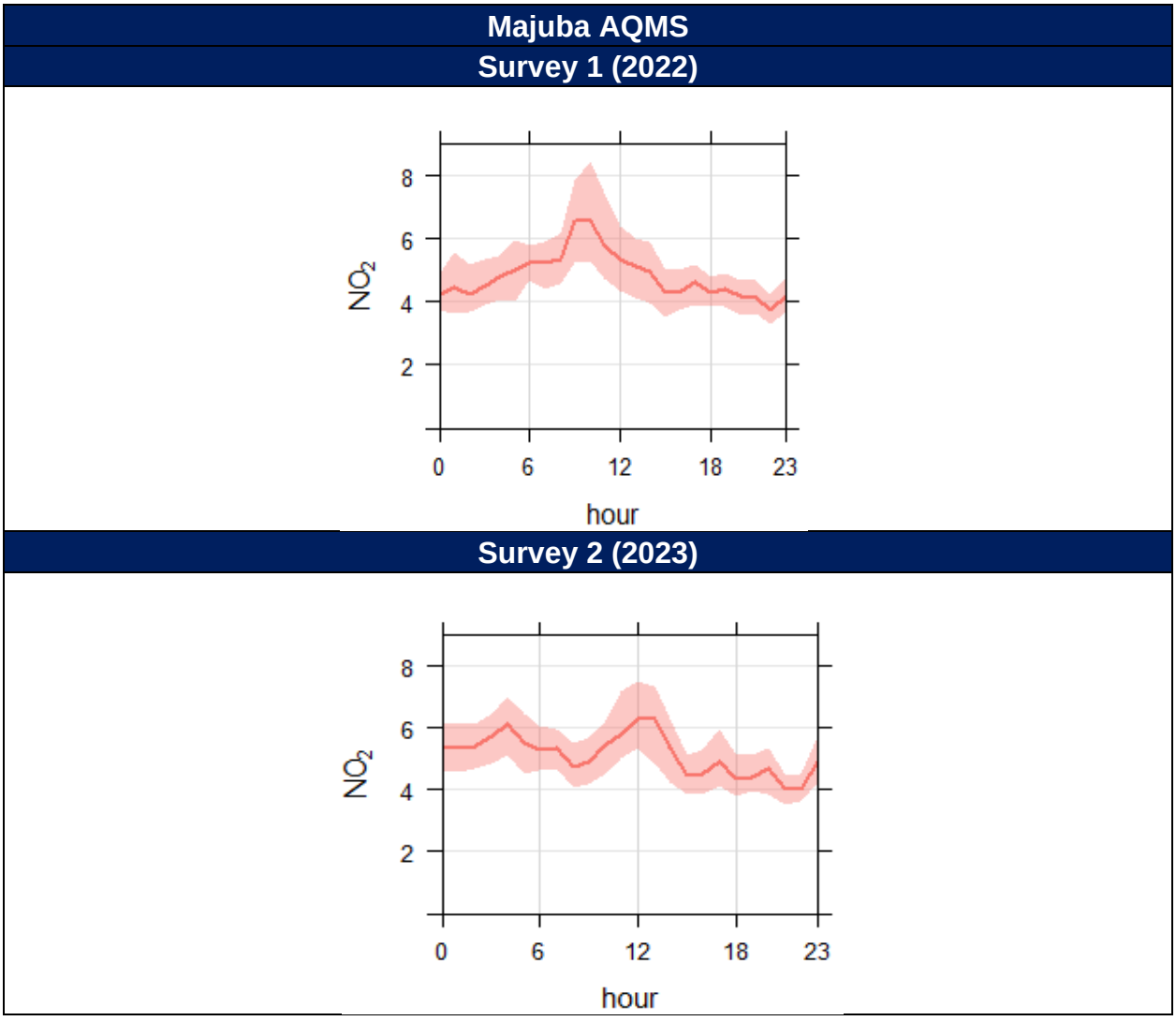

Figure 64B: Mean hourly diurnal NO_2 concentrations (ppb) measured at the Majuba AQMS during the two sampling surveys.

eZamokuhle AQMS

Survey 1 (2022)

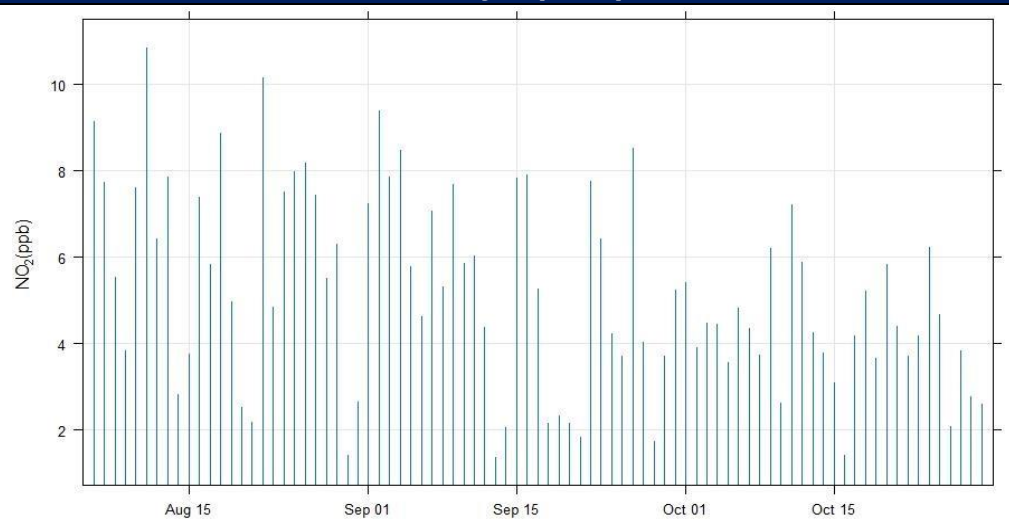

Survey 2 (2023)

No data available.

Figure 65A: Daily ambient NO_2 concentrations (ppb) measured at Eskom eZamokuhle AQMS during the two sampling surveys.

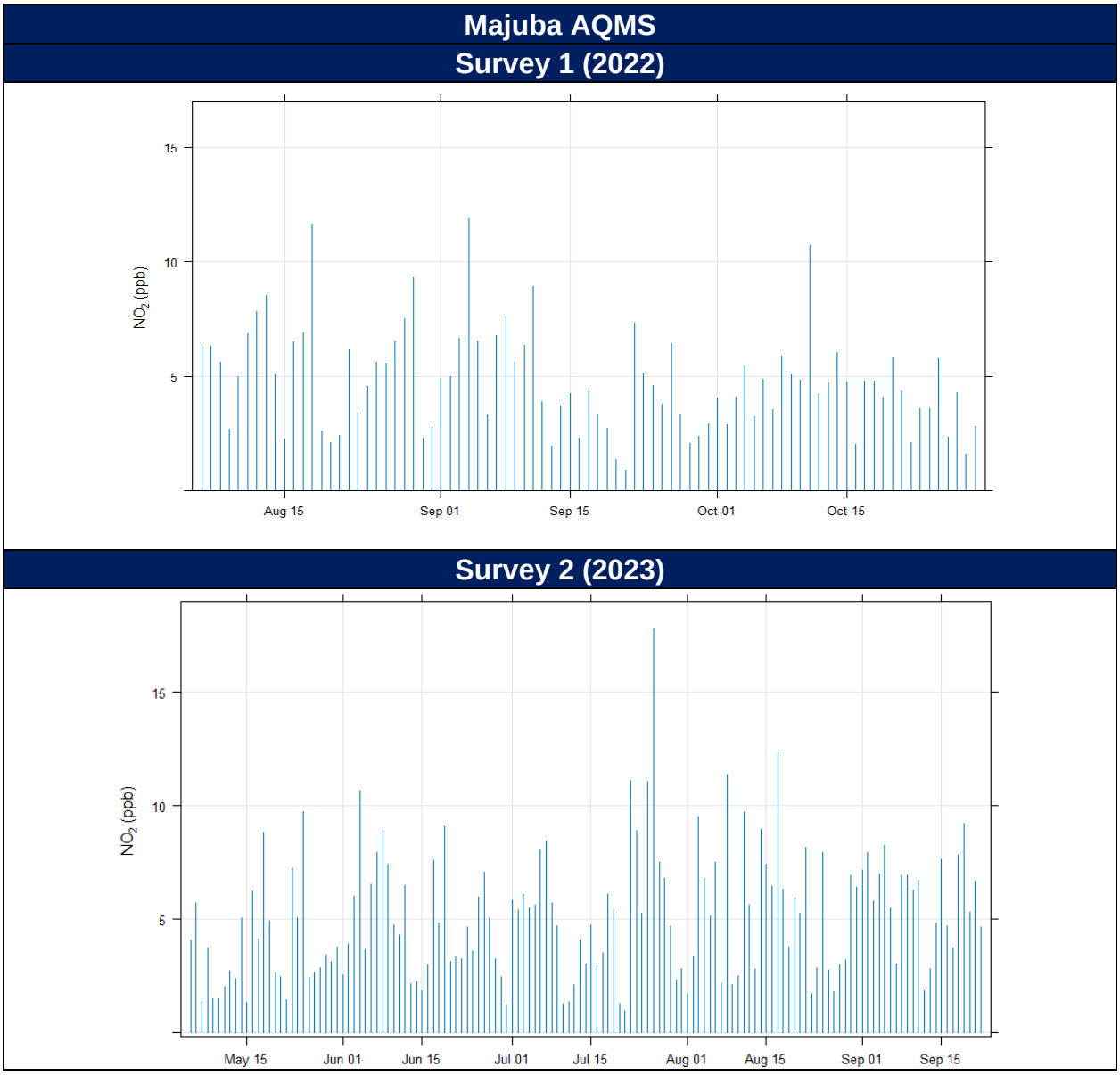

Figure 66B: Daily ambient NO_2 concentrations (ppb) measured at Eskom Majuba AQMS during the two sampling surveys.

eZamokuhle AQMS

Survey 1 (2022)

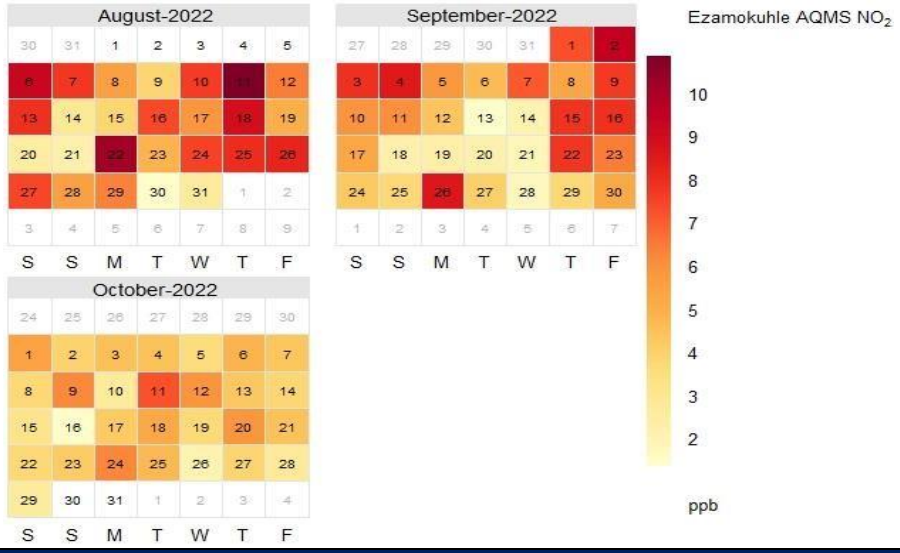

Survey 2 (2023)

No data available.

Figure 67A: Daily ambient NO_2 concentrations (ppb) measured at Eskom eZamokuhle AQMS during the two sampling surveys.

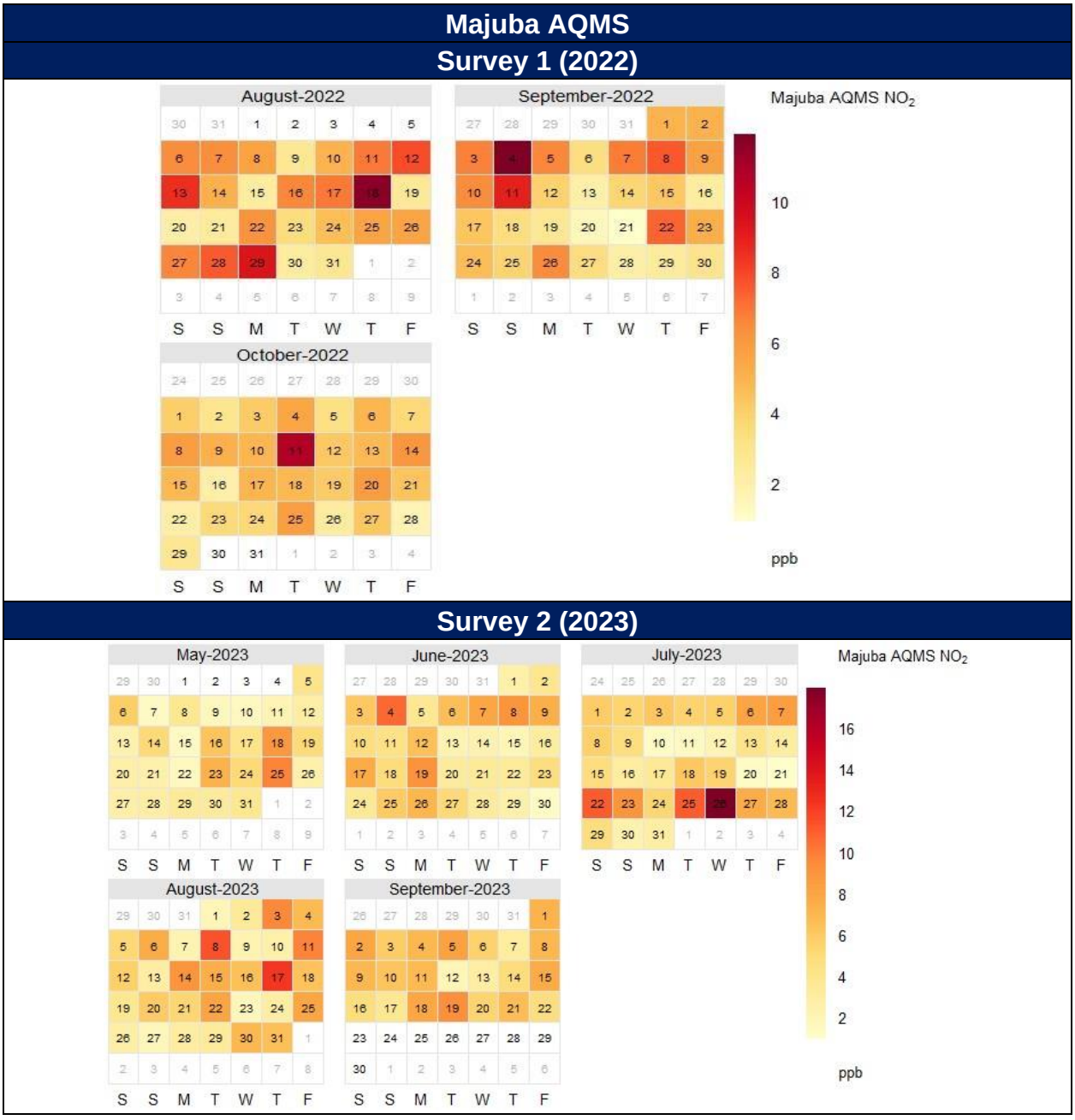

Figure 68B: Daily ambient NO_2 concentrations (ppb) measured at Eskom Majuba AQMS during the two sampling surveys.

eZamokuhle AQMS	
Survey 1 (2022)	
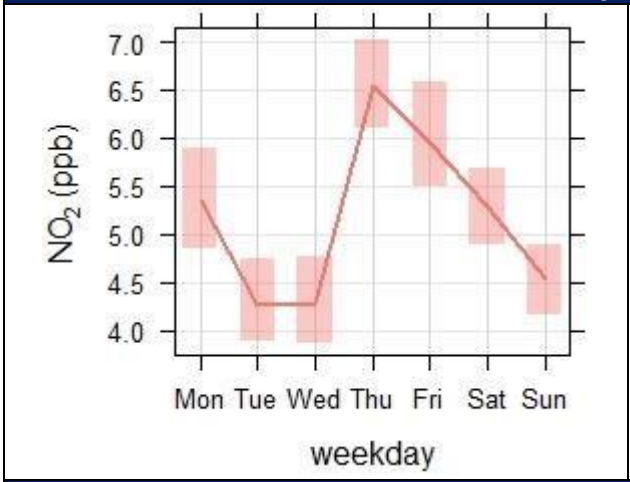	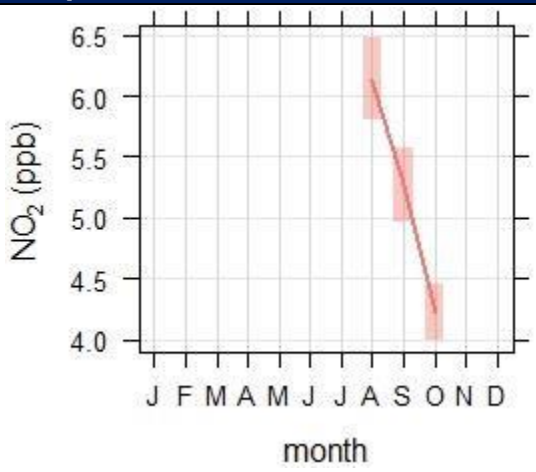
Survey 2 (2023)	
No data available.	No data available.

Figure 69A: Mean weekday and mean monthly ambient NO_2 concentrations (ppb) measured at the eZamokuhle AQMS during the two sampling surveys.

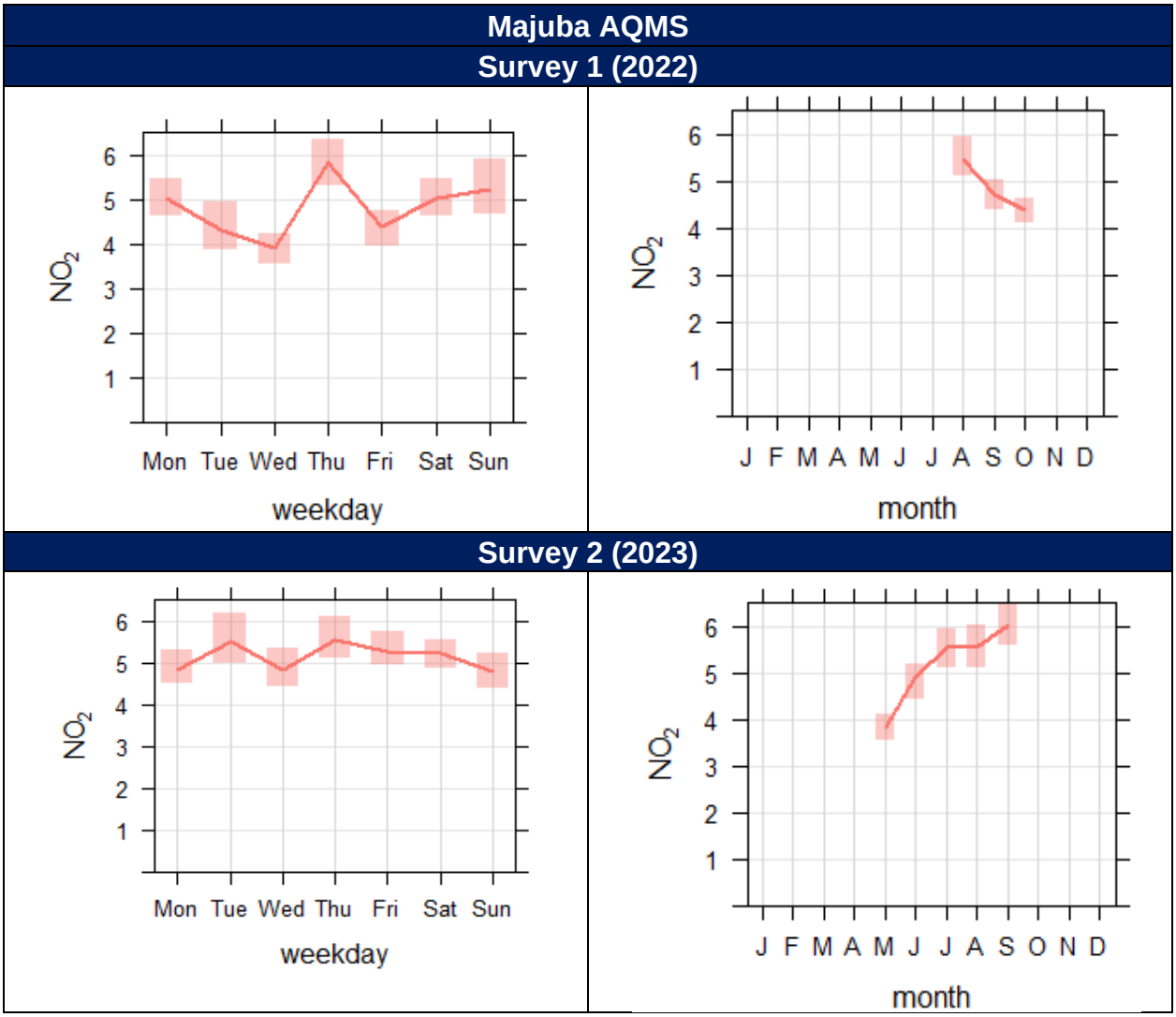

Figure 70B: Mean weekday and mean monthly ambient NO_2 concentrations (ppb) measured at the Majuba AQMS during the two sampling surveys.

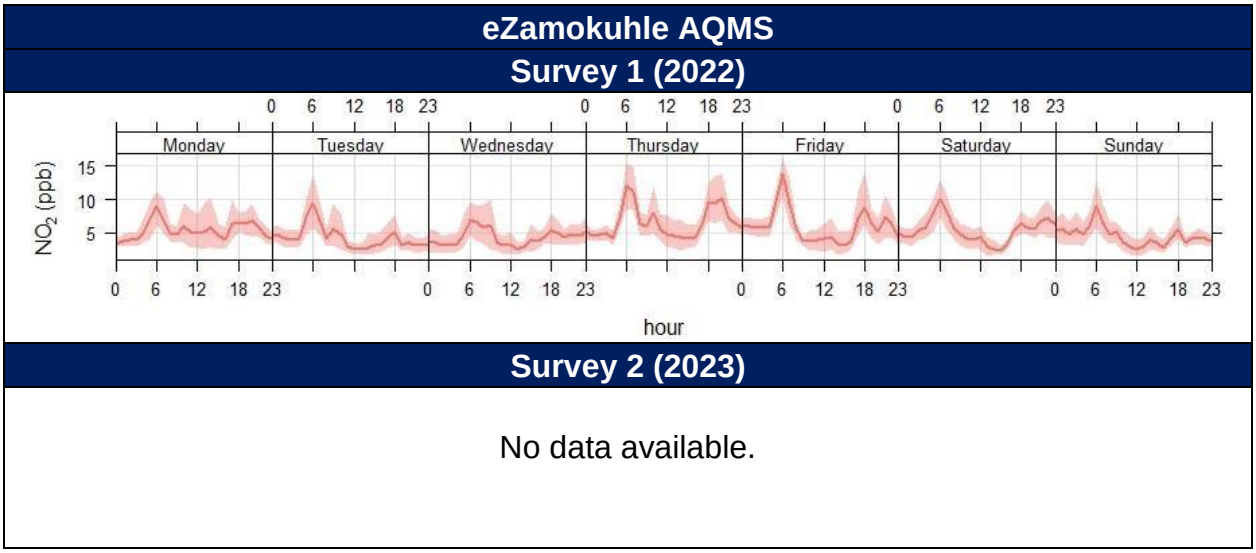

Figure 71A: Weekly diurnal NO_2 concentrations (ppb) measured at sampling sites during the two sampling surveys.

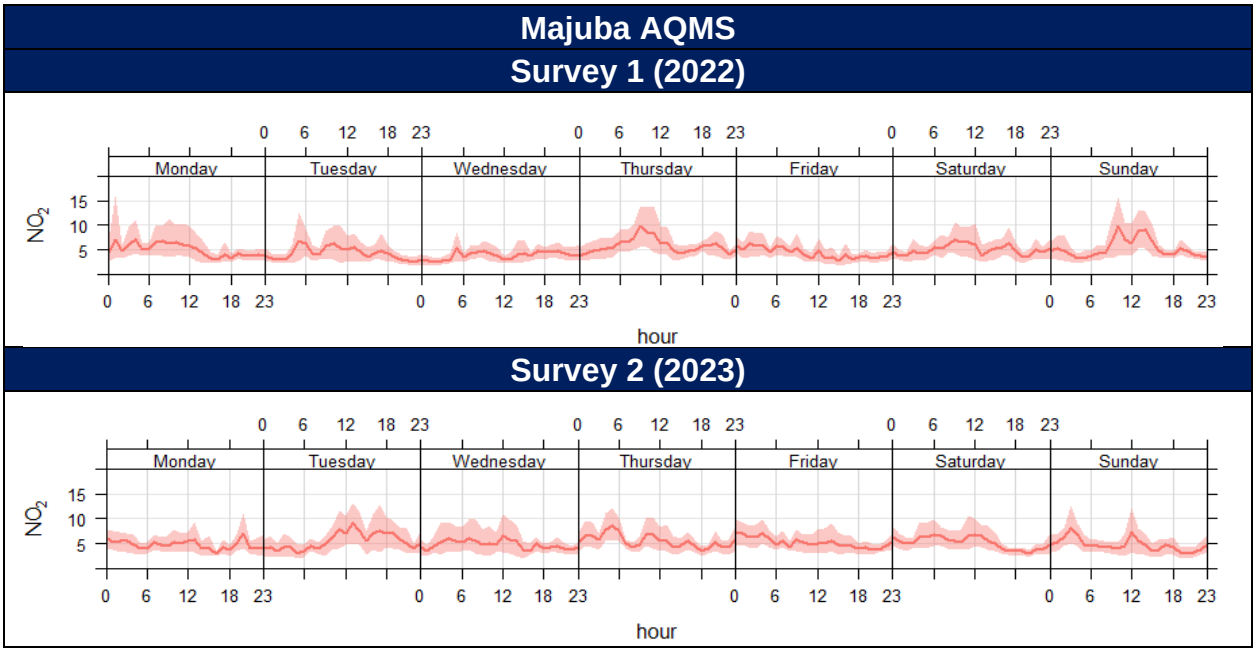

Figure 72B: Weekly diurnal NO_2 concentrations (ppb) measured at the Majuba AQMS during the two sampling surveys.

4.3 EMISSION SOURCE CONTRIBUTION

The emission performance of an individual air-pollution source can be inferred from an ambient record by isolating its signal of impacts. However, ambient data are not conventionally used for such purposes because individual signals tend to be modified, obscured, or complicated by confounding factors (Szulecka et al., 2017). However, more detailed and source-specific information can be extracted if analyses are performed using a subset of the data that has been "conditionally-selected" to exclude superimposed impacts from non-relevant sources (Malby et al., 2013). Numerous studies (Carslaw, 2007; Griffin et al., 2009; Malby et al., 2008; Shu et al., 2017) have demonstrated that these signals can successfully be used for source attribution. A common method for source characterisation is the use of pollution roses and bivariate polar plots (Carslaw et al., 2006; Westmoreland et al., 2007; Carslaw and Beevers, 2013; Uria Tellaetxe and Carslaw, 2014).

Bivariate polar plots have proved to be extremely valuable for identifying and understanding sources of air pollution (Carslaw et al., 2006; Westmoreland et al., 2007). Bivariate polar plots provide an effective graphical means of discriminating different source types and characteristics as these plots show how the concentration of a pollutant varies by two different variables at a specific receptor.

4.3.1 POLLUTION ROSES

The pollution rose is useful for considering pollutant concentrations by wind direction, or more specifically the percentage time the concentration is in a particular range. This type of approach can be very informative for air pollutant species (Henry et al. 2009).

4.3.1.1 Particulate Matter (PM_{10})

Figure 73 illustrates the pollution roses for PM_{10} measured at the Eskom eZamokuhle & Majuba stations. These plots are very useful for understanding which wind directions control the overall mean concentrations. The pollution rose clearly indicates that high episodes of pollutant levels are primarily related to winds from the: west-, north-westerly direction; east-, north easterly direction, as well a south westerly direction. A comparison of the annual wind rose for the Eskom eZamokuhle station and the Eskom Majuba station (Figure 8) to the pollution roses (Figure 73) shows higher pollutant concentrations occur at higher wind speeds. Conversely lower wind speeds (Figure 8) are associated with lower concentrations (Figure 73). It should be noted that higher wind speeds are typically associated with elevated emissions from tall stack sources whilst low-level emissions behave differently, and higher concentrations would normally be observed during weak-wind conditions.

4.3.1.2 Particulate Matter ($PM_{2.5}$)

Figure 74 illustrates the pollution roses for $PM_{2.5}$ measured at the Eskom eZamokuhle & Majuba stations. The pollution roses clearly indicate that high episodes of pollutant levels are primarily related to winds from the: west-, north-westerly direction; east-, north easterly direction, as well a south westerly direction. Please note that data was not available for the 2023 period at the Eskom eZamokuhle AQMS.

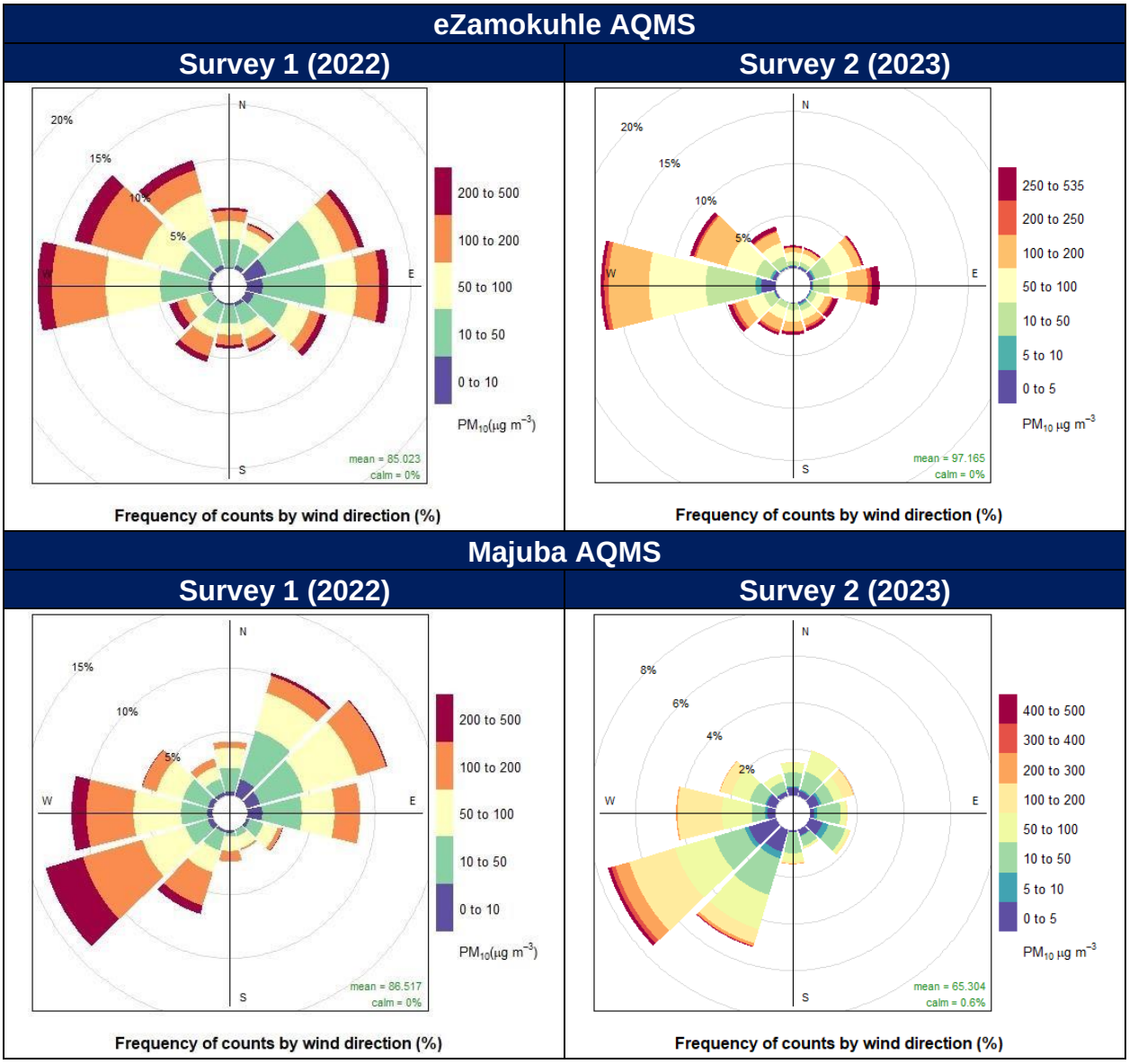

Figure 73: Pollution roses indicating which wind directions contribute most to overall mean concentrations for PM_{10}.

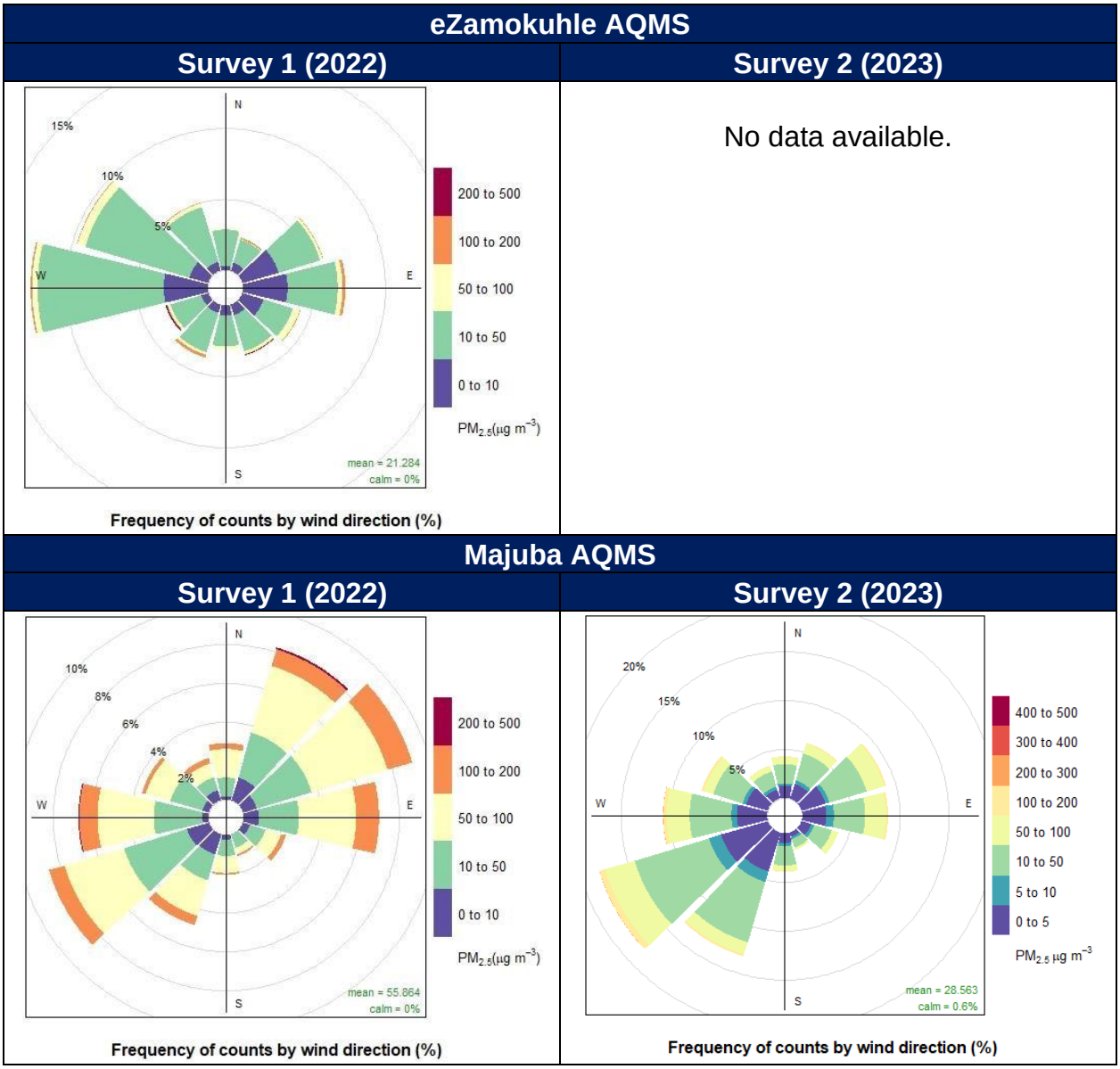

Figure 74: Pollution roses indicating which wind directions contribute most to overall mean concentrations for $PM_{2.5}$.

4.3.1.3 Sulphur Dioxide (SO_2)

Figure 75 illustrates the pollution roses for SO_2 measured at the Eskom eZamokuhle & Majuba stations. The pollution rose clearly indicates that high episodes of pollutant levels are primarily related to winds from the: west-, north-westerly direction; east-, north easterly direction, as well a south westerly direction. Figure 75 illustrates that hourly mean concentrations of 10 to 50ppb SO_2, recorded at the Eskom eZamokuhle station are predominantly associated with sources emanating from a westerly/west north-westerly direction.

4.3.1.4 Nitrogen Oxide (NO_2)

Figure 76 illustrates the pollution roses for NO_2 measured at the Eskom eZamokuhle & Majuba stations. The pollution rose clearly indicates that high episodes of pollutant levels are primarily related to winds from the: west-, north-westerly direction; east-, north easterly direction, as well a south westerly direction. Figure 76 illustrates those hourly mean concentrations of 10 to 50 ppb NO_2, recorded at the Eskom eZamokuhle station are predominantly associated with sources emanating from a westerly/south-westerly direction. Please note that data was not available for the 2023 period at the Eskom eZamokuhle AQMS.

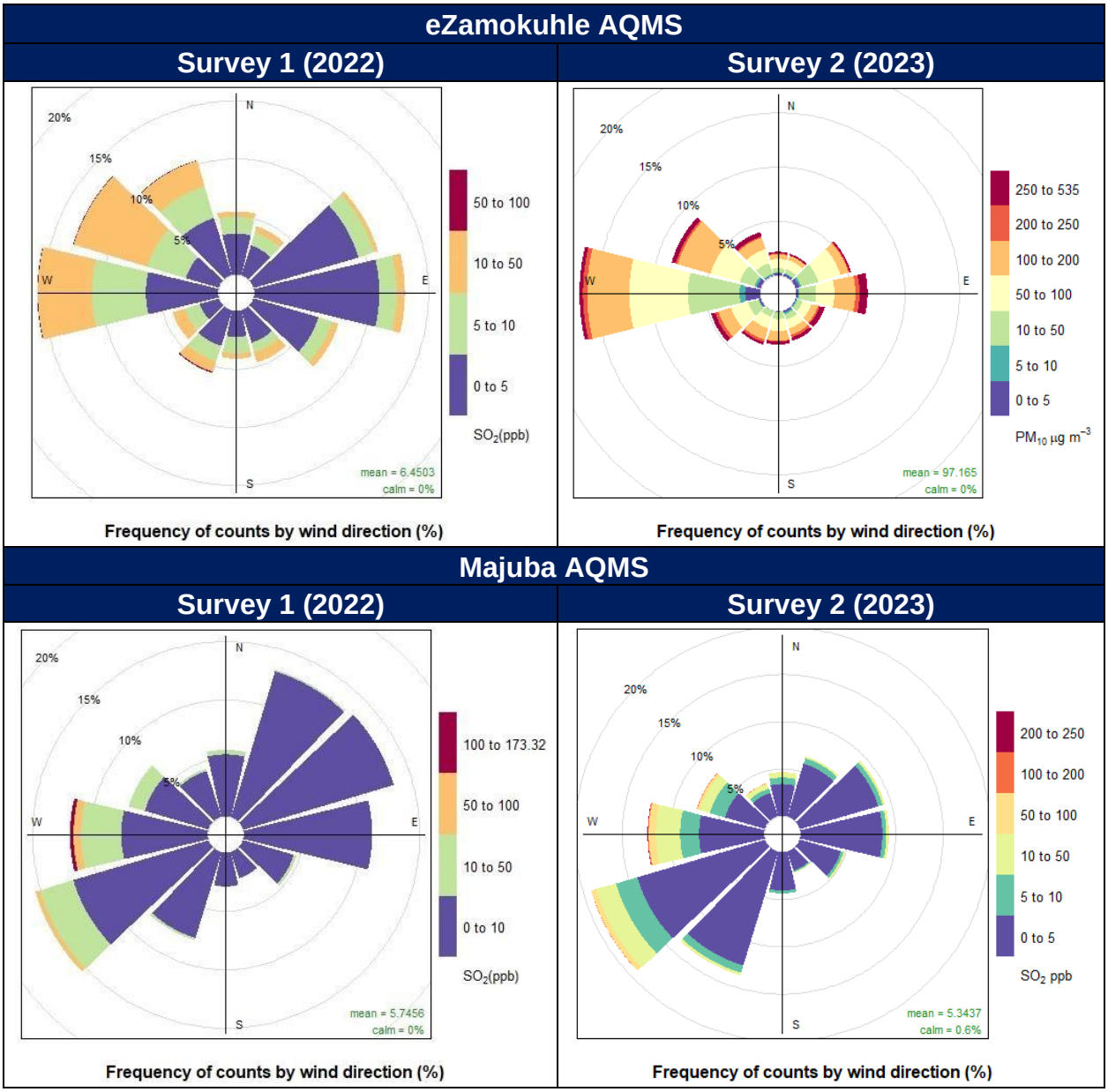

Figure 75: Pollution roses indicating which wind directions contribute most to overall mean concentrations for SO_2.

eZamokuhle AQMS

Survey 1 (2022)

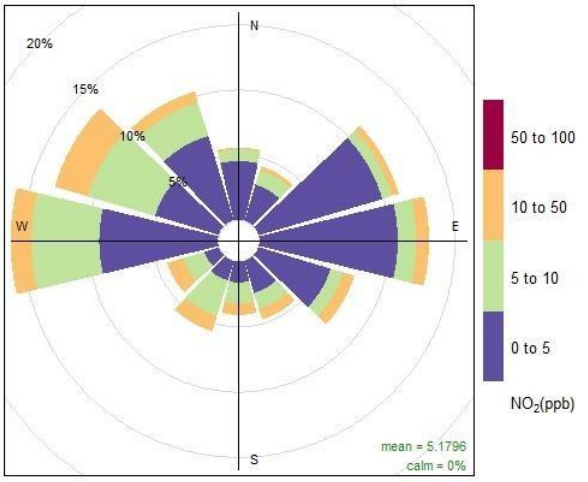

Frequency of counts by wind direction (%)

Survey 2 (2023)

No data available.

Majuba AQMS

Survey 1 (2022)

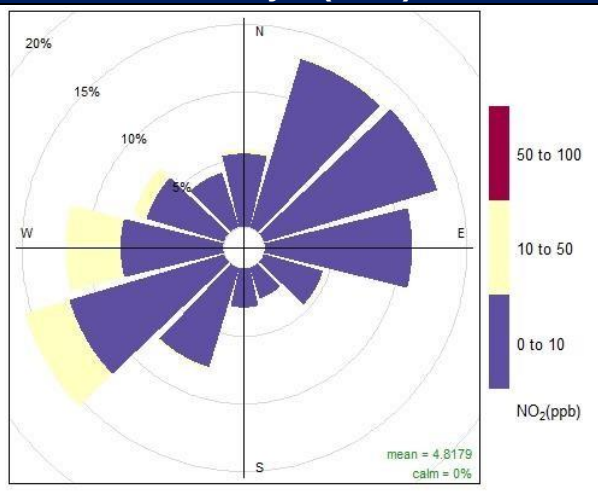

Frequency of counts by wind direction (%)

Survey 2 (2023)

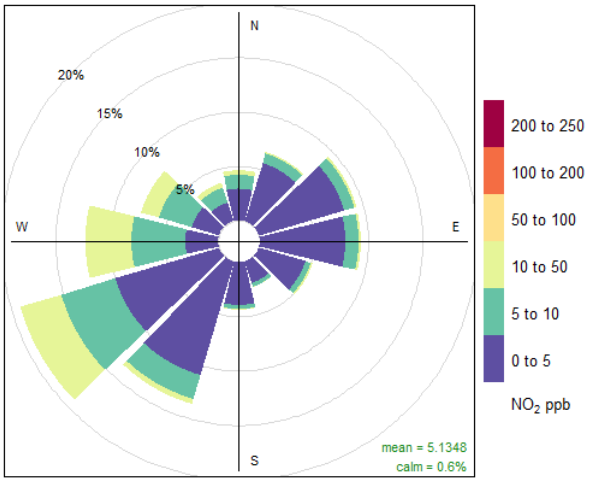

Frequency of counts by wind direction (%)

Figure 76: Pollution roses indicating which wind directions contribute most to overall mean concentrations for NO_2.

4.3.2 Bivariate Polar Plots for Mean Concentration & Wind Speed

Bivariate plots indicate how the concentration of a pollutant varies by wind direction and wind speed at a receptor. The wind speed dependence of a source can provide important information concerning the source type and characteristics (Carslaw et al., 2006; Jones et al., 2010). High ground level concentrations from tall stack emissions are more prevalent during stronger wind speeds during stable conditions whilst conversely low-level emissions, and higher concentrations would normally be observed during weak-wind conditions.

4.3.2.1 Particulate Matter (PM_{10})

Elevated particulate (PM_{10}) concentrations at Eskom eZamokuhle show source contributions from the north-west and the south-east at higher (between 8 and 12 m/s) wind speeds (Figure 77). At low wind speeds the symmetrical plot shows a localised contribution, most likely the result of residential fuel burning (Figure 77). The Eskom Majuba station indicate source contributions from a westerly, south-westerly as well as a north-easterly direction. The higher concentrations (400 to 450 ug/m^3) are associated with sources from a south-westerly direction (10 to 14m/s).

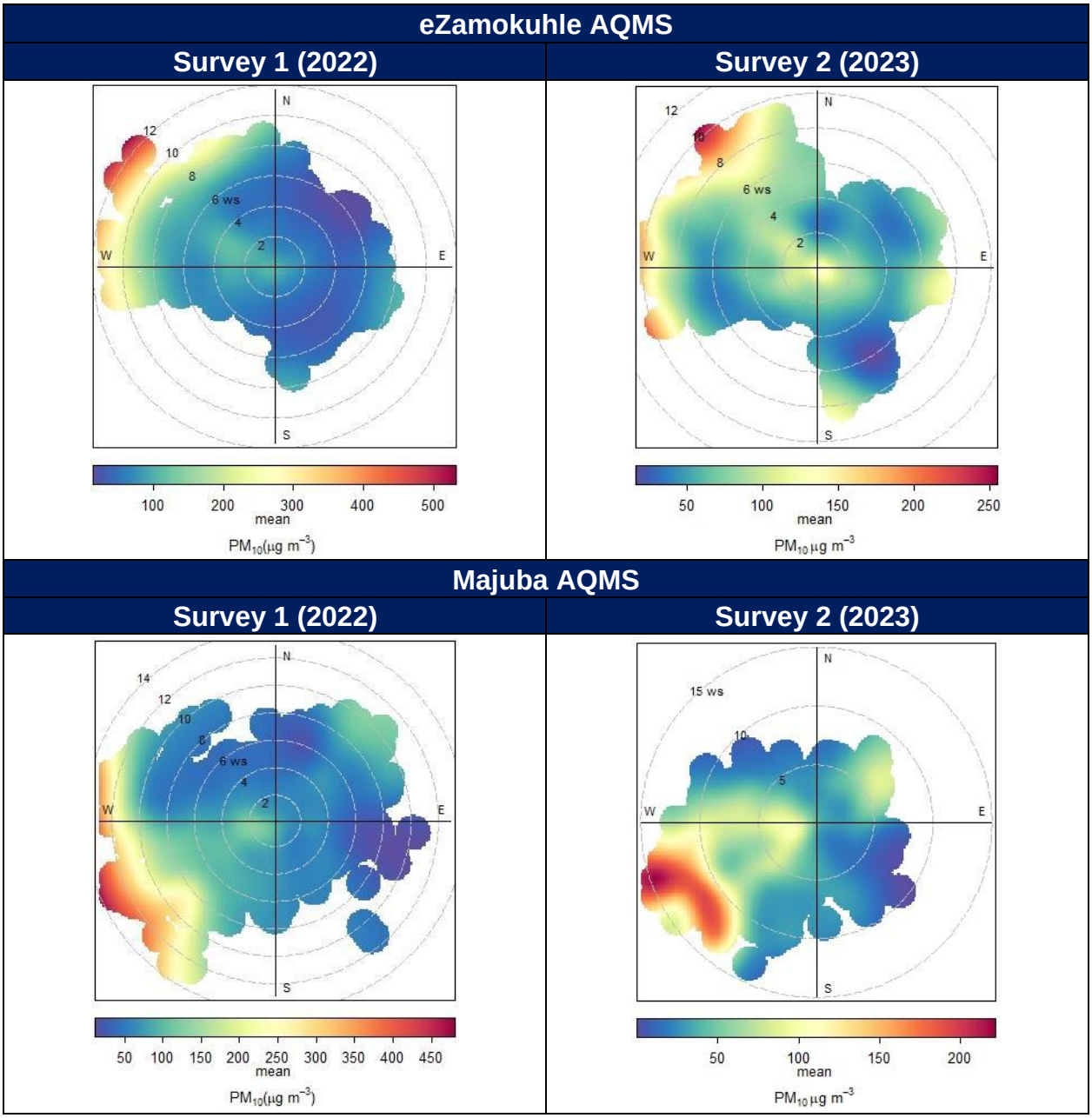

Figure 77: Polar plot of hourly mean PM_{10} concentrations at the Eskom AQMS for the two sampling periods.

4.3.2.2 Particulate Matter ($PM_{2.5}$)

Elevated particulate ($PM_{2.5}$) concentrations at Eskom eZamokuhle show source contributions from the north-west and the south-east at higher (between 8 and 12 m/s) wind speeds (Figure 78). At low wind speeds the symmetrical plot shows a localised contribution, most likely the result of residential fuel burning (Figure 78). The Eskom Majuba station indicate the highest source contribution from a westerly direction. These high concentrations (>120 ug/m^3) is associated with sources from a westerly direction and wind speeds of 12 to 14 m/s. Please note that data was not available for the 2023 period at the Eskom eZamokuhle AQMS.

eZamokuhle AQMS	
Survey 1 (2022)	**Survey 2 (2023)**
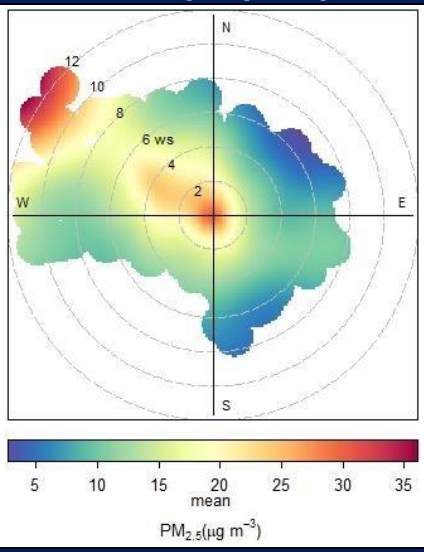	No data available.
Majuba AQMS	
Survey 1 (2022)	**Survey 2 (2023)**
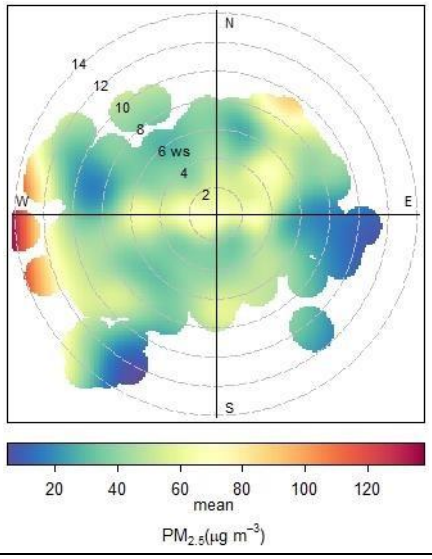	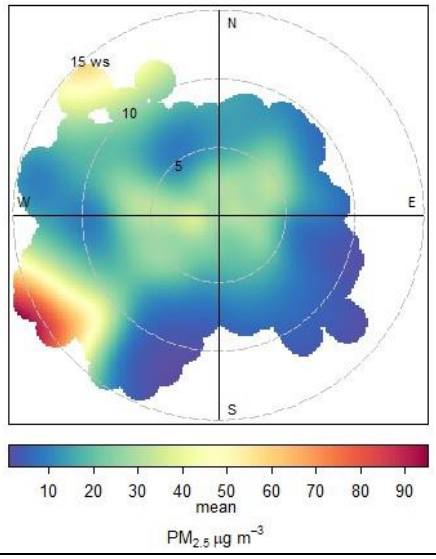

Figure 78: Polar plot of hourly mean $PM_{2.5}$ concentrations at the Eskom AQMS for the two sampling periods.

4.3.2.3 Sulphur Dioxide (SO_2)

The SO_2 concentrations observed at the Eskom eZamokuhle station (Figure 79) show two distinct wind directions, namely from the south-west and the north-west. High concentrations present at high wind speeds are indicative of emissions from stacks rather than non-buoyant ground-level sources. Hence the higher SO_2 concentrations associated with the south-westerly winds are most likely due to emissions from the Eskom Majuba power station. Similarly, the SO_2 concentrations from the north-west indicates a distinct tall stack emission source and this corresponds to the exact direction of a significant petrochemical facility located in Secunda which may be the likely emission source.

SO_2 concentrations (Figure 79) observed at the Eskom Majuba AQMS clearly show that the highest SO_2 concentrations occur when the wind is blowing from the west/north-west. These high concentrations occur under very high wind speeds conditions (between 10 to 15 m/s) from the north-west which is most likely due to emissions from the Eskom Majuba power station. At low wind speeds the symmetrical plot shows a localised contribution, most likely the result of residential fuel burning (Figure 79).

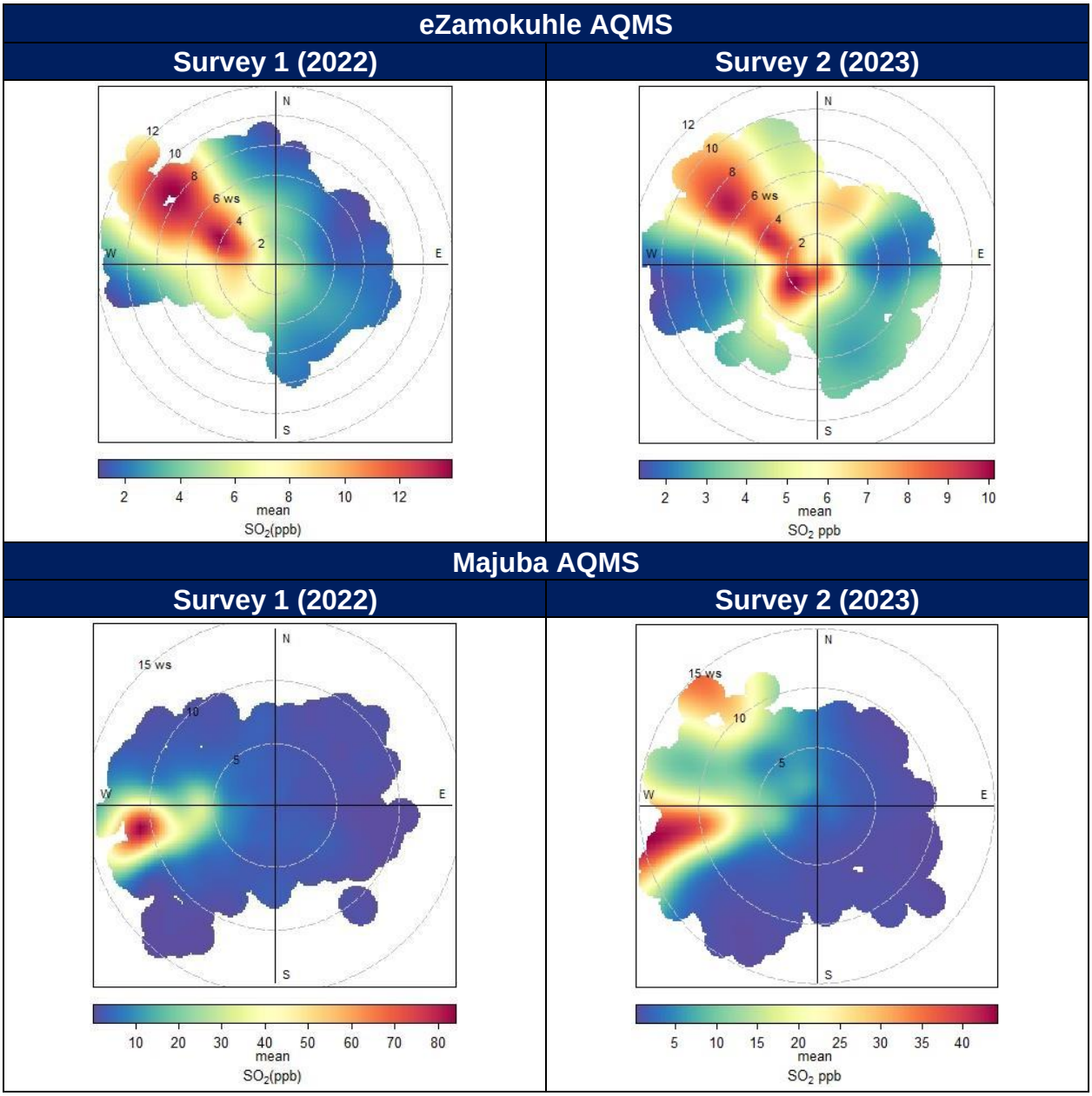

Figure 79: Polar plot of hourly mean SO_2 concentrations at the Eskom AQMS for the two sampling periods.

4.3.2.3 Nitrogen Dioxide (NO_2)

Figure 80 indicate the bivariate NO_2 polar plots for the Eskom eZamokuhle and Majuba AQMS. The highest concentrations occur under very low wind speed conditions (0 to 2m/s) from the south-west. These high concentrations occur under stable atmospheric conditions when non-buoyant ground-level sources are important such as road transport emissions. Figure 78 confirms that these NO_2 concentrations are the likely impact of vehicle emissions. The bivariate polar plot also indicates an area of high concentration to the north-west that occur at high wind speeds (8 to 12m/s), possibly corresponding to the activities of a petrochemical facility located in Secunda. Please note that data was not available for the 2023 period at the Eskom eZamokuhle AQMS.

NO_2 concentrations (Figure 80) observed at the Eskom Majuba station clearly show that the highest NO_2 concentrations occur when the wind is blowing from the north-west. The high concentrations occur under very high wind speeds conditions (between 10 to 15 m/s) from the north-west which is most likely due to emissions from the Eskom Majuba power station. At low wind speeds the symmetrical plot shows a localised contribution, most likely the result of residential fuel burning in the region.

eZamokuhle AQMS	
Survey 1 (2022)	**Survey 2 (2023)**
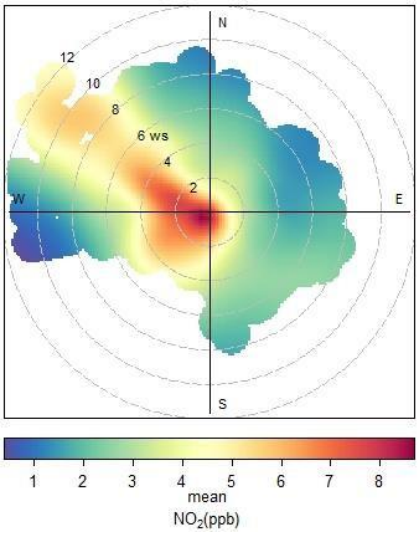	No data available.
Majuba AQMS	
Survey 1 (2022)	**Survey 2 (2023)**
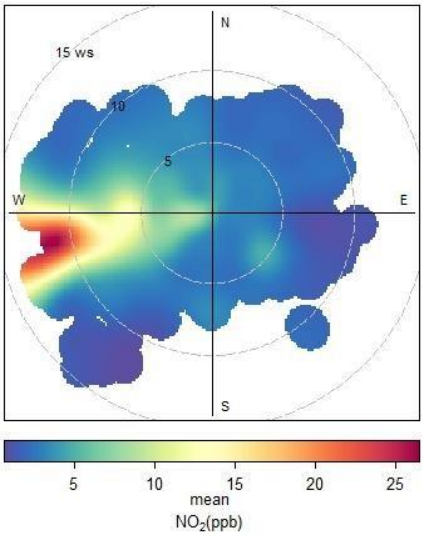	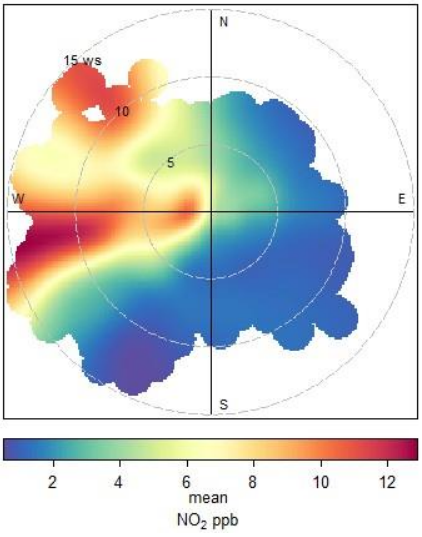

Figure 80: Polar plot of hourly mean NO_2 concentrations at the Eskom AQMS for the two sampling periods.

4.3.3 Bivariate Polar Plot for Mean Concentration & Temperature

These plots indicate how the concentration of a pollutant varies by wind direction and temperature at a receptor. Temperature can help reveal high-level sources brought down to ground level in unstable atmospheric conditions or show the effect a source emission dependent on temperature e.g., residential burning for space heating. Please note that data was not available for the 2023 period at the Eskom eZamokuhle AQMS.

4.3.3.1 Particulate Matter (PM_{10})

Figure 81 indicates the bivariate polar plots for PM_{10} concentrations as a function of wind direction and surface temperature for both the Eskom eZamokuhle and Eskom Majuba AQMS. The highest concentrations occur during low temperatures, which results mostly from residential fuel burning.

4.3.3.2 Particulate Matter ($PM_{2.5}$)

Figure 82 indicates the bivariate polar plots for $PM_{2.5}$ concentrations as a function of wind direction and surface temperature for both the Eskom eZamokuhle and Eskom Majuba AQMS. Lower localised concentrations occur during low temperatures, which results mostly from residential fuel burning.

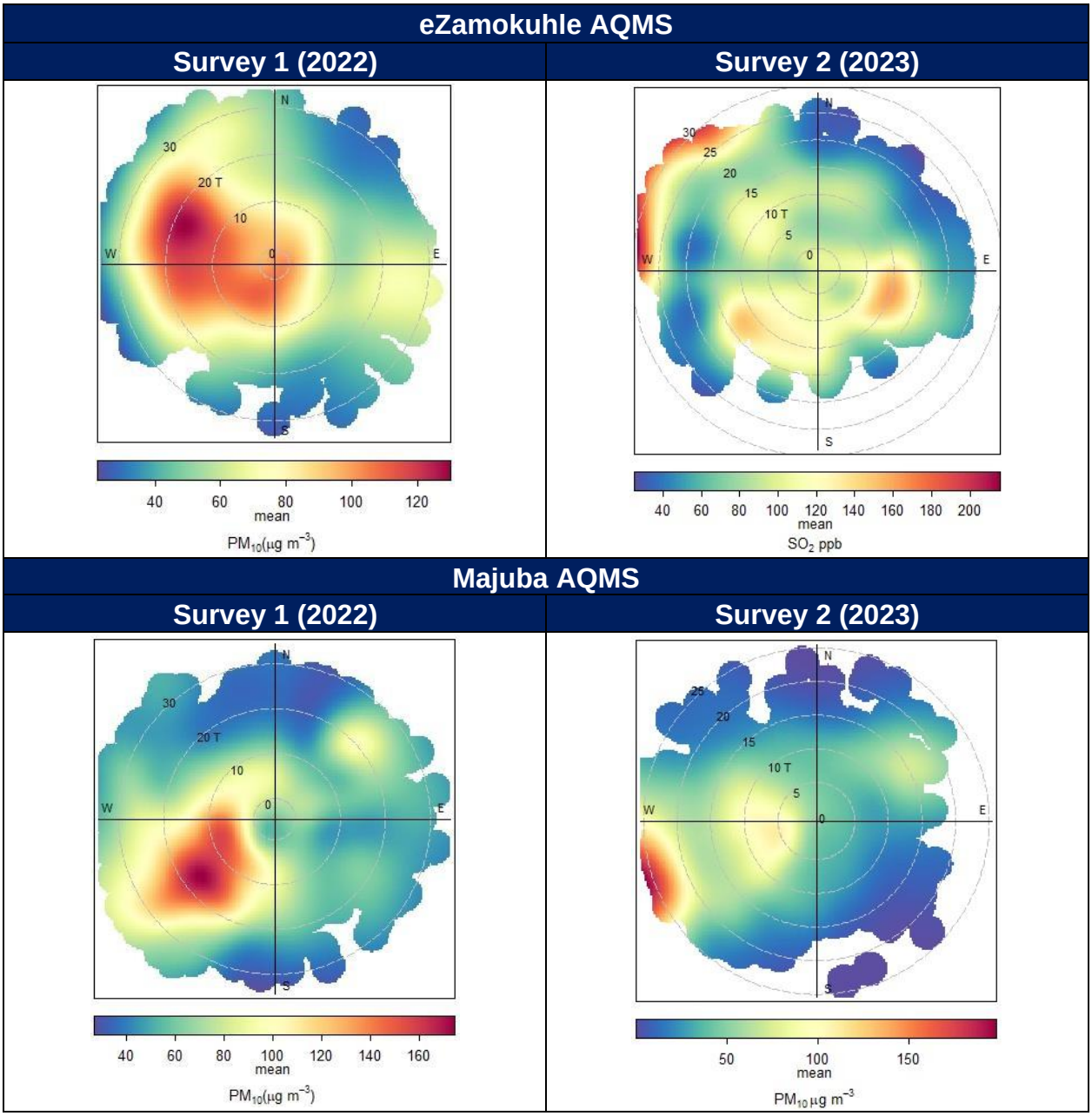

Figure 81: Polar plot of hourly mean PM_{10} concentrations at the Eskom AQMS for the two sampling periods.

eZamokuhle AQMS	
Survey 1 (2022)	**Survey 2 (2023)**
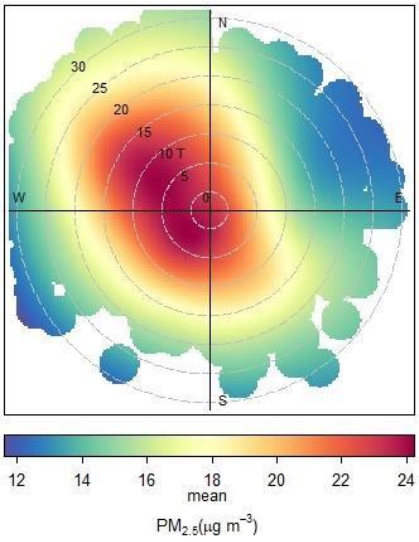	No data available.
Majuba AQMS	
Survey 1 (2022)	**Survey 2 (2023)**
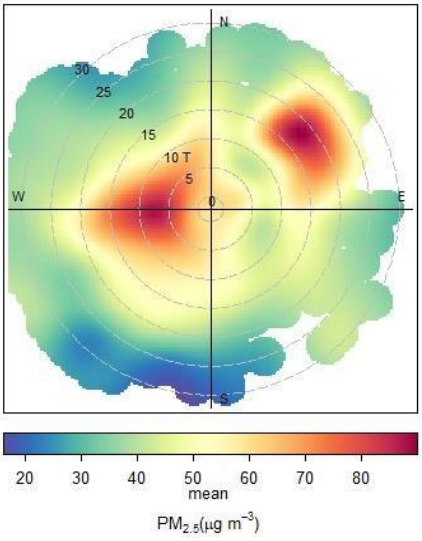	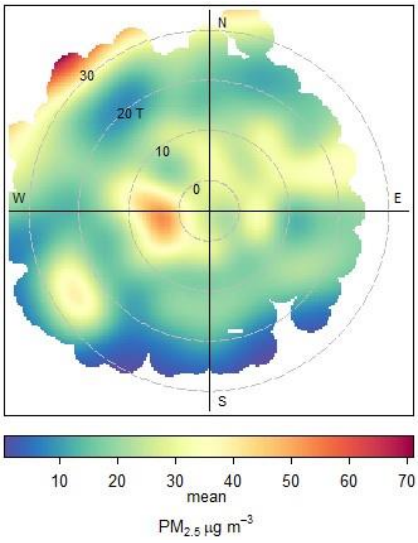

Figure 82: Polar plot of hourly mean $PM_{2.5}$ concentrations at the Eskom AQMS for the two sampling periods.

4.3.3.3 Sulphur Dioxide (SO_2)

Figure 83 indicate the bivariate polar plot for hourly SO_2 concentrations as a function of wind direction and surface temperature. It is apparent that there is a clear dependence of SO_2 concentrations with increasing ambient temperature for both the Eskom eZamokuhle and Eskom Majuba AQMS. These concentrations increase with increasing temperature can be attributed to dispersing plumes from tall stacks that are brought down to ground level under unstable atmospheric conditions when thermal turbulence is increased. The bivariate polar plot (Figure 83) also indicates an area of high concentration to the north-west that occur at higher temperatures (20 to 30°C), possibly corresponding to the activities of a petrochemical facility located in Secunda.

The area of high concentration for the Eskom Majuba station toward the west could possibly correspond to the Eskom Majuba power station, located towards the west of the Eskom Majuba AQMS.

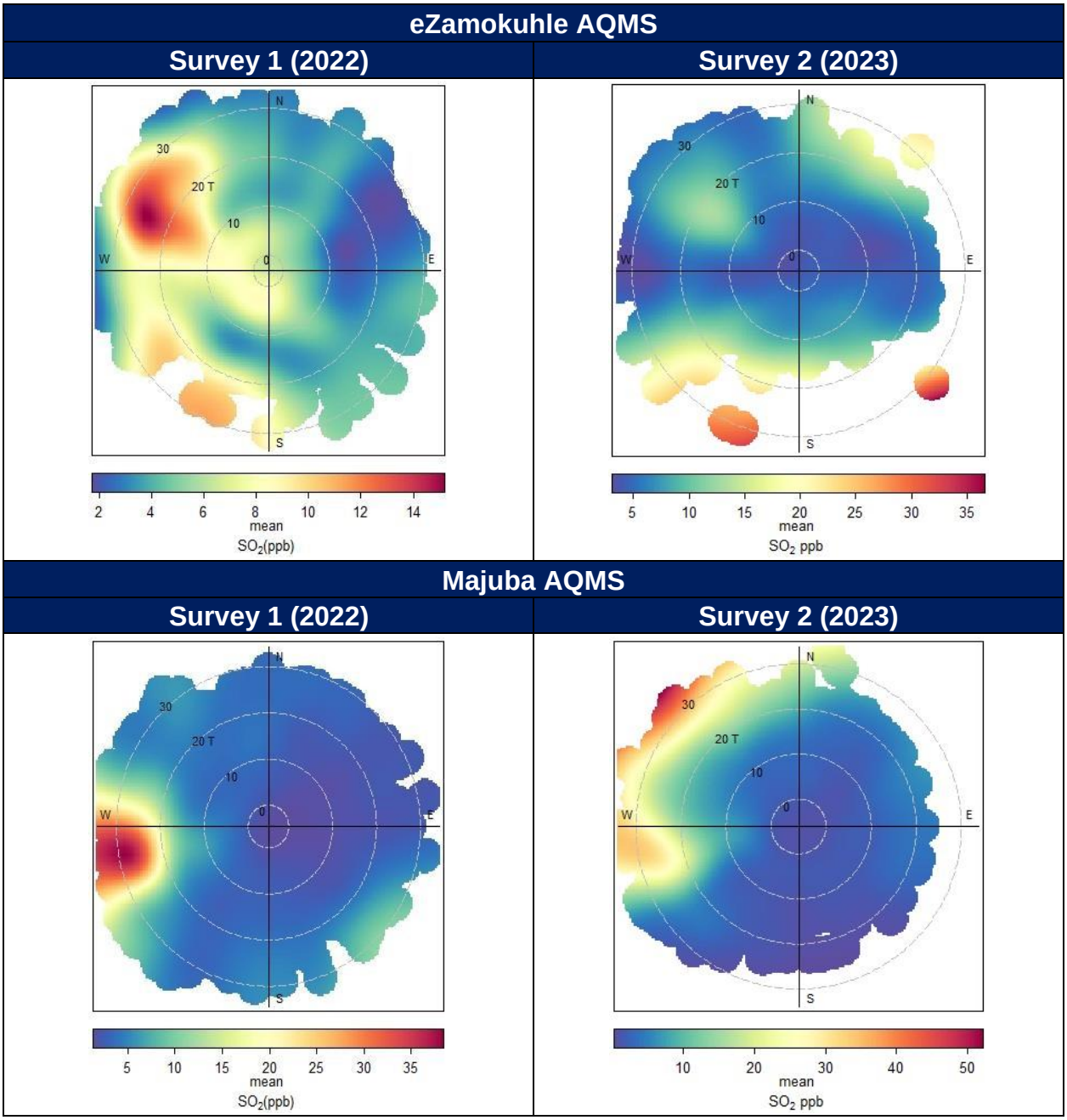

Figure 83: Polar plot of hourly mean SO_2 concentrations at the Eskom AQMS for the two sampling periods.

4.3.3.4 Nitrogen Dioxide (NO_2)

Figure 84 indicate the bivariate polar plot for hourly NO_2 concentrations as a function of wind direction and surface temperature. It is apparent that there is a clear dependence of NO_2 concentrations with increasing ambient temperature for both the Eskom eZamokuhle and Eskom Majuba AQMS. These concentrations increase with increasing temperature can be attributed to dispersing plumes from tall stacks that are brought down to ground level under unstable atmospheric conditions when thermal turbulence is increased. The bivariate polar plot (Figure 84) also indicates an area of high concentration to the north-west that occur at higher temperatures (20°C), possibly corresponding to the activities of a petrochemical facility located in Secunda. The area of high concentration in the south-westerly direction ate temperatures from 0 to 30°C could correspond to vehicle emissions.

The area of high concentration for the Eskom Majuba station (Figure 84) toward the west could possibly correspond to the Eskom Majuba power station, located towards the west of the Eskom Majuba AQMS.

eZamokuhle AQMS	
Survey 1 (2022)	**Survey 2 (2023)**
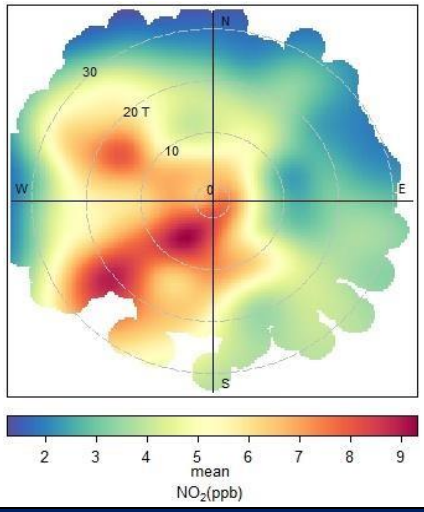	No data available.
Majuba AQMS	
Survey 1 (2022)	**Survey 2 (2023)**
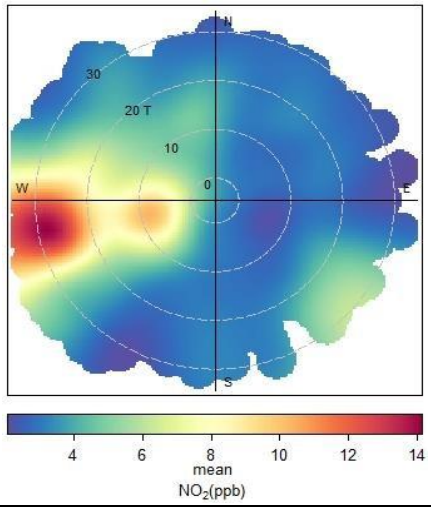	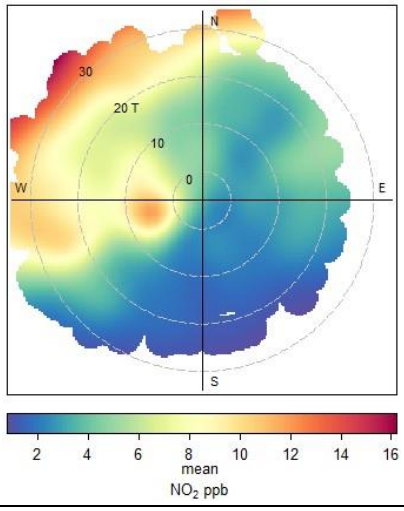

Figure 84: Polar plot of hourly mean NO_2 concentrations at the Eskom AQMS for the two sampling periods.

5. CONCLUSIONS

The daily NAAQS for particulate matter (both PM_{10} & $PM_{2.5}$) was exceeded at all three residential sampling sites in eZamokuhle. The elevated particulate concentrations were predominant during the colder winter months which is attributable to residential fuel burning. Its noted due to constraints and delays encountered by the insulation contractors in eZamokuhle, the roll-out of the Eskom AQO Project interventions herein was not at a significant scale for the sampling period. Going forward, post the large-scale rollout of Eskom AQO Project interventions at Ezamokuhle, a number of scientific studies (*inter alia* source apportionment; indoor air quality monitoring and dispersion modelling) will be utilized to assess the subsequent air quality impact herein.

An analysis of the Eskom eZamokuhle ambient air quality stations (AQMS) showed that there were no recorded exceedances of the hourly NAAQS SO_2 and/or NO_2 standards. The SO_2 concentrations were generally associated with a typically industrial signature whereas the analysis indicated that the variability of NO_2 concentration was associated with vehicle emissions.

It's clear from both survey campaigns that residential fuel burning poses a significant health risk to the community of eZamokuhle. Thus, supporting the roll-out of Eskom's PMV air quality offset intervention project in Ezamokuhle.

6. ACKNOWLEDGEMENTS

Air Resource Management would like to thank the following individuals for their assistance in this study:

- Ms Bontle Moiloa for timeously providing the team with the ambient air quality monitoring data for the Eskom Majuba and eZamokuhle stations;
- Mr Motshewa Matimolane and Mr Bryan McCourt for their technical comments and support.

7. REFERENCES

1. S. Munir, T. M. Habeebullah, A. M. F. Mohammed, E. A. Morsy, M. Rehan, and K. Ali, “Analysing $PM_{2.5}$ and its association with PM_{10} and meteorology in the arid climate of Makkah, Saudi Arabia,” Aerosol and Air Quality Research, vol. 17, no. 2, pp. 453–464, 2017.
2. J. Hu, Y. Wang, Q. Ying, and H. Zhang,2014. “Spatial and temporal variability of $PM_{2.5}$ and PM_{10} over the north China plain and the Yangtze River Delta, China,” Atmospheric Environment, vol. 95, pp. 598–609, 2014.
3. Doucet, P., Sloep, P.B. 1992. “Mathematical Modeling in the Life Sciences”, King’s College, London,1992
4. Tiwary, A., Colls, J. “Air Pollution: Measurement, Modeling, and Mitigation”, 3rd Edition, Routledge,New York, 2010
5. Carslaw D.C., Ropkins K. 2012. “Openair – an r package for air quality data analysis”. Environmental Modelling and Software, pp27–28: pp52–61
6. Appel, K.W., Gilliam, R.C., Davis, N., Zubrow, A., and Howard, S.C., 2011. “Overview of the atmospheric model evaluation tool (amet) v1.1 for evaluating meteorological and air quality models”. Environmental Modelling and Software ,Vol 26 (4), pg434-443. http://www.sciencedirect.com/science/article/pii/S1364815210002653
7. Carslaw, D. “The Openair Manual Open-Source Tools for Analysing Air Pollution Data”, King’s College, London, 2015.
8. Czernecki B., Pólrolniczak M., Kkolendowicz L., Marosz M., Kendzierski S., Pilguj N. 2016. “Influence of the Atmospheric Conditions on PM_{10} Concentrations in Poznan, Poland”. Journal of Atmospheric Chemistry,vol 74(1),pp. 1-25. View at: https://www.researchgate.net/publication/308477377_Influence_of_the_atmospheric_conditions_on_PM_{10}_concentrations_in_Poznan_Poland

9. Crilley L.R., Lucarelli F., Bloss W.J., Harrison R.M., Beddows D.C., Calzolai G., Navab S., Vallid G., Bernardonid V., Vecchi R. 2017. “Source apportionment of fine and coarse particles at a roadside and urban background site in London during the 2012 summer ClearfLo campaign”. Environmental Pollution 220: pp766–778
10. Pattinson W., Kingham S., Longley I., Salmond J. 2016. “Potential Pollution Exposure Reductions from Small-Distance Bicycle Lane Separations”. Journal of Transport & Health,Vol 4,pp40-52. View at: https://www.sciencedirect.com/science/article/abs/pii/S2214140516303504
11. Salvador P., Alonso-Pérez S., Pey J., Artíñano B., Debustos J.J., Alastuey A., Querol X. 2014. “African dust outbreaks over the western Mediterranean Basin: 11-year characterization of atmospheric circulation patterns and dust source areas”. Atmospheric Chemistry and Physics Vol 14(13): pp6759–6775. View at: https://www.researchgate.net/publication/263036412_African_dust_outbreaks_over_the_western_Mediterranean_Basin_11-Year_characterization_of_atmospheric_circulation_patterns_and_dust_source_areas
12. Schweizer D.,and Cisneros R. 2014. “Wildland Fire Management and Air Quality in the Southern Sierra Nevada: Using the Lion Fire as a case study with a multi-year perspective on $PM_{2.5}$ impacts and fire policy”. Journal of Environmental Management Vol 144: pp 265–278. View at: https://www.sciencedirect.com/science/article/pii/S0301479714003089?via%3Dihub
13. Crilley L.R., Bloss W.J., Yin J., Beddows D.C., Harrison R.M., Allan J.D., Young D.E., Flynn M., Williams P., Zotter P., Prevot A.S.H., Heal M.R., Barlow J.F.,Halios C.H., Lee J.D., Szidat S., Mohr C., Prevot A.S. 2015. “Sources and contributions of wood smoke during winter in London: Assessing local and

regional influences". Atmospheric Chemistry and Physics Vol 15(6): pp 3149–3171. View at: https://acp.copernicus.org/articles/15/3149/2015/

14. Jang E., Do W., Park,G., Kim M., Yoo E. 2016. "Spatial and temporal variation of urban air pollutants and their concentrations in relation to meteorological conditions at four sites in Busan, South Korea". Atmospheric Pollution Research Vol 8(1): pp 89–100. View at: https://www.sciencedirect.com/science/article/abs/pii/S1309104216301192?via%3Dihub
15. Szulecka,A., Oleniacz R , and Rzeszutek,M. 2017. "Functionality of Openair Package in Air Pollution Assessment and Modeling — A Case Study of Krakow". Environmental Protection and Natural Resources,Vol 28(2):pp 22-27. View at: https://content.sciendo.com/view/journals/oszn/28/2/article-p22.xml?language=en&tab_body=abstract
16. Malby, A.R., Whyatt, J.D., and Timmis, R.J. 2013. "Conditional Extraction of Air-Pollutant Source Signals from air-quality monitoring". Atmospheric Environment, Vol 74(2013):pp 112-122
17. Carslaw, D.C.,and Carslaw, N., 2007. "Detecting and characterising small changes in ur-ban nitrogen dioxide concentrations". Atmospheric Environment Vol 41(22): pp 4723-4733.View at: http://dx.doi.org/10.1016/j.atmosenv.2007.03.034
18. Malby, A.R., Timmis, R.J., Whyatt, J.D., 2008. "Combining modelling and monitoring to Estimate Fugitive Releases from a Heavily-Industrialised Site". Proceedings from the 12th Conference on Harmonisation within Atmospheric Dispersion Modelling for Regulatory Purposes (HARMO 12), Cavtat, Croatia,October 6-9, 2008, pp. 939-943. View at: http://www.harmo.org/Conferences/ Cavtat/12harmo.asp

19. Shu,M., Dang,D., Nguyen,T., Hsu,B., and Pham,K. 2017. “The application of bivariate polar plots and k-means clustering to analysis air pollution in Taoyuan, Taiwan”. International Journal of Advance Engineering and Research Development, Vol 4(4),pp 553-557
20. Carslaw, D.C., Beevers, S.D., Ropkins, K., Bell, M.C., 2006. “Detecting and quantifying aircraft and other on-airport contributions to ambient nitrogen oxides in the vicinity of a large international airport”. Atmospheric Environment 40 (28),pp 5424-5434. View at: https://www.sciencedirect.com/science/article/abs/pii/S1352231006004250?via%3Dihub
21. Westmoreland, E.J., Carslaw, N., Carslaw, D.C., Gillah, A., and Bates, E., 2007. “Analysis of air quality within a street canyon using statistical and dispersion modelling techniques”. Atmospheric Environment, Vol 41(39), pp 9195-9205. View at: https://doi.org/10.1016/j.atmosenv.2007.07.057
22. Carslaw D.C., and Beevers S.D. 2013. “Characterising and understanding emission sources using bivariate polar plots and k-means clustering”. Environmental Modelling and Software, Vol 40: pp 325–329. View at: https://doi.org/10.1016/j.envsoft.2012.09.005
23. Jones, A.M., Harrison, R.M., Baker, J., 2010. “The wind speed dependence of the concentrations of airborne particulate matter and nox”. Atmospheric Environment Vol 44(13), pp 1682-1690. View at:http://www.sciencedirect.com/science/article/B6VH3-4Y7P72C-2/2/f6c65e5f49ac3e9862d4c1803d4735c0.
24. Tellaetxe, I.U., and Carslaw, D.C. “Conditional bivariate probability function for source identification”,Environmental Modelling & Software,Vol 59,pp 1-9. View at: https://www.sciencedirect.com/science/article/pii/S1364815214001339?via%3Dihub

25. Thangprasert, N.,and Suwanarat,S. 2017. “The Relationships between Wind Speed and Temperature Time Series in Bangkok, Thailand. Journal of Physics: Conference Series, 901 (2017) 01204. View at: https://iopscience.iop.org/article/10.1088/1742-6596/901/1/012043
26. Grundstrom, M., Tang, L., Hallquist, M., Nguyen, H., Chen, D., and Pleijel,H. “Influence of atmospheric circulation patterns on urban air quality during the winter” Atmospheric Pollution Research,Vol 6(2), pp 278-285. View at: https://doi.org/10.5094/APR.2015.032.
27. Garstang, M., Tyson, P.D., Swap, R., Edwards, M., Kållberg, P. and Lindesay, J.A. (1996). Horizontal and vertical transport of air over Southern Africa. Journal of Geophysical Research, 101 (D19), 23721-23736.
28. Swap, R., Garstang, M., Macko, S.A., Tyson, P.D., Maenhaut, W., Artaxo, P., Kallberg, P. and Talbot, R. (1996). The long-range transport of southern African aerosols to the tropical south Atlantic. Journal of Geophysical Research, 101 (D19), 23777-23791.
29. Held, G., Gore, B.J., Surridge, A.D., Tosen, G.R. and Walmsley, R.D. (eds) (1996), Air Pollution and its Impacts on the South African Highveld, Environmental Scientific Association, Cleveland, 144 pp.
30. DEFF (2010), Air Quality Baseline Assessment for the Highveld Priority Area
31. Merrill, J.T., Bleck, R. and Boudra, D.B. (1986). Techniques of Lagrangian trajectory analysis in isentropic coordinates. Monthly Weather Review, 114, 571-581.
32. Lacaux J.P (2003), IGACtivities Newsletter, issue no.27, January 2003, (http://www.igac.noaa.gov/newsletter/igac27/Jan_2200_IGAC_27.pdf)
33. Martins J.J, Dhammapala R.S, Lachmann G, Galy-Lacaux C and Pienaar J.J., (2007): ‘Long-term measurements of sulphur dioxide, nitrogen dioxide, ammonia,

nitric acid and ozone in southern Africa using passive samplers", South African Journal of Science, 103, 1-7

34. Mphepya J.N. 2004, 'Precipitation Chemistry in Semi-Arid Areas of Southern Africa: A Case Study of a Rural and an Industrial Site', Journal of Atmospheric Chemistry 47: 1–24.
35. Van Zyl, P.G., Conradie, E.H., Pienaar, J.J., Beukes, J.P., Galy-Lacaux, C., Swartz, J., Liousse, C., and Mkhatshwa, G.V., An assessment of precipitation chemistry at the South African DEBITS sites, 13th Quadrennial Symposium of the International Commission on Atmospheric Chemistry and Global Pollution, (iCACGP) 13th Science Conference of the International Global Atmospheric Chemistry Project, (IGAC), Natal Convention Center (NCC), Natal, Brazil 22-26th September 2016
36. Van Zyl, P.G., Beukes, J.P.;Conradie, E.H.; Pienaar, J.J.; Mkhatshwa, G.; Fourie, G.D. and Galy-Lacaux, C., Deposition measurements in southern Africa, Workshop on Atmospheric Depostion Processes, The Abdus Salam International Centre for Theoretical Physics, Trieste, Italy, 21-25 May 2012.
37. P. Maritz, J.P. Beukes, P.G. van Zyl, E.H. Conradie, A.D. Venter, J.J. Pienaar, C. Liousse, C. Galy-Lacaux, Spatial and temporal assessment of atmospheric organic and black carbon concentrations at South African DEBITS sites, 16th International Union of Air Pollution Prevention Association (IUAPPA) Congress, 29 September – 4 October 2013, International Convention Centre, Cape Town, South Africa.

DISCLAIMER

Air Resource Management (Pty) Ltd has prepared this report based on an agreed scope of work and acts in all professional matters as an advisor to the Client and exercises all reasonable skill and care in the provision of its professional services in a manner consistent with the level of care and expertise exercised by air quality management professionals.

Reports are commissioned by and prepared for the exclusive use of the Client. They are subject to and issued in accordance with the agreement between the Client and Air Resource Management (Pty) Ltd. Air Resource Management (Pty) Ltd is not responsible and will not be liable to any other person or organisation for or in relation to any matter dealt within this Report, or for any loss or damage suffered by any other person or organisation arising from matters dealt with or conclusions expressed in this report (including without limitation matters arising from any negligent act or omission of Air Resource Management (Pty) Ltd or for any loss or damage suffered by any other party relying upon the matters dealt with or conclusions expressed in this Report). Other parties should not rely upon the report or the accuracy or completeness of any conclusions and should make their own inquiries and obtain independent advice in relation to such matters.

Except where expressly stated, Air Resource Management (Pty) Ltd has not verified the validity, accuracy or comprehensiveness of any information supplied to Air Resource Management (Pty) Ltd for its reports.

Reports prepared by Air Resource Management (Pty) Ltd cannot be copied or reproduced in whole or part for any purpose without the prior written agreement of Air Resource Management (Pty) Ltd.

Where site inspections, testing or fieldwork have taken place, the report is based on the information made available by the client or their nominees during the visit, visual observations and any subsequent discussions with regulatory authorities. The validity and comprehensiveness of supplied information has not been independently verified and, for

the purposes of this report, it is assumed that the information provided to Air Resource Management (Pty) Ltd is both complete and accurate. It is further assumed that normal activities were being undertaken at the site on the day of the site visit(s), unless explicitly stated otherwise.

COPYRIGHT